AK-Mechanika, s.r.o.

Computational analysis of strength, fatigue and excessive vibrations of machines and machinery

OVERVIEW OF EXPERIENCE OF STAFF WITH COMERCIAL WORKS IN

- TRANSPORTATION
- ENERGY INDUSTRY
- PROCESS INUSTRY
- ELECTRICAL INDUSTRY
- OTHER AREAS

TRANSPORTATION

Overview of selected computational finite element analyses

Fig. 1. Road tank for bulk materials.

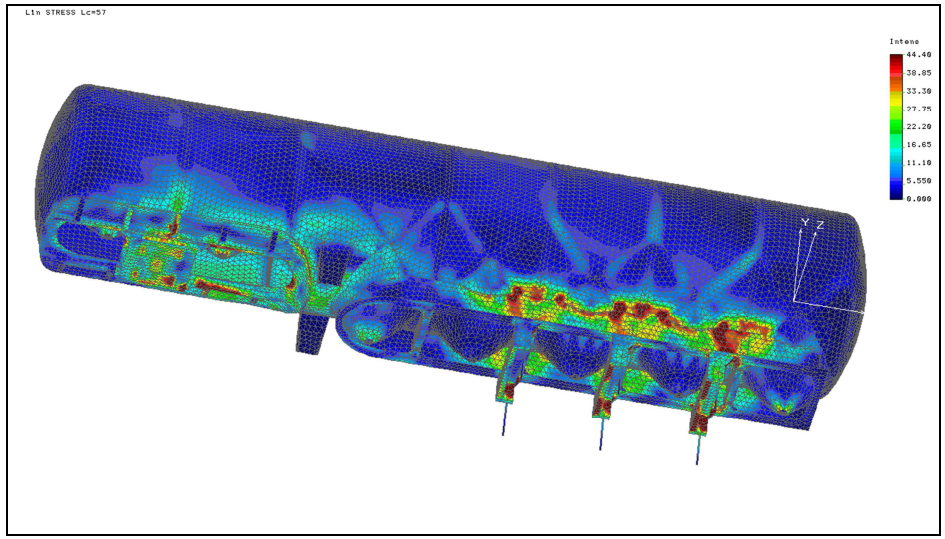

Fig. 2. Critical points - stress from the simulated load.

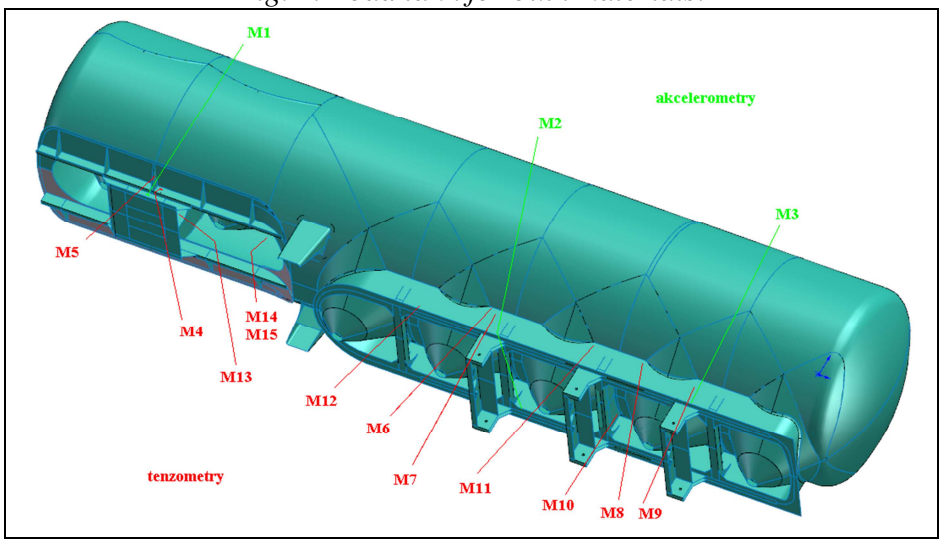

Fig. 3. Draft positions of accelerometers and strain gauges during testing.

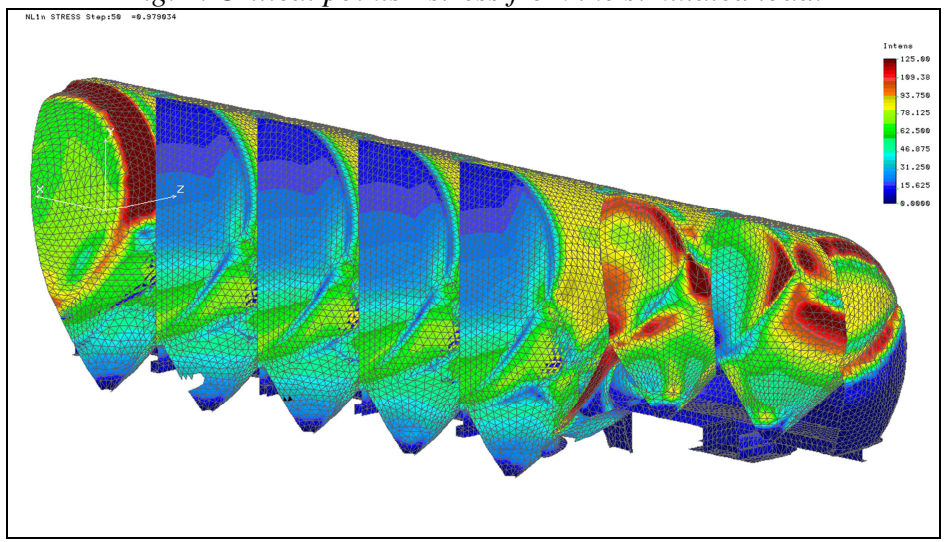

Fig. 4. Check of the limit state of stability and plasticity.

.

Overview of selected computational finite element analyses

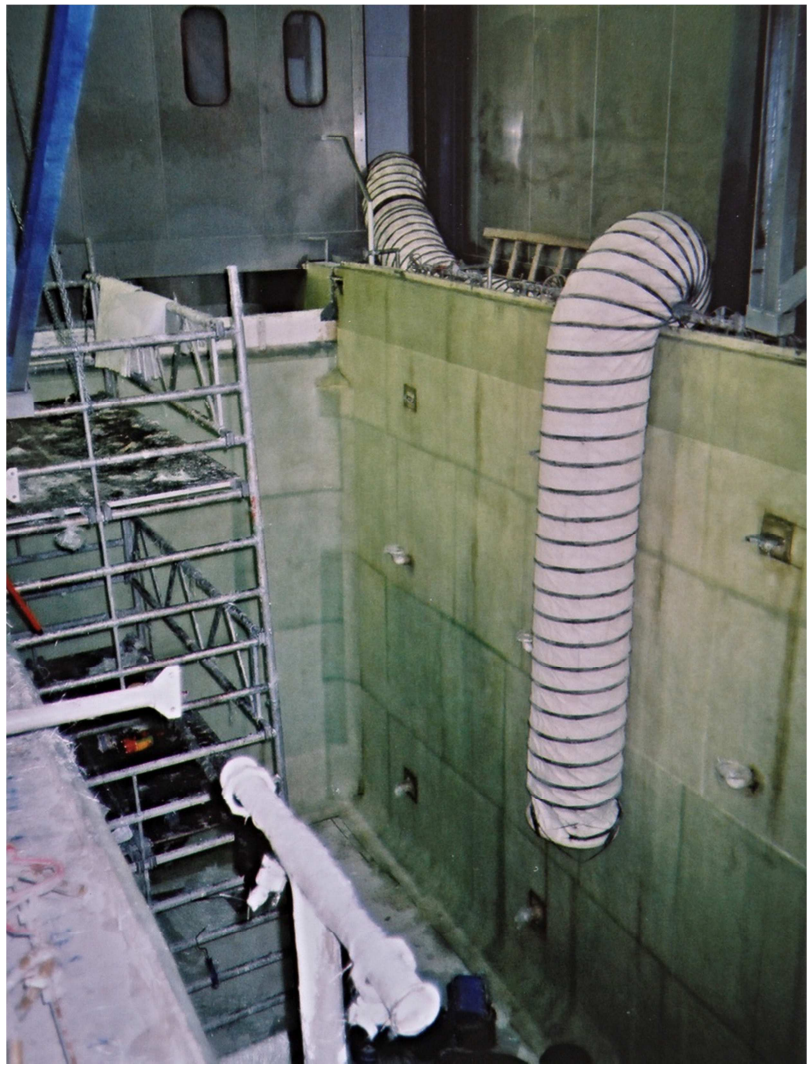

Fig. 1. Photo of inner space of KTL tank.

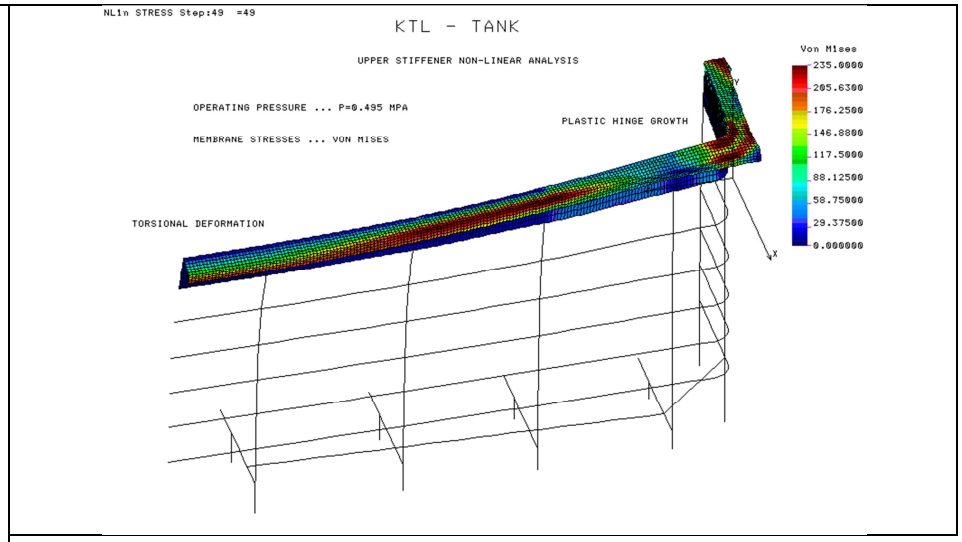

Fig. 2. Strength and stability check of the collapsed outer ring.

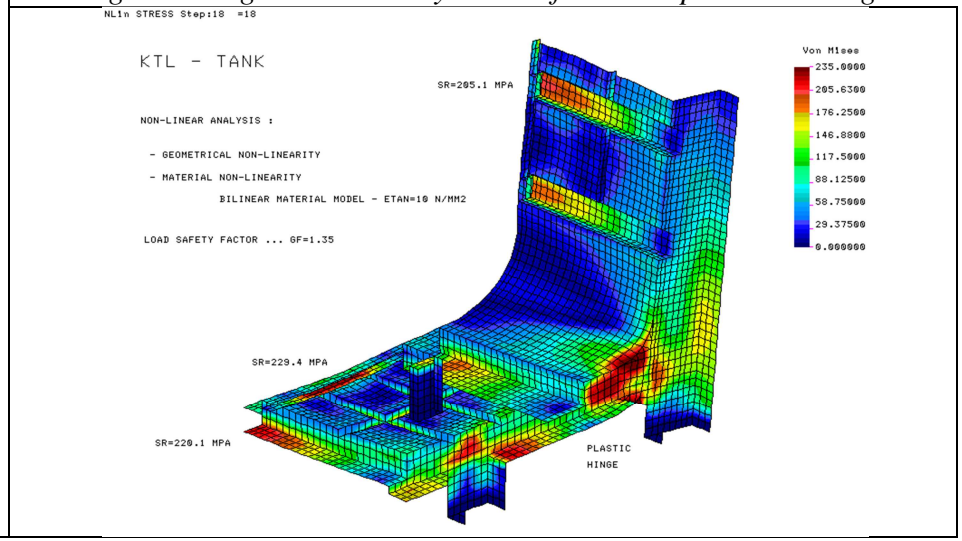

Fig. 3. Computational strength analysis of undersized joint of bottom and side wall of the tank.

Overview of selected computational finite element analyses

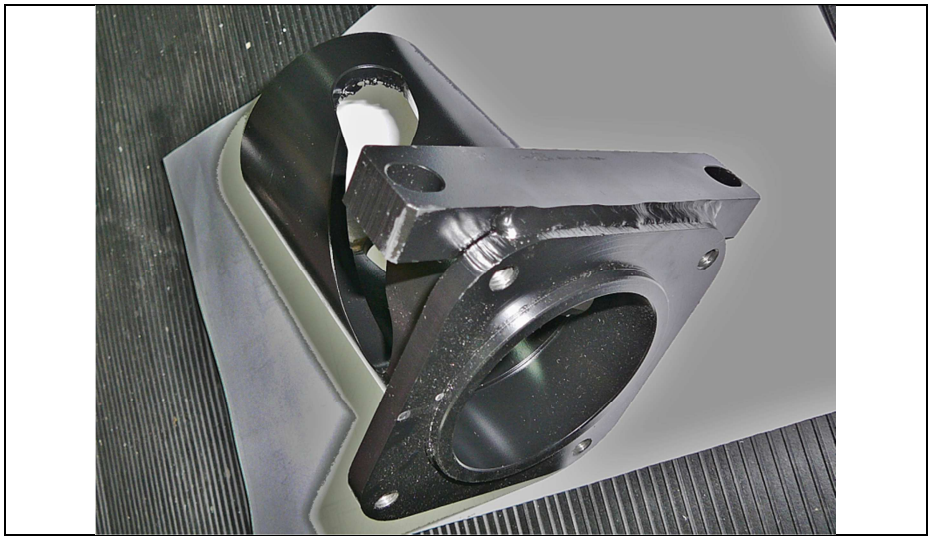

Fig. 1. Console L/140 of bus door closing mechanism.

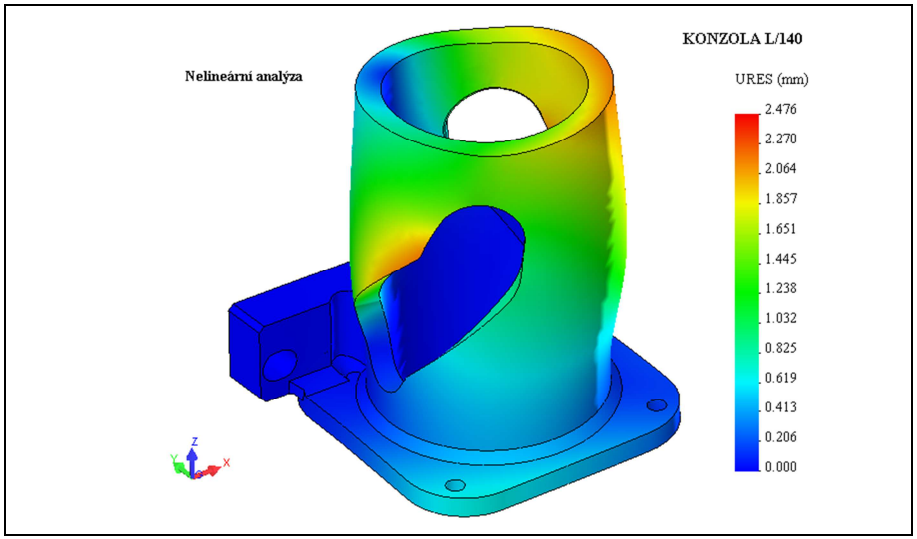

Fig. 2. Limit state of plasticity of console L/140 – displacements.

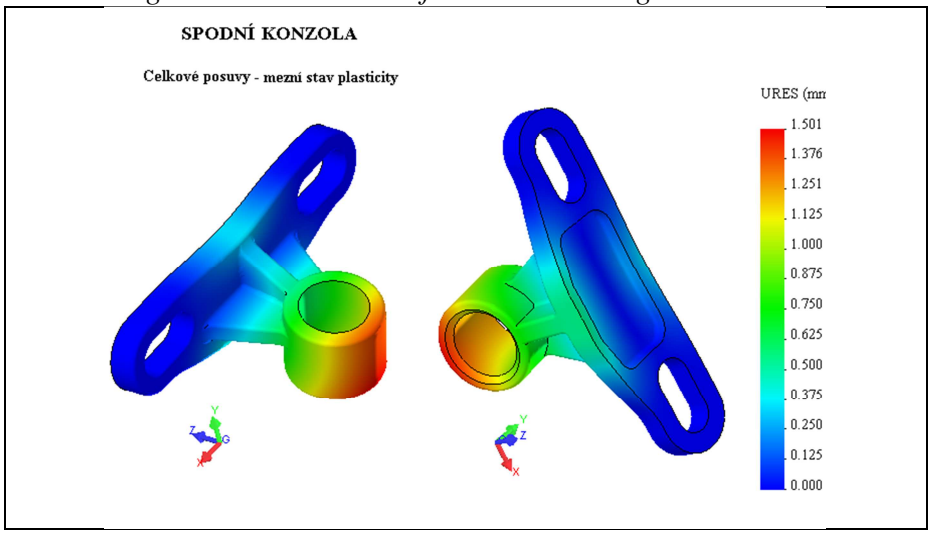

Fig. 3. Limit state of plasticity of lower console – displacements.

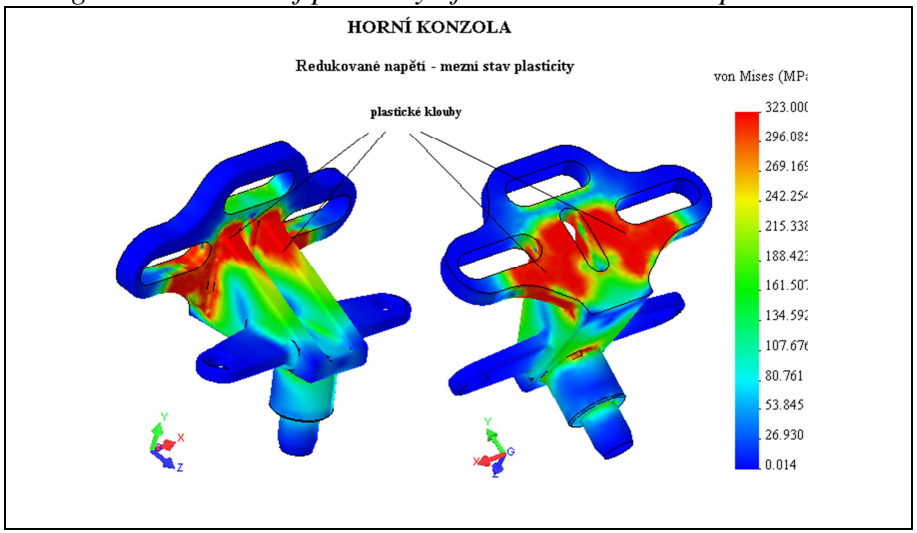

Fig. 4. Limit state of plasticity of upper console – equivalent stresses.

Overview of selected computational finite element analyses

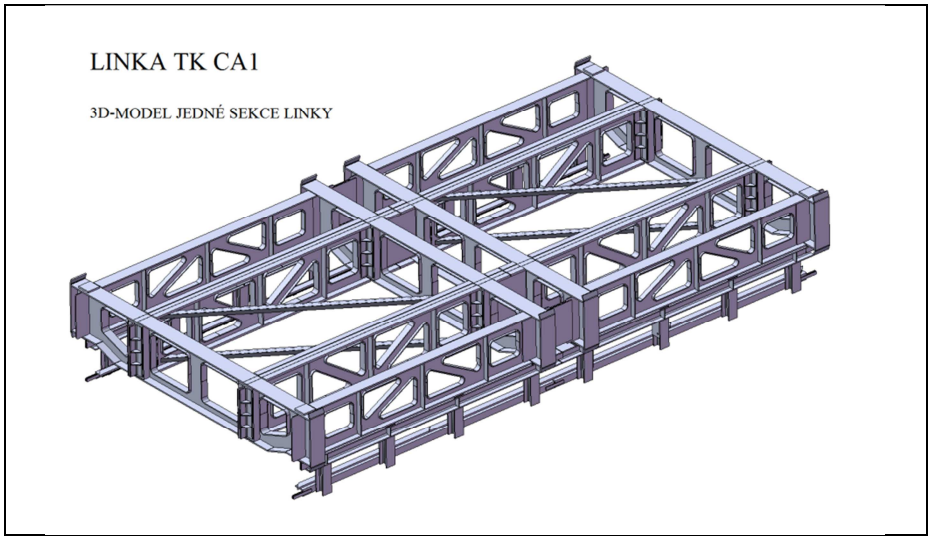

Fig. 1. Model of one section of the conveyor line.

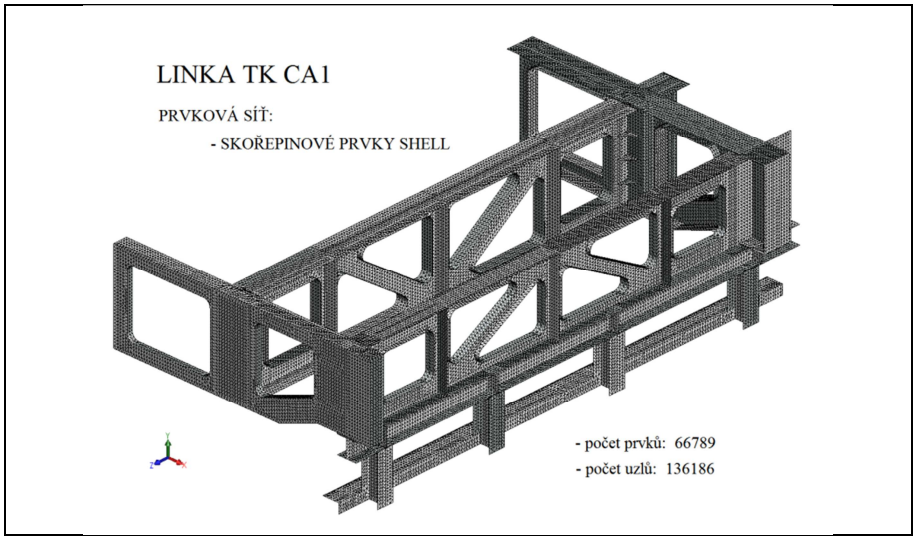

Fig. 2. Computational model (one quarter of the structure).

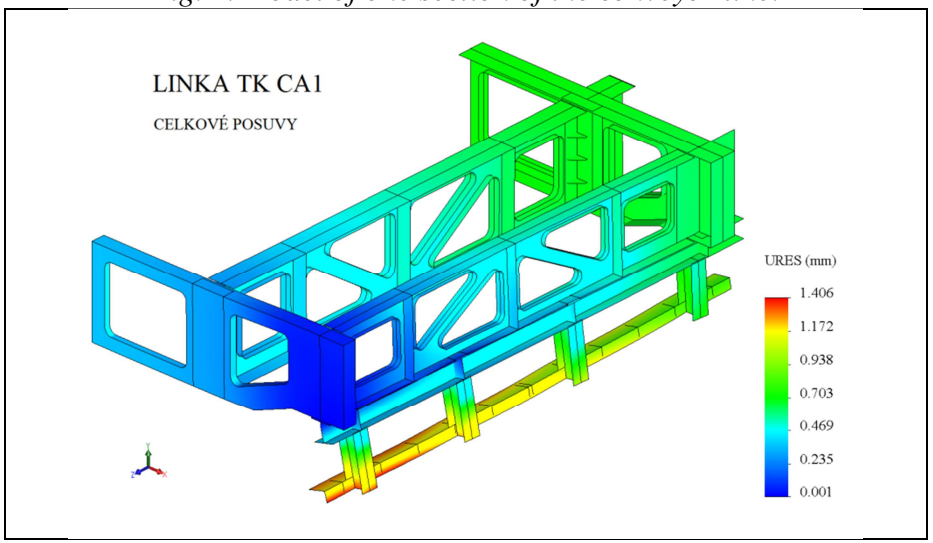

Fig. 3. Displacements due to weight and weight of trolleys.

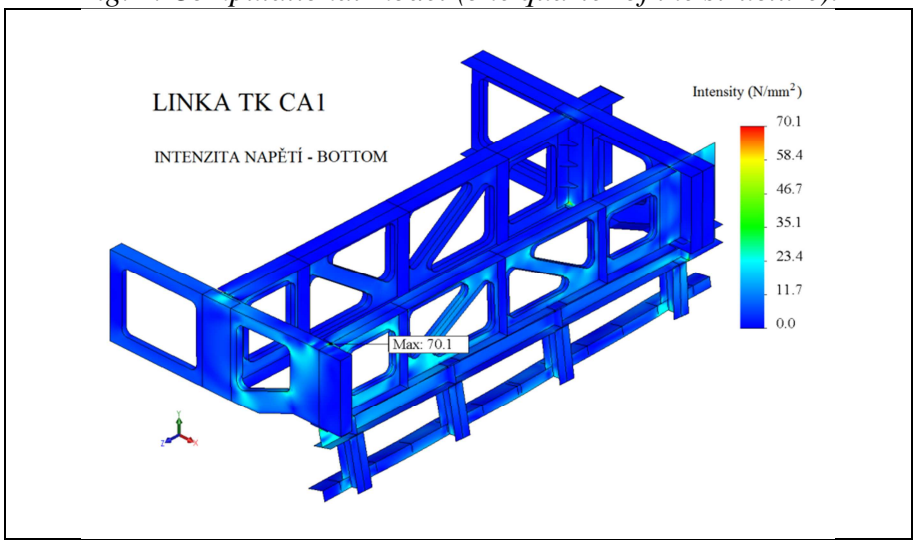

Fig. 4. Stress intensity due to weight and weight of trolley.

Overview of selected computational finite element analyses

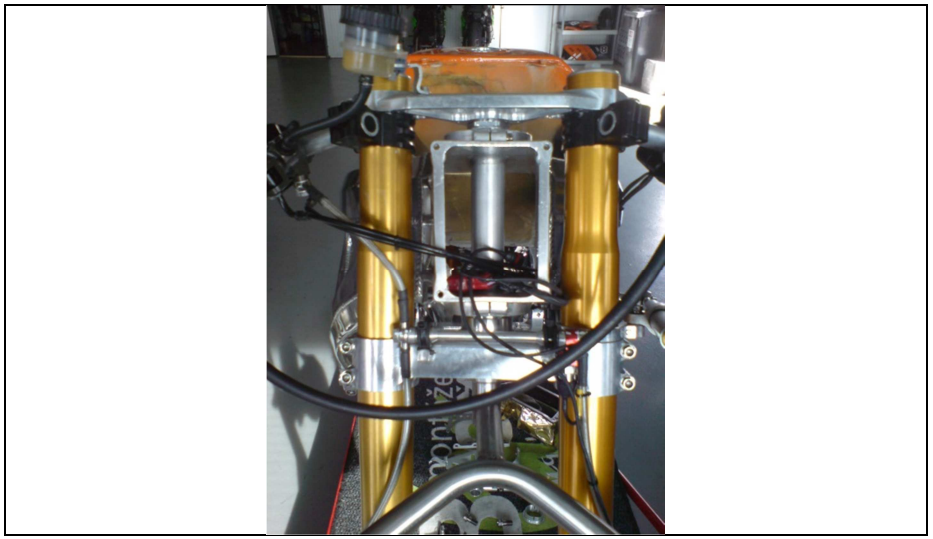

Fig. 1. Forks of race motorcycle.

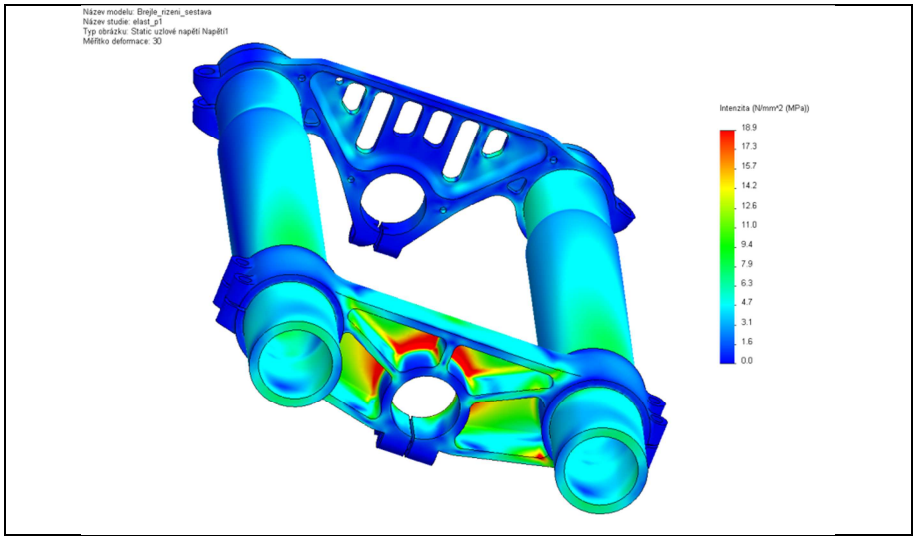

Fig. 2. Equivalent stress of computational model.

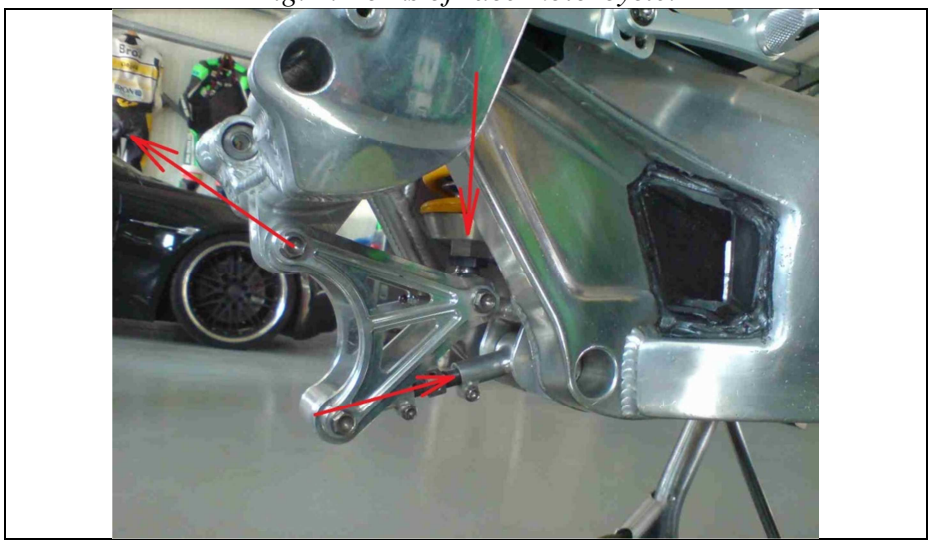

Fig. 3. Connecting element of the base frame and swingarm.

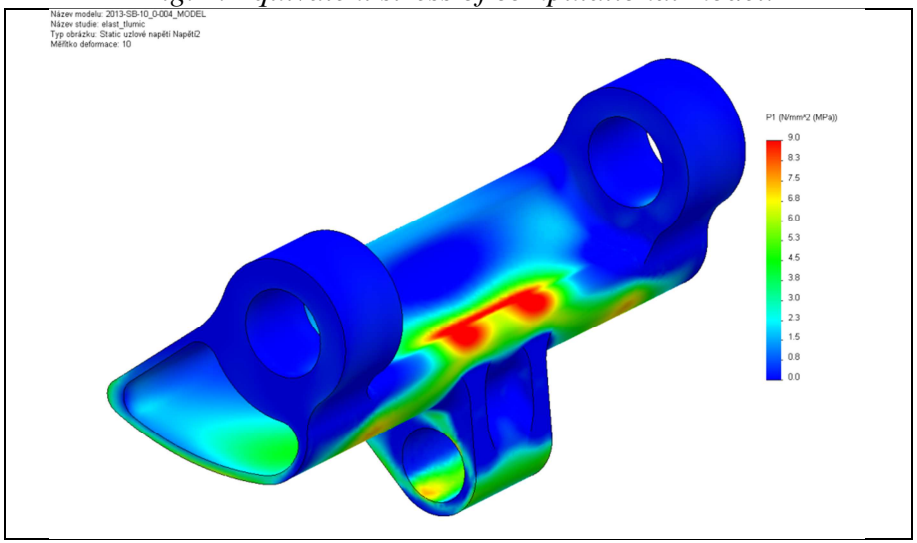

Fig. 4. Equivalent stress of computational model.

Overview of selected computational finite element analyses

Fig. 1. Photo of rescue car.

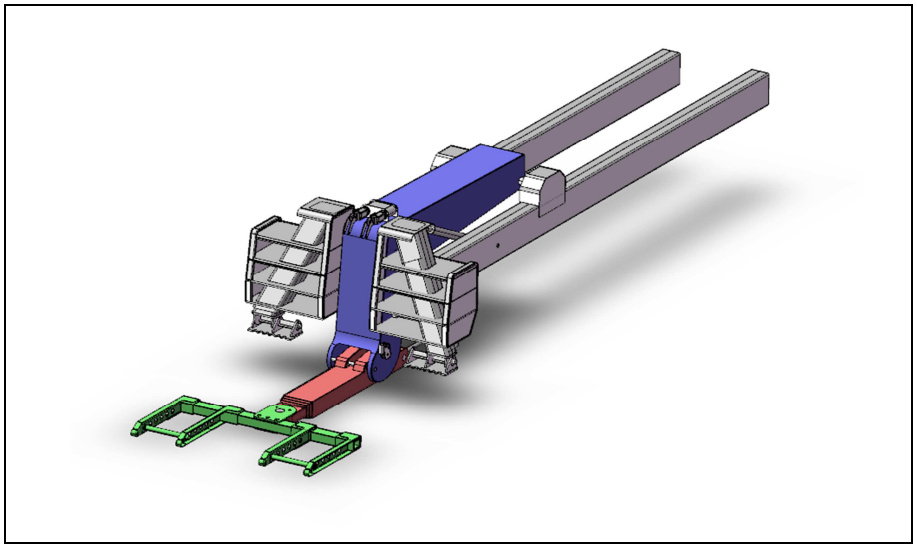

Fig. 2. Scheme of drawing arm with telescopic tube.

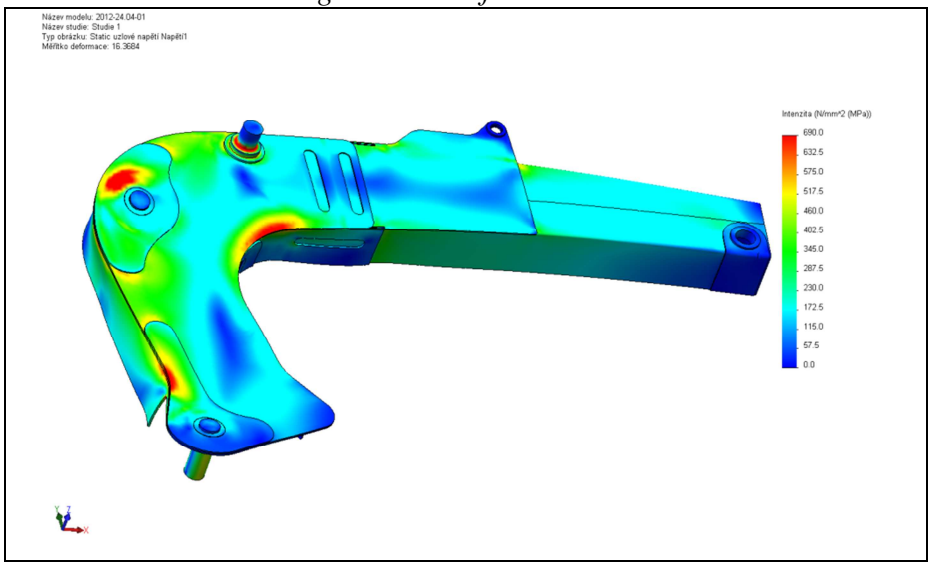

Fig. 3. Stress intensity of computational model of drawing arm.

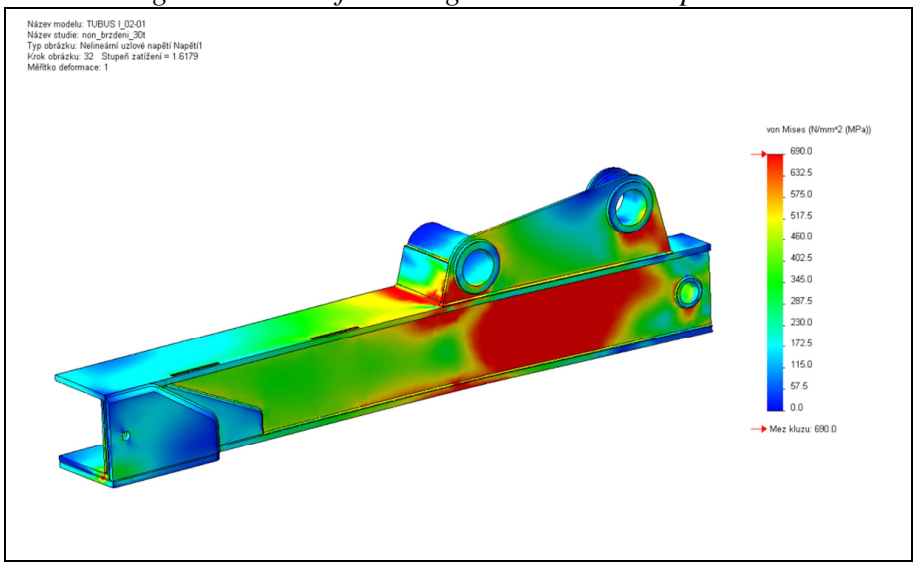

Fig. 4. Equivalent stress of computational model of drawing arm.

Overview of selected computational finite element analyses

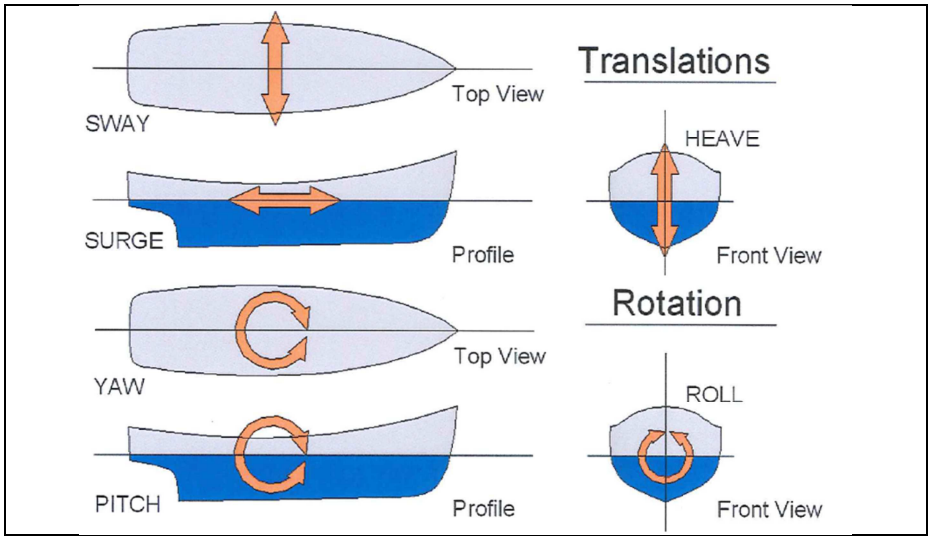

Fig. 1. Movement pattern of line ship with a steel structure suspended below deck 20 m above sea level.

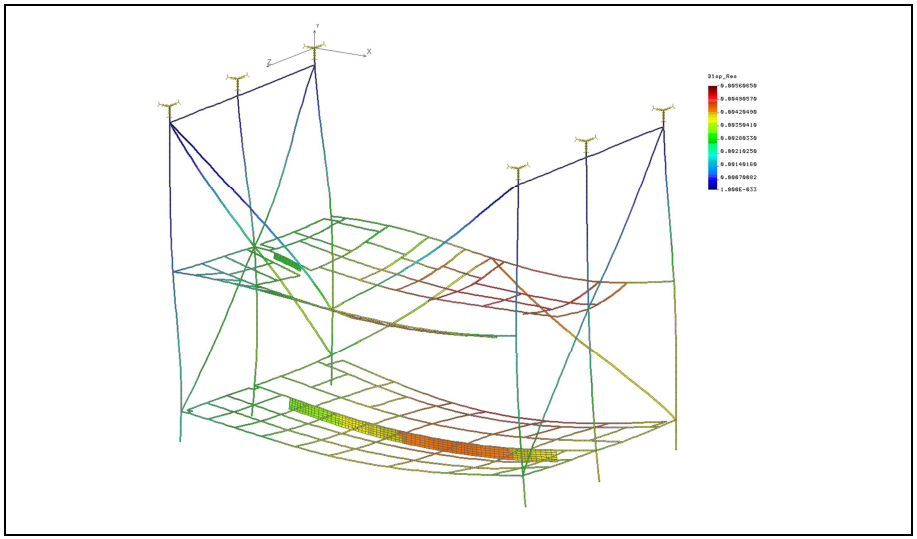

Fig. 2. Deformation of the total beam model of the structure due to quasi-static loading.

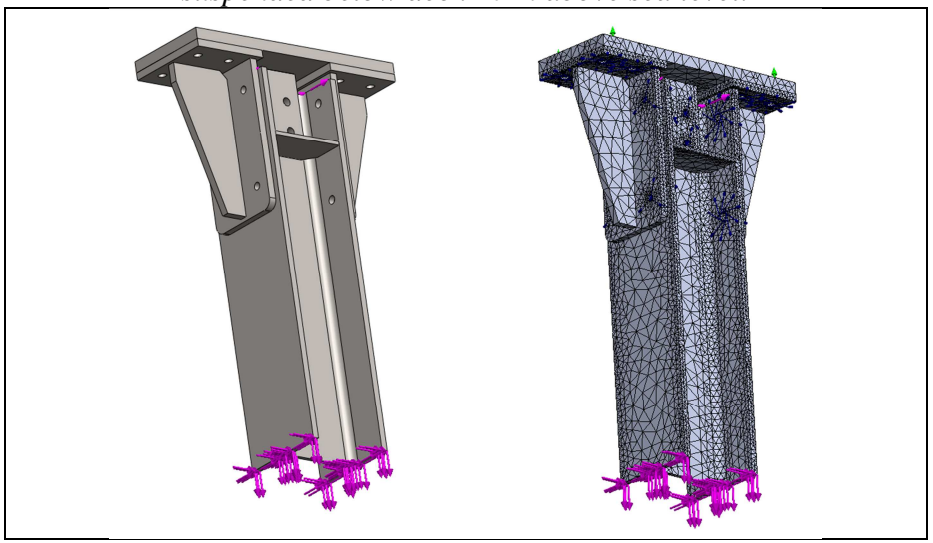

Fig. 3. One of computational models of beam joints.

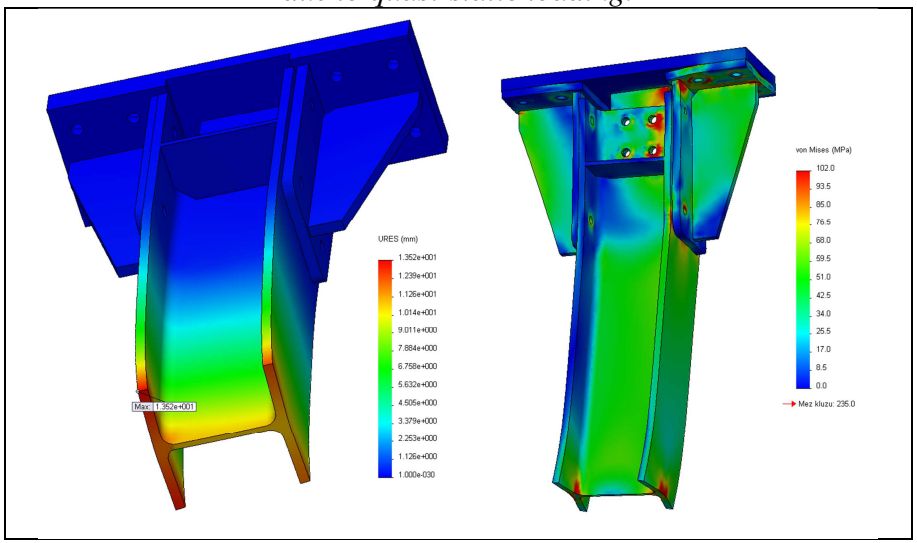

Fig. 4. Equivalent stress of model in limit state of plasticity.

ENERGY INDUSTRY

(CLASICAL, NUCLEAR)

Overview of selected computational finite element analyses

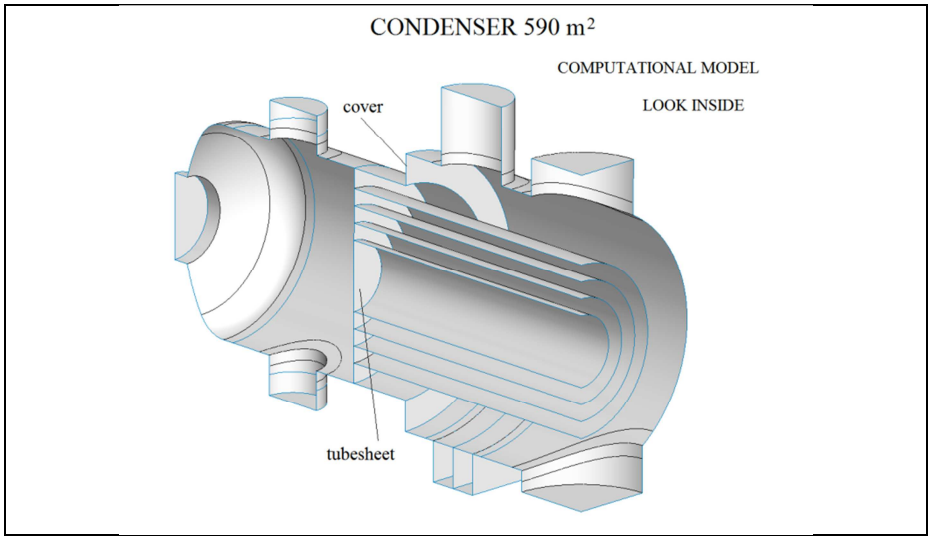

Fig. 1. Model of heat exchanger.

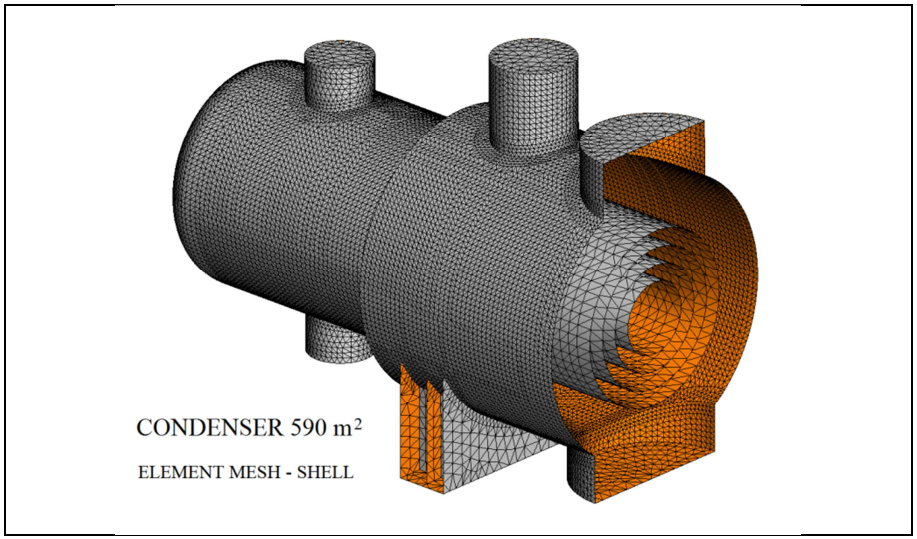

Fig. 2. Computational model of heat exchanger.

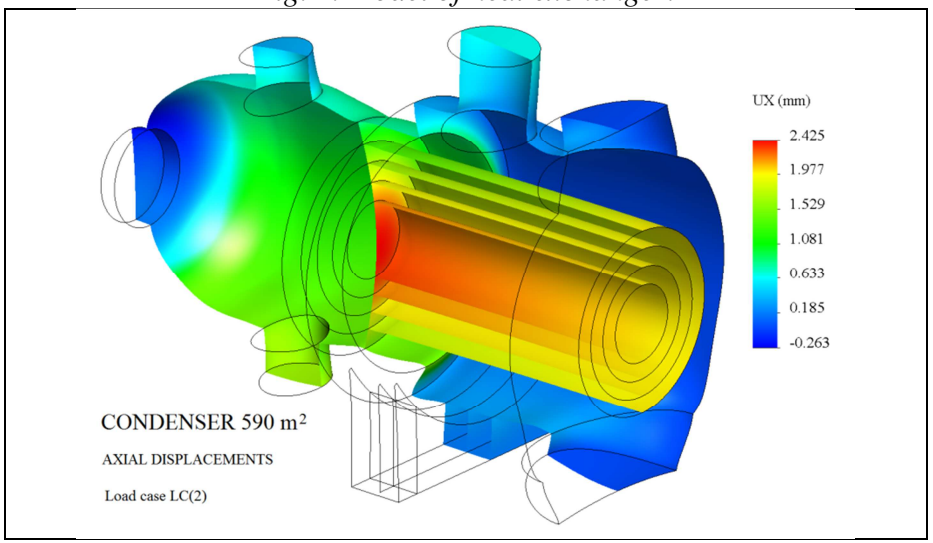

Fig. 3. Displacements due to internal pressure and thermal expansions.

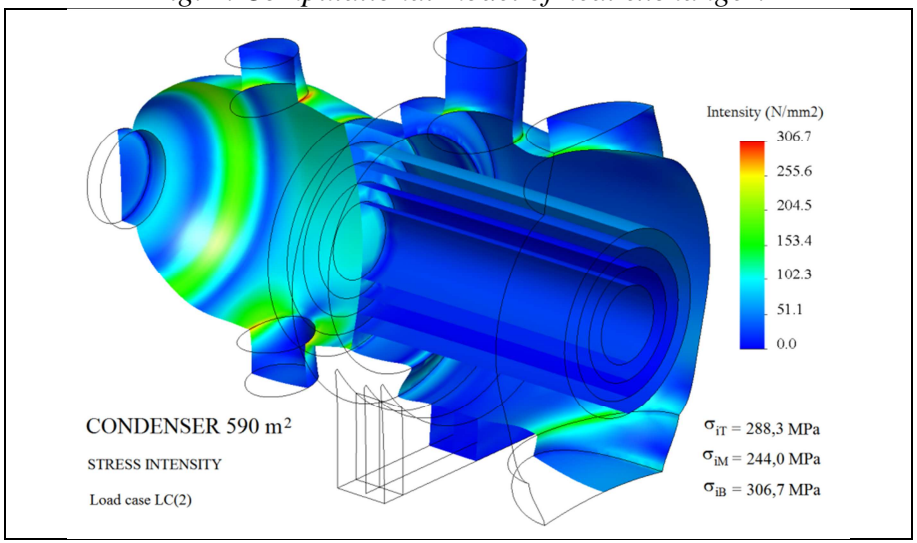

Fig. 4. Equivalent stresses due to internal pressure and thermal expansions.

Overview of selected computational finite element analyses

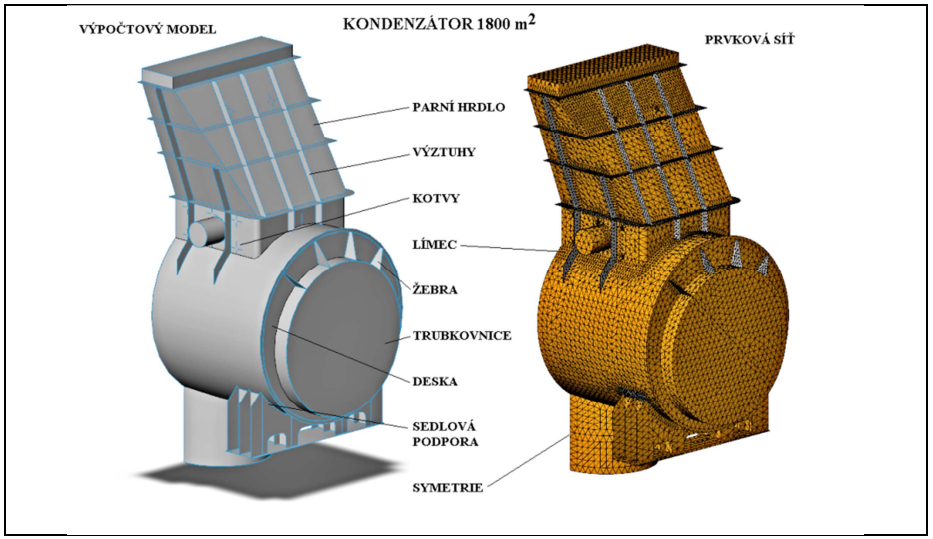

Fig. 1. Computational model of condenser with steam nozzle.

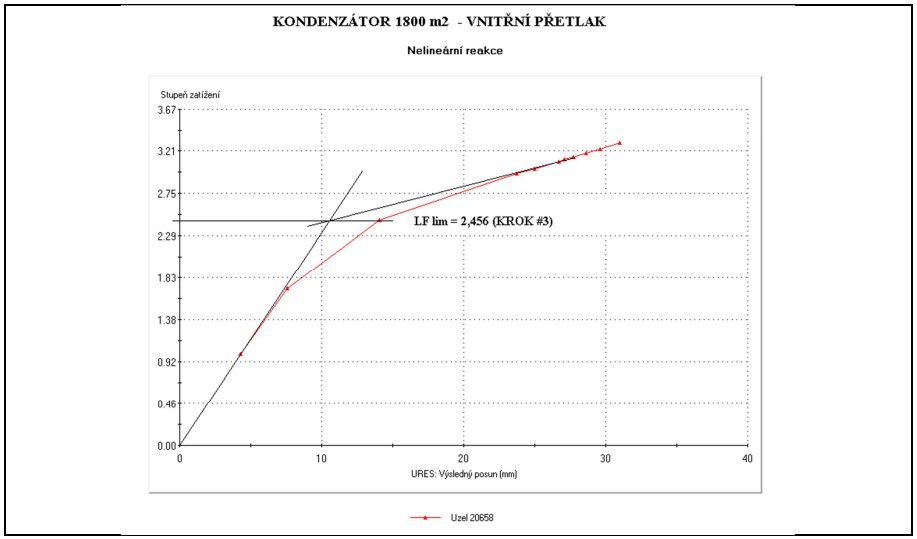

Fig. 2. Load curve due to inner pressure.

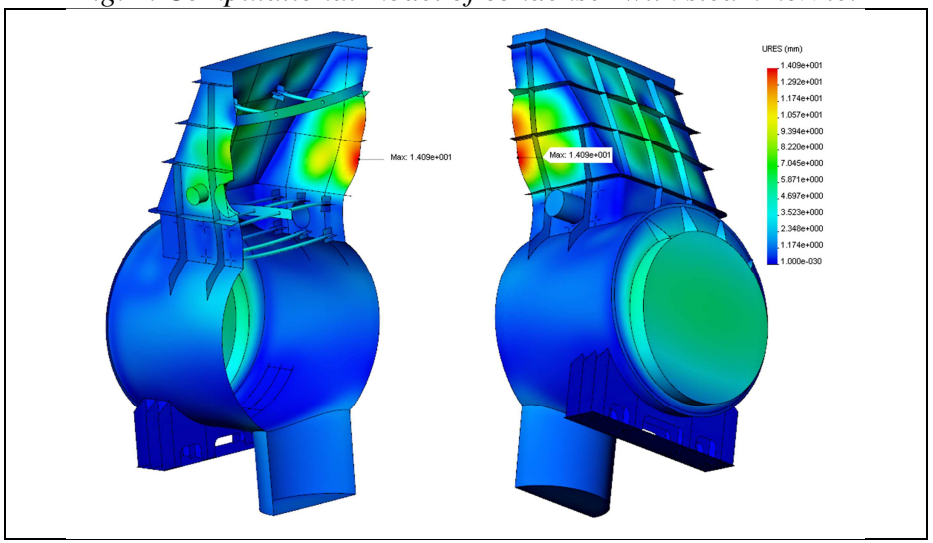

Fig. 3. Total displacements of model in limit state of plasticity.

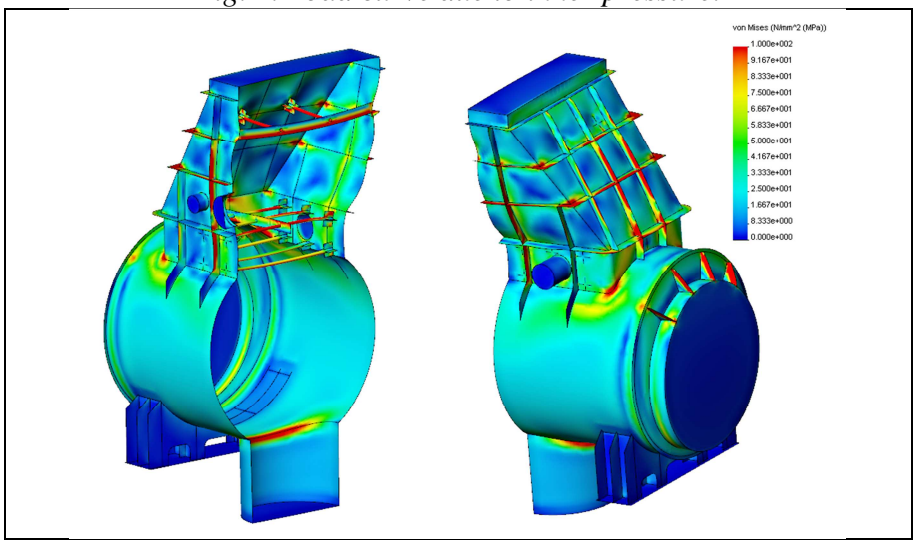

Fig. 4. Equivalent stress of model in limit state of plasticity MIDDLE surface.

Overview of selected computational finite element analyses

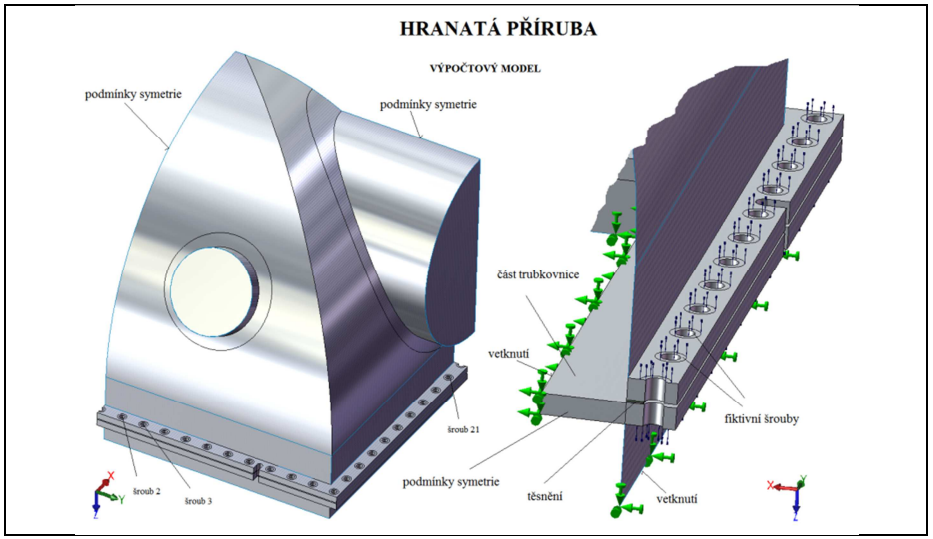

Fig. 1. Rectangular flange of water chamber of condenser.

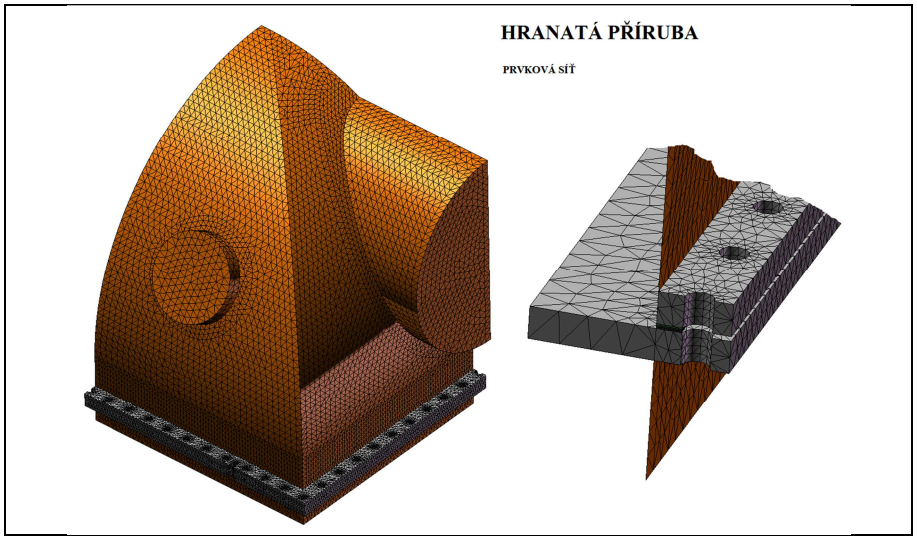

Fig. 2. Element mesh of flange and shell of water chamber.

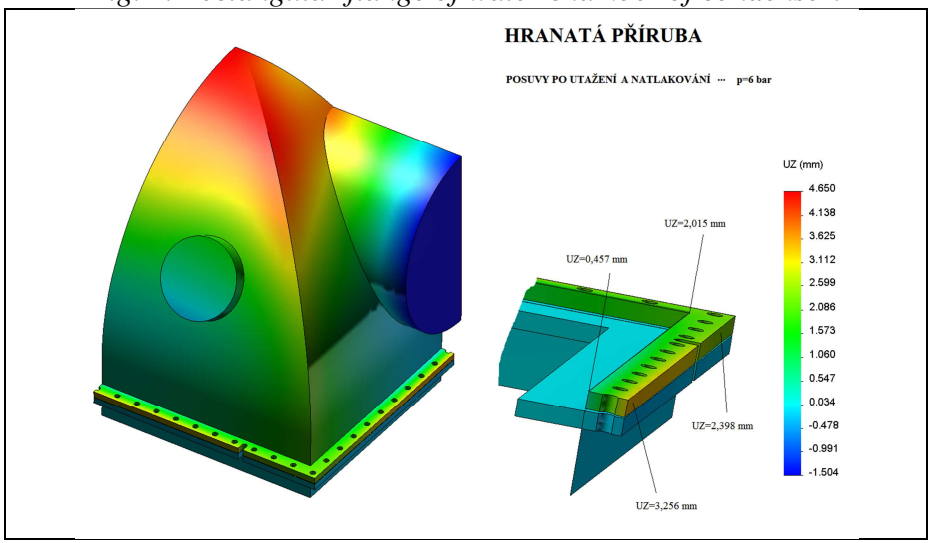

Fig. 3. Displacements of model after assembly and pressurization.

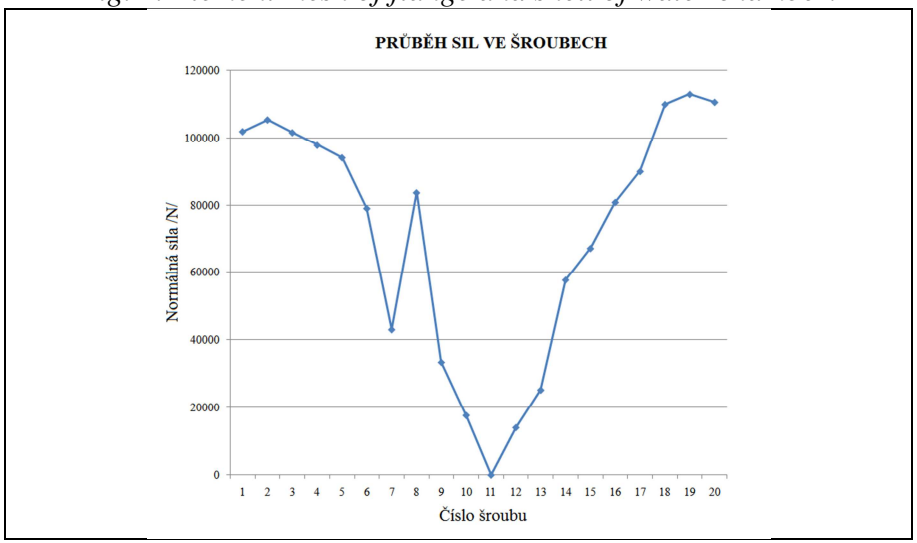

Fig. 4. Resulting force distribution in bolt of deformed flange.

Overview of selected computational finite element analyses

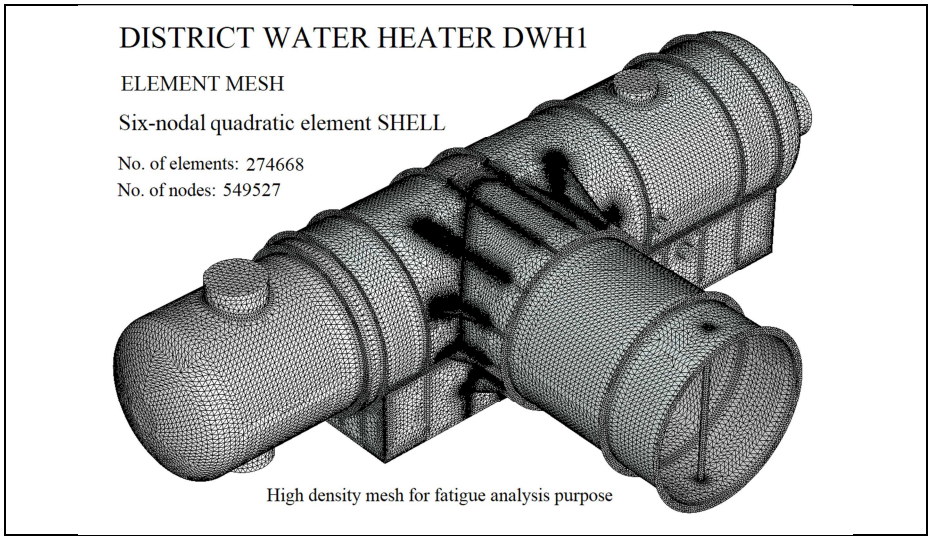

Fig. 1. Computational model with element mesh.

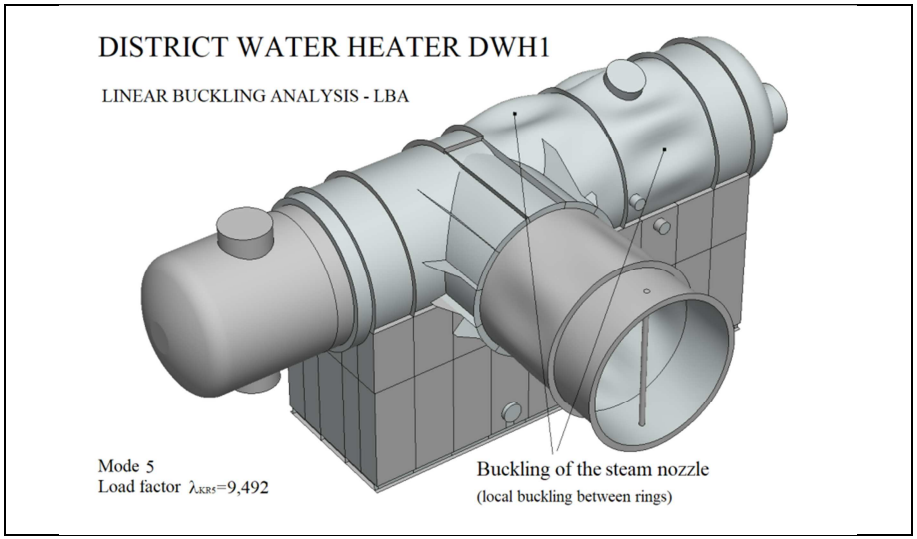

Fig. 2. Loss of stability (linear buckling).

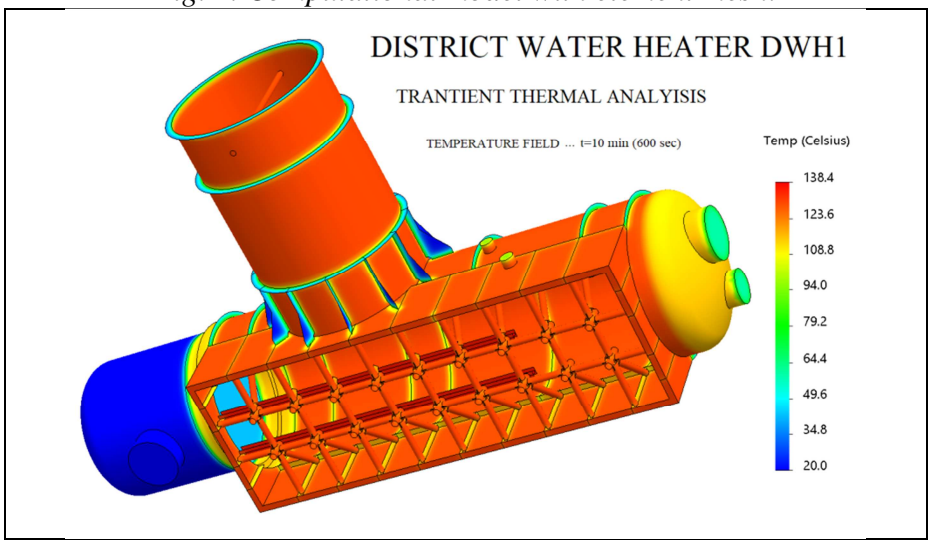

Fig. 3. Temperature field at time t=10 min.

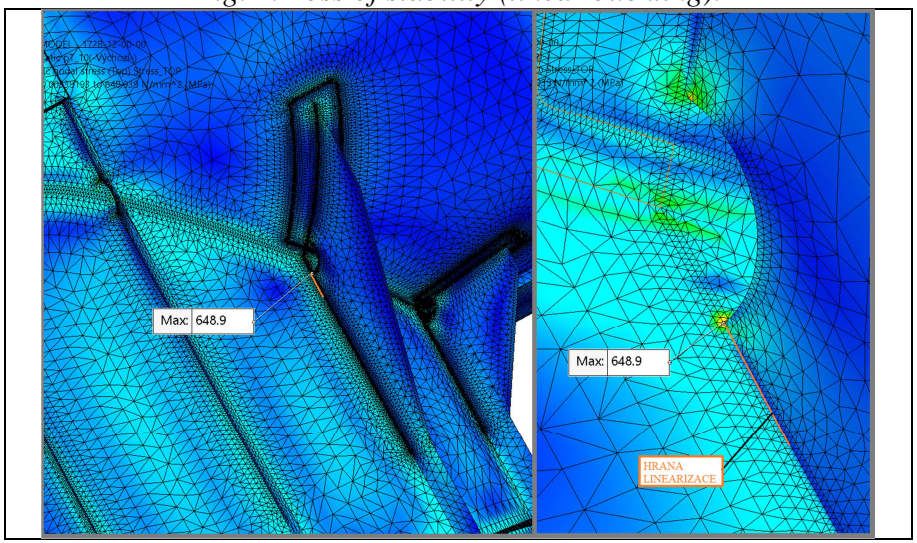

Fig. 4. Stress intensity for fatigue evaluation.

Overview of selected computational finite element analyses

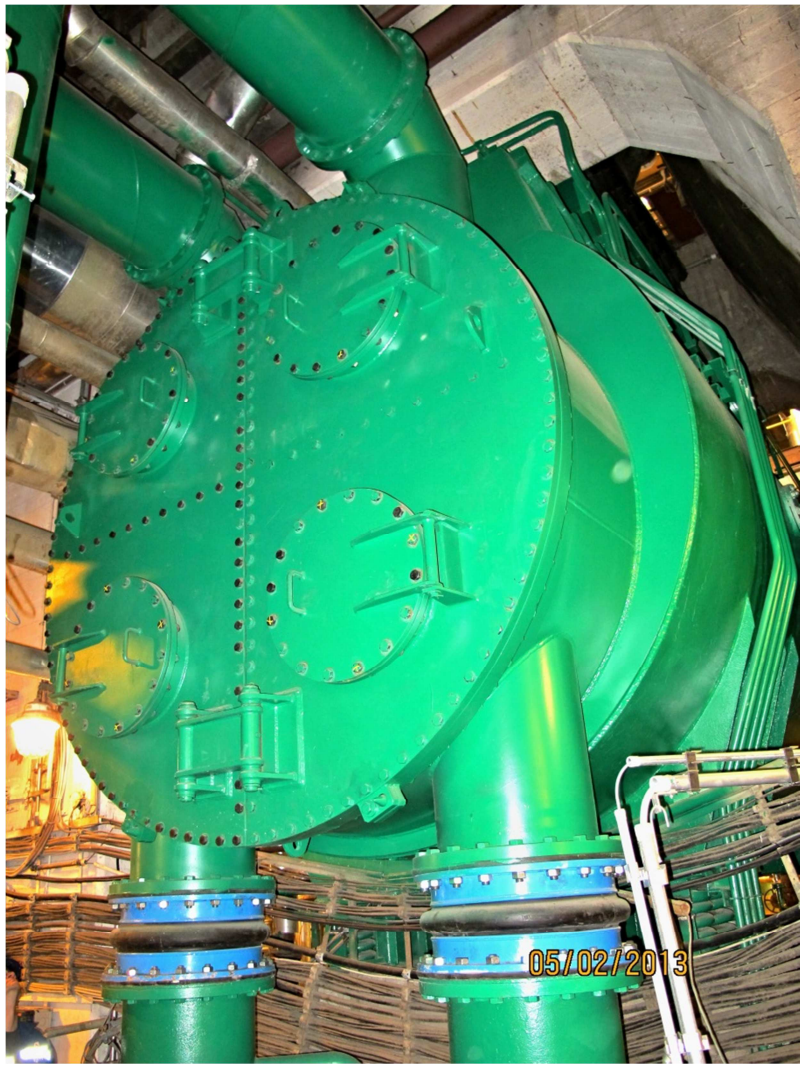

Fig. 1. Photo of gate of condenser.

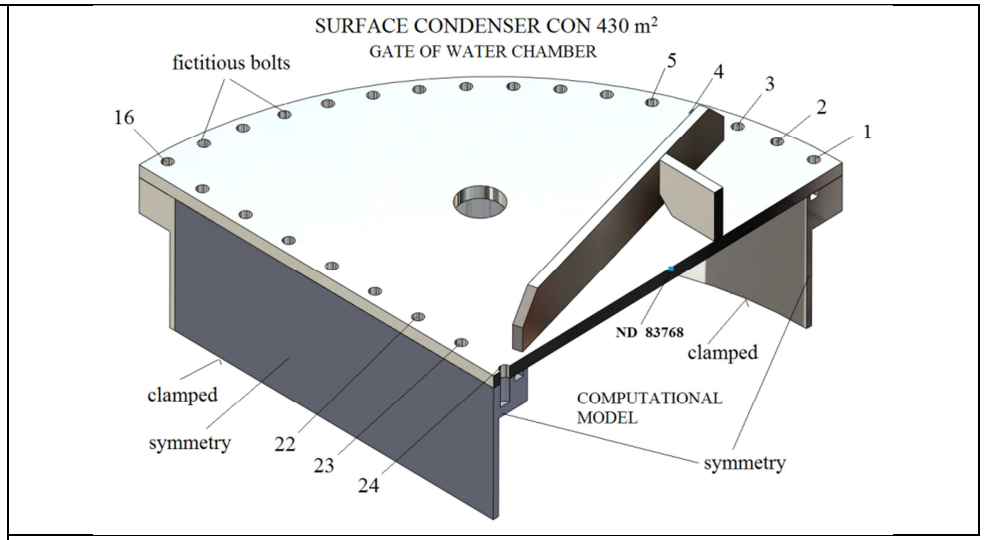

Fig. 2. Computational model.

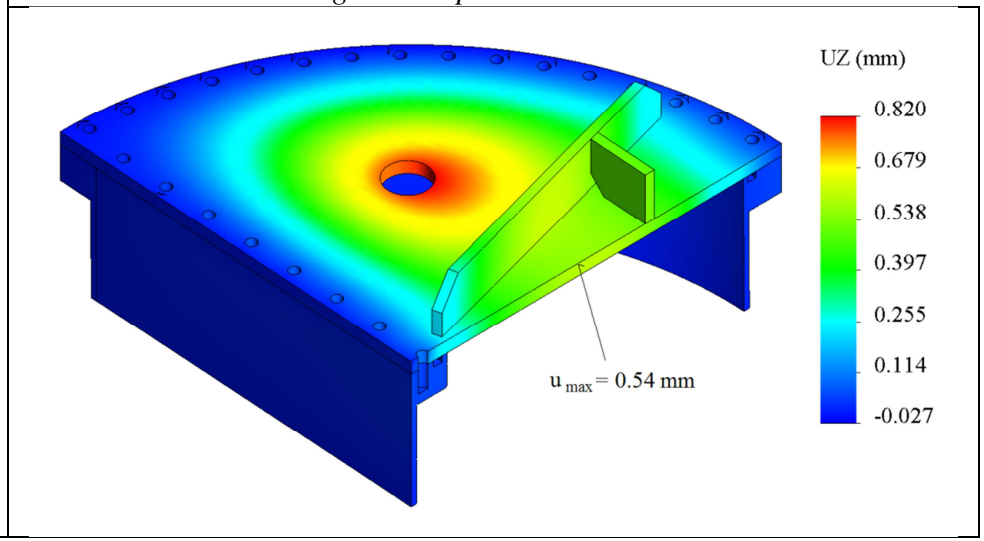

Fig. 3. Deflection due to pressure.

Overview of selected computational finite element analyses

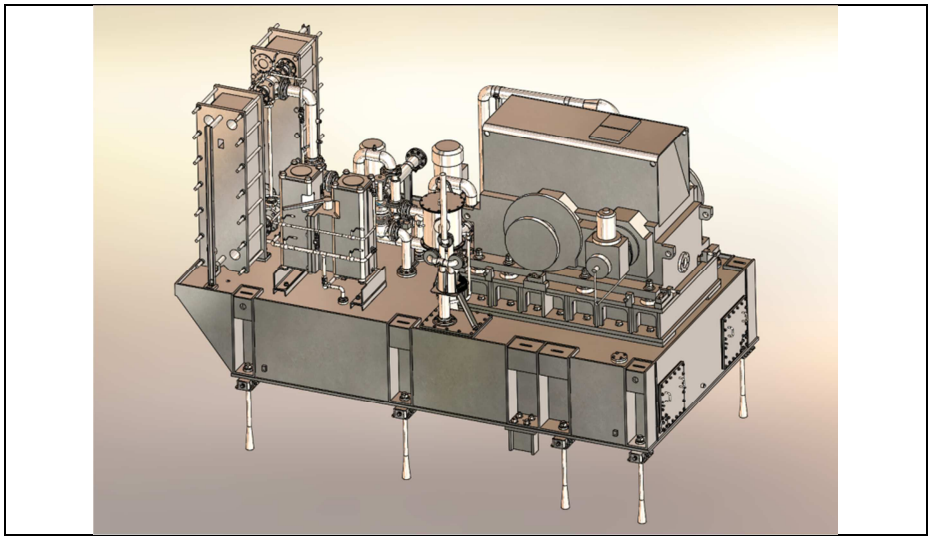

Fig. 1. Steel frame under the gear box (3D-model).

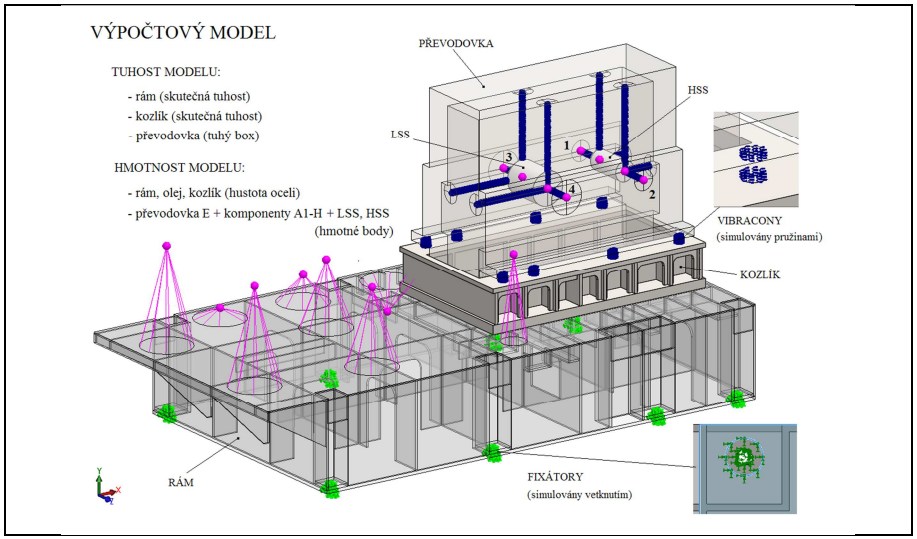

Fig. 2. Computational model of the frame.

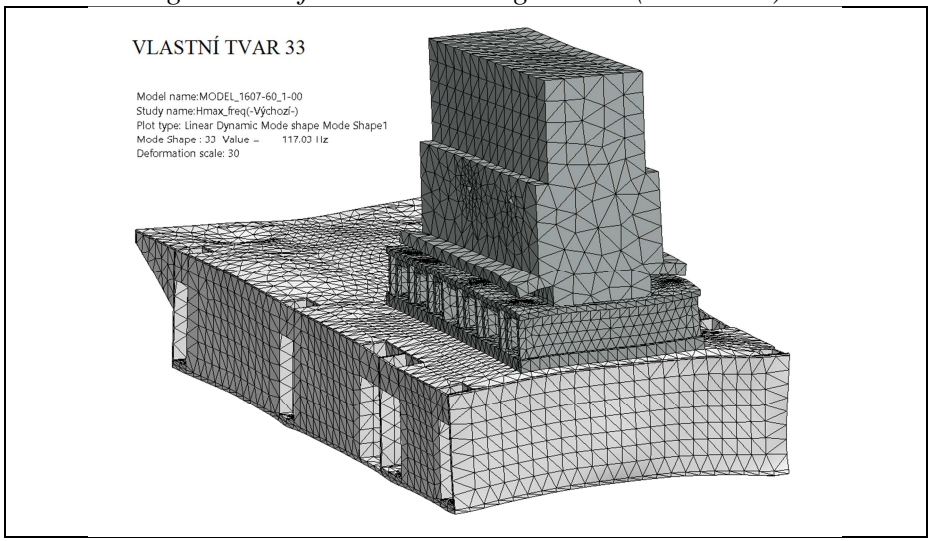

Fig. 3. Modal analysis - the most significant mode (f_{033}=117.03 Hz).

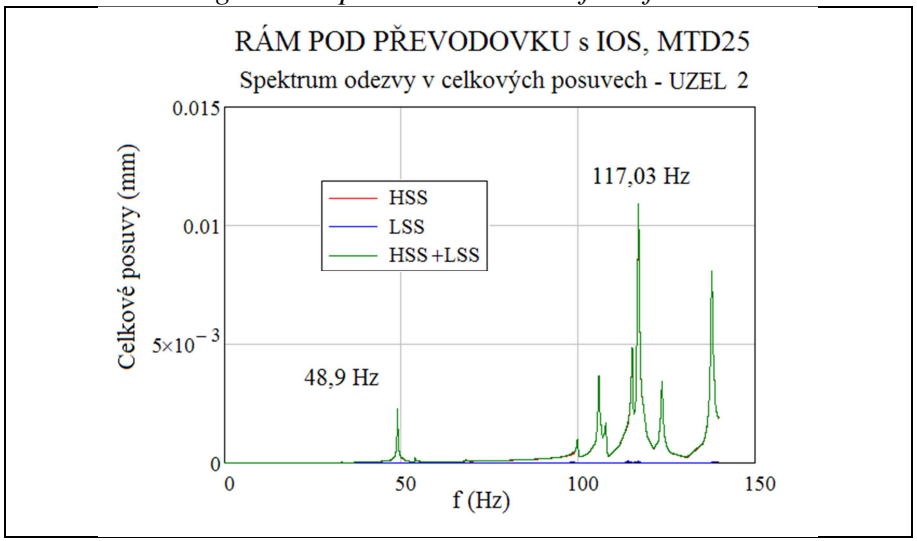

Fig. 4. Harmonic analysis – response spectrum in point 2.

Overview of selected computational finite element analyses

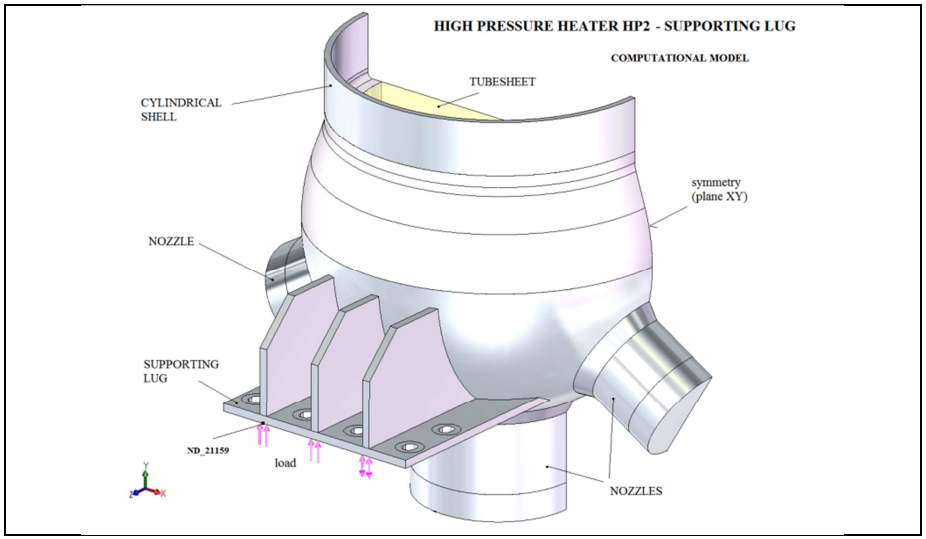

Fig. 1. Model of lower part of high pressure heater.

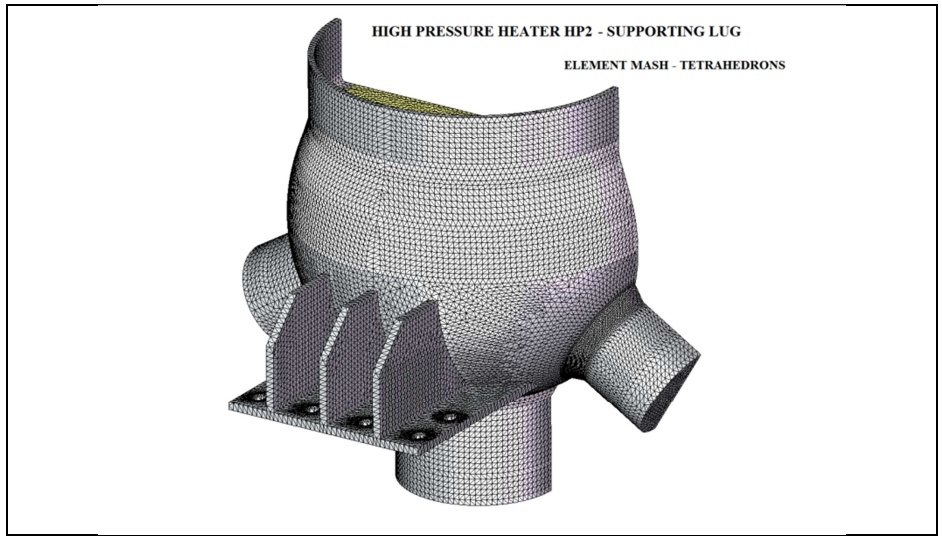

Fig. 2. Computational model loaded by internal pressure and seismicity.

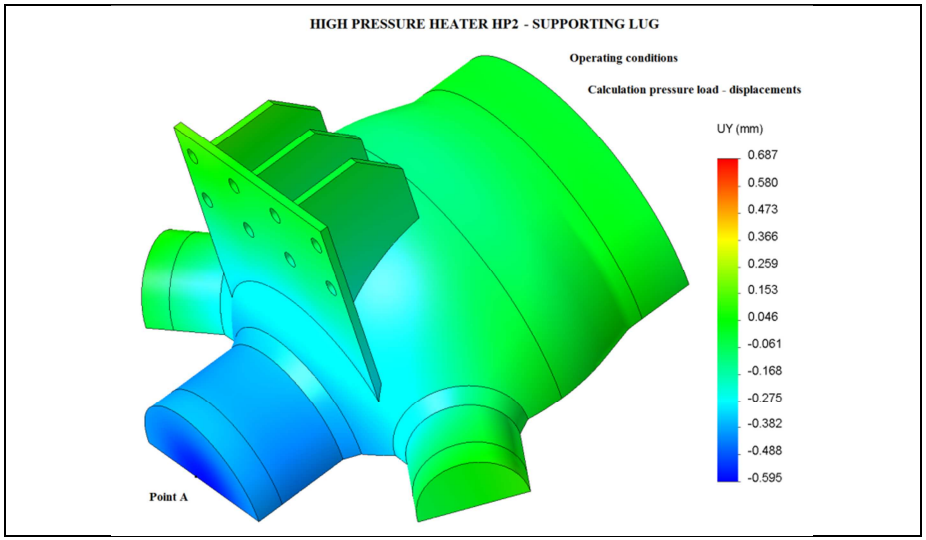

Fig. 3. Vertical displacements of model in limit state of plasticity.

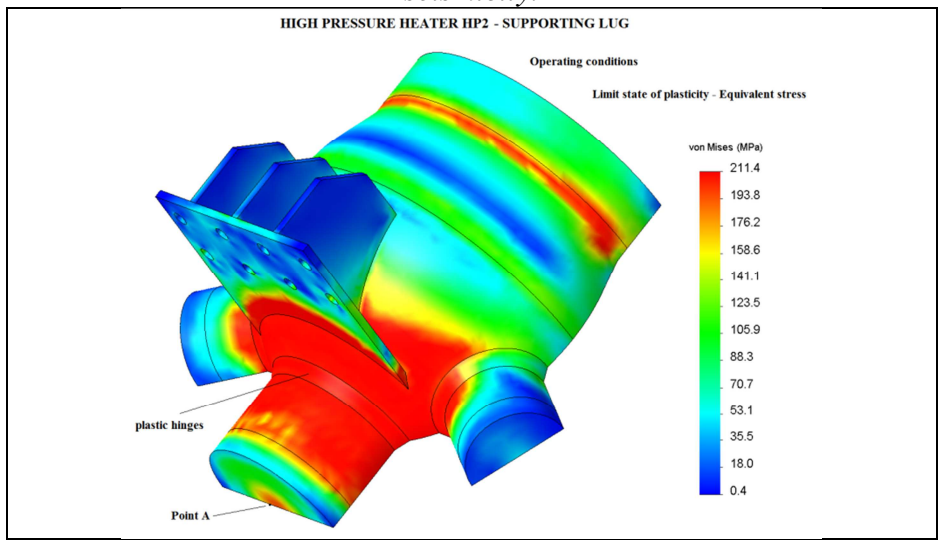

Fig. 4. Equivalent stress of model in limit state of plasticity.

Overview of selected computational finite element analyses

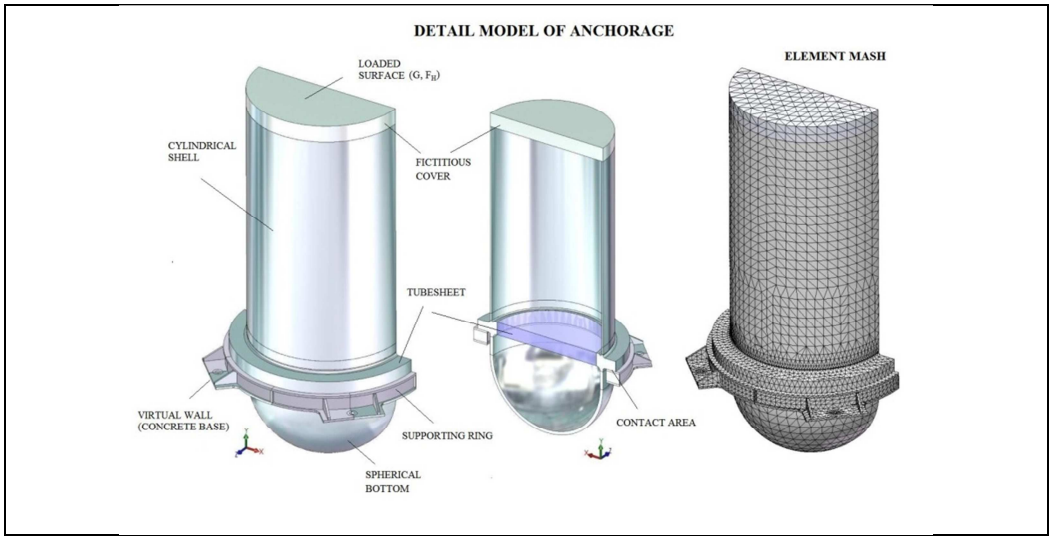

Fig. 1. Lower part of high pressure heater HPH at atomic plant (seismic analysis).

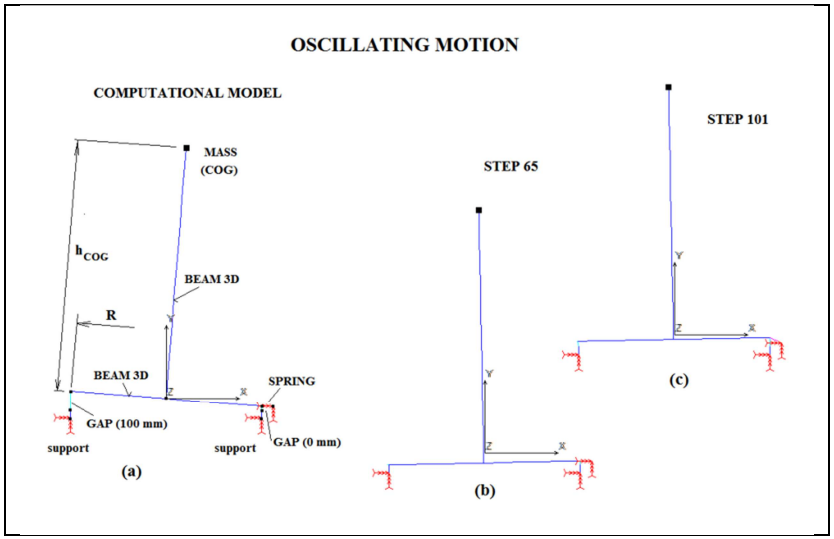

Fig. 2. The swinging motion - nonlinear dynamic analysis of simplified beam model.

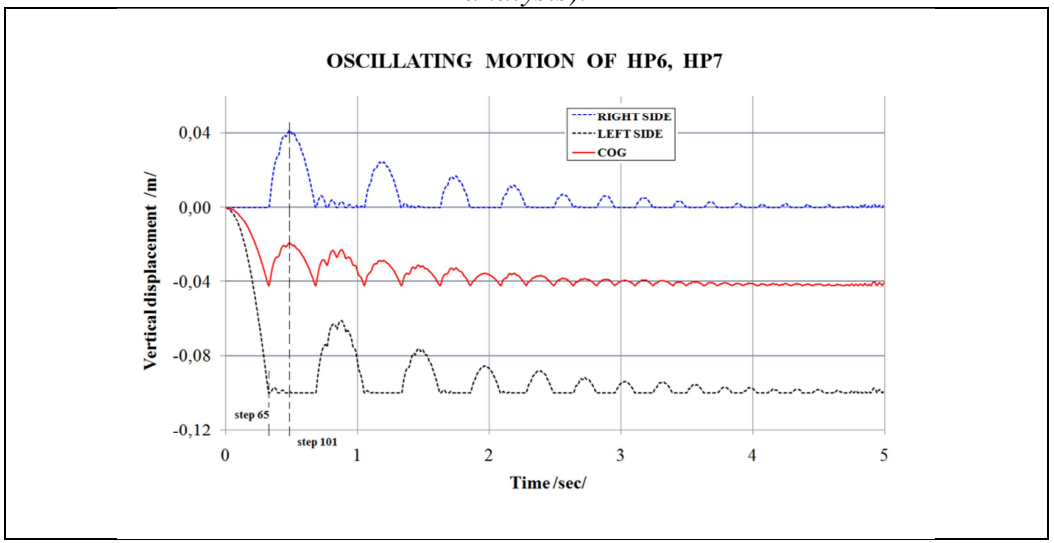

Fig. 3. Displacements of heater in COG and support.

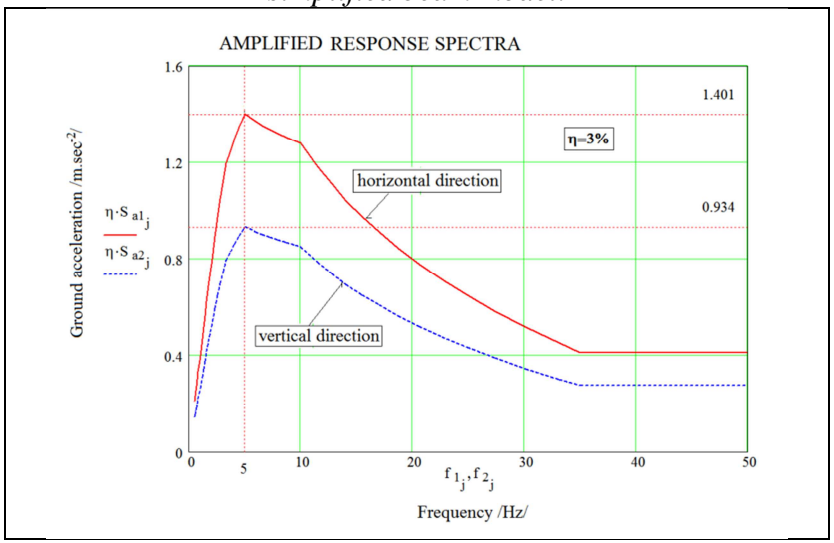

Fig. 4. Design base response spectrum.

Overview of selected computational finite element analyses

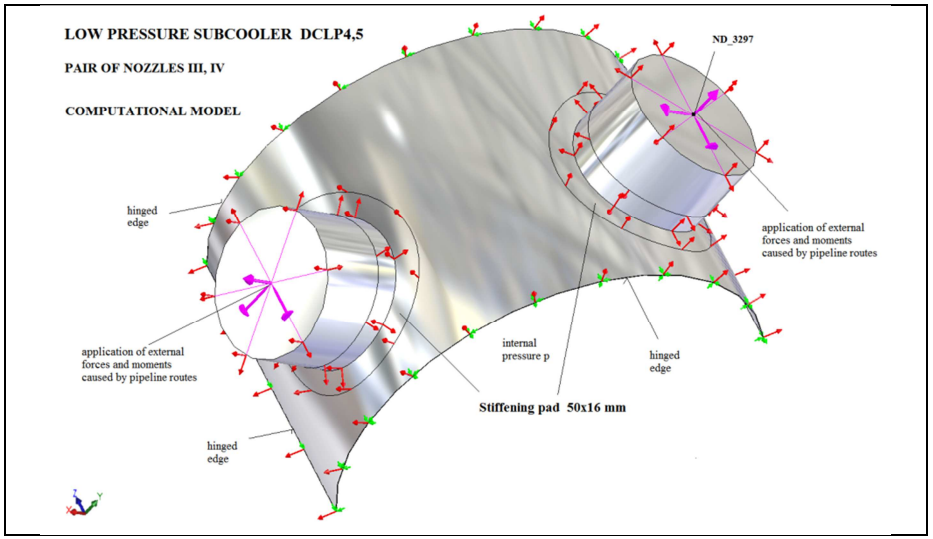

Fig. 1. Nozzles of low pressure subcooler in atomic plant.

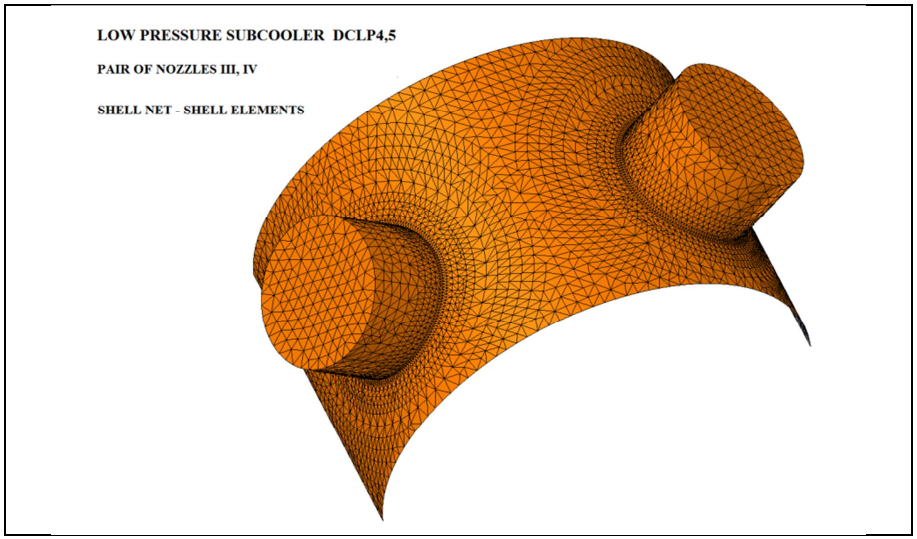

Fig. 2. Computational model with shell element mesh.

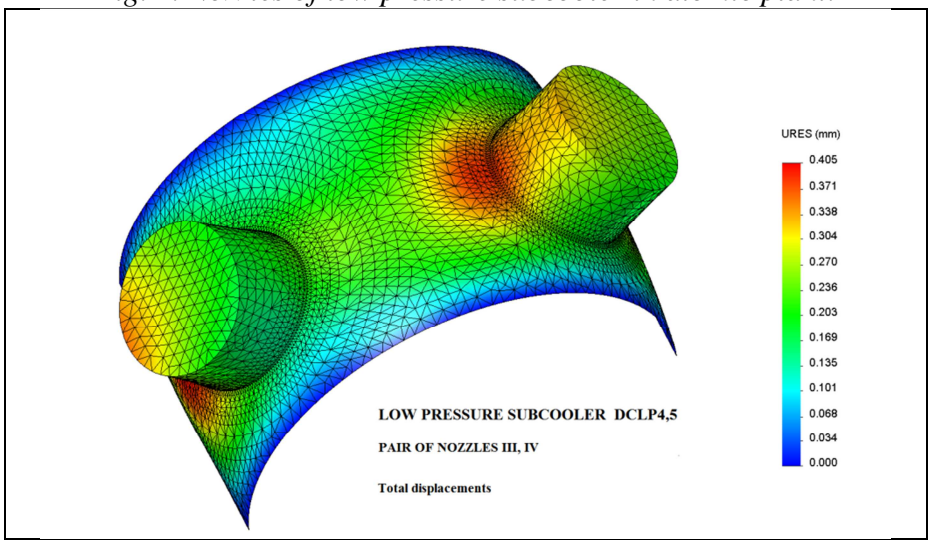

Fig. 3. Total displacements in limit state of plasticity.

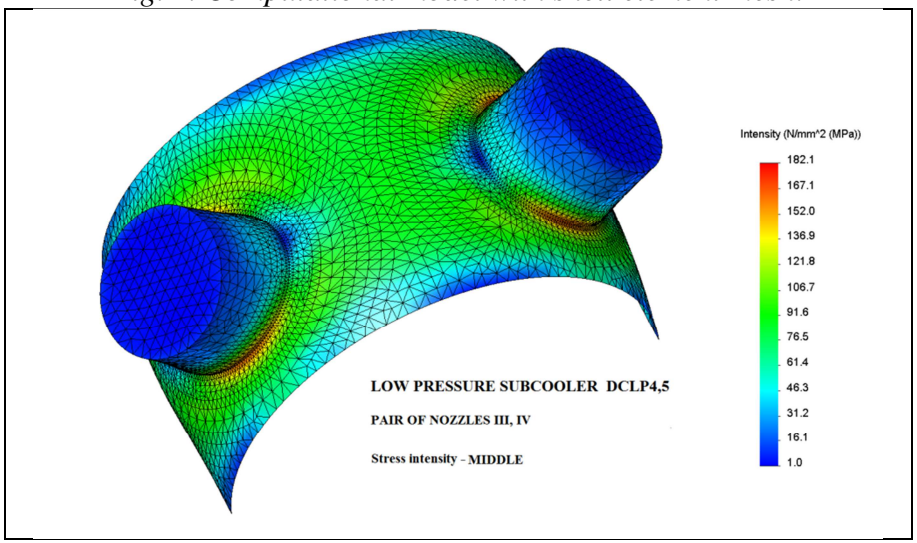

Fig. 4. Stress intensity in limit state of plasticity – MIDSURFACE.

Overview of selected computational finite element analyses

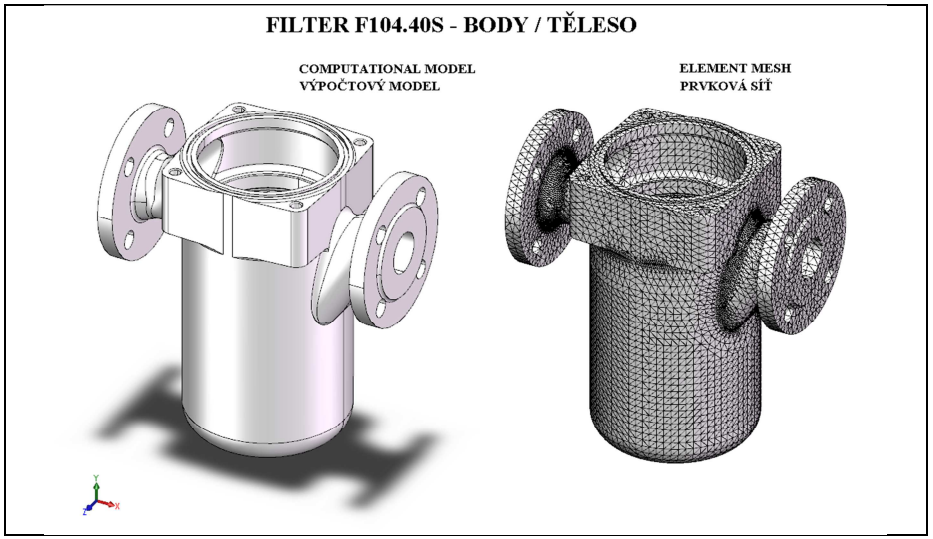

Fig. 1. Strength check of body of filter F104.40S in atomic plant.

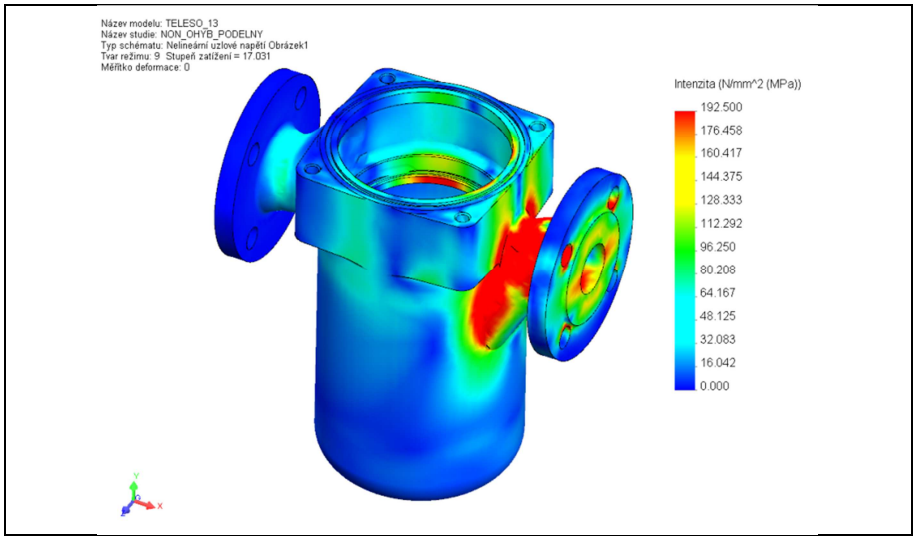

Fig. 2. Limit state of plasticity due to horizontal force.

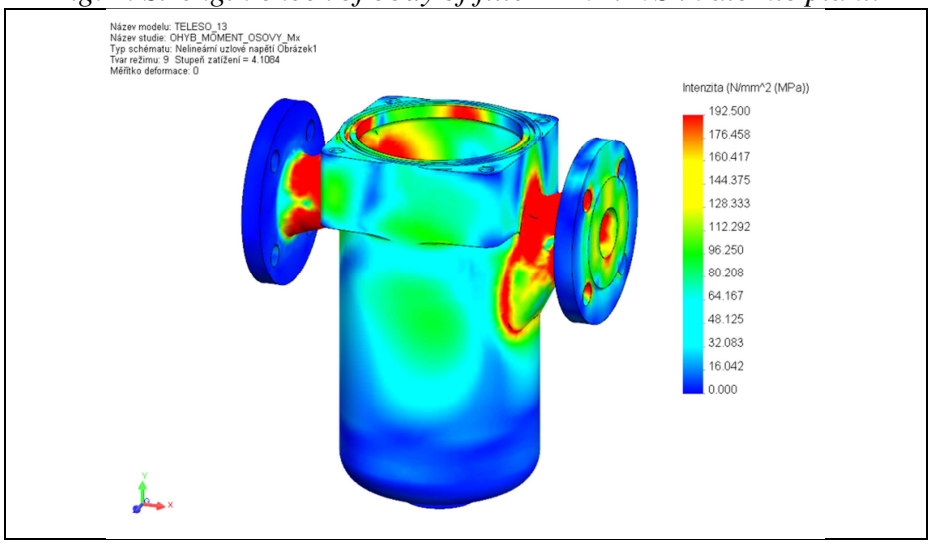

Fig. 3. Limit state of plasticity due to bending moment.

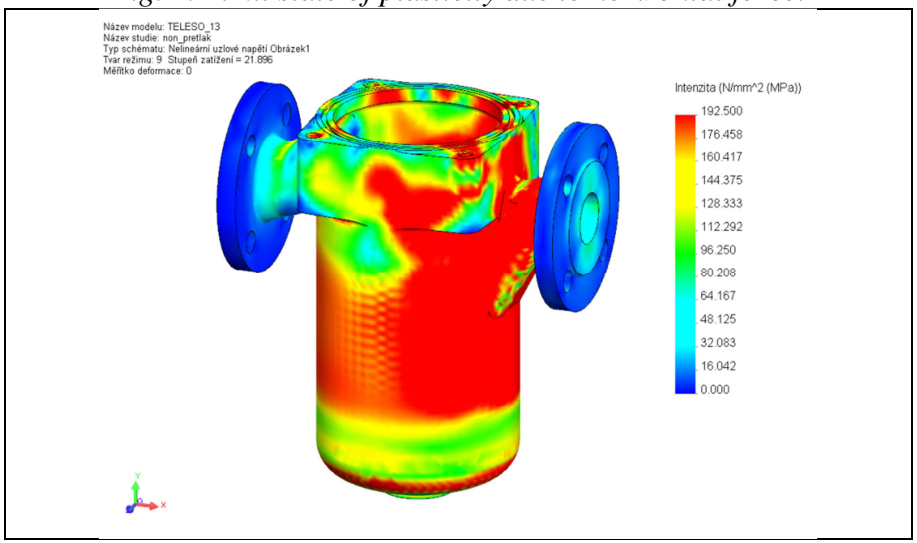

Fig. 4. Limit state of plasticity due to internal pressure.

Overview of selected computational finite element analyses

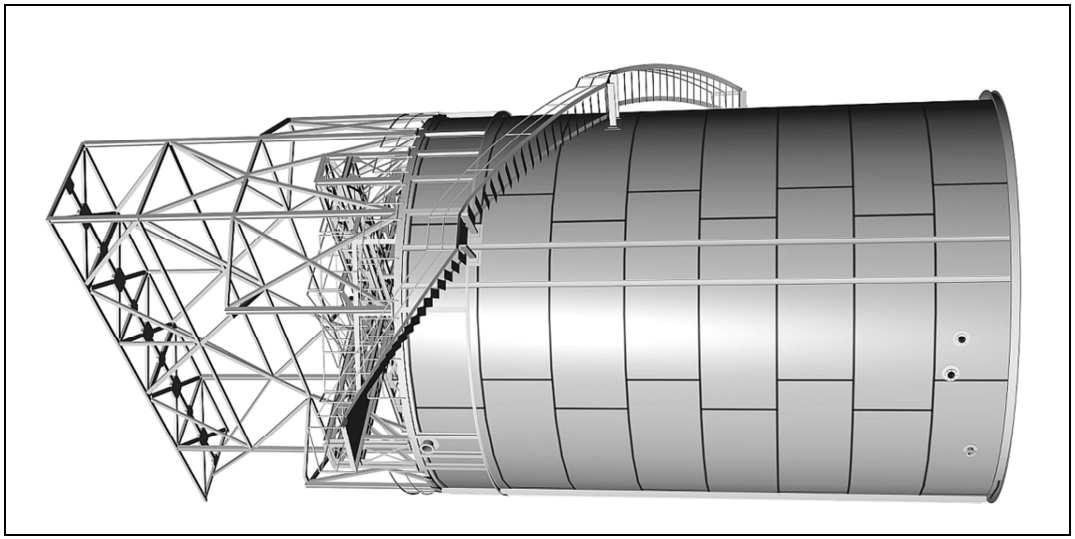

Fig. 1. Desulphurization tank (operation, wind, seismicity).

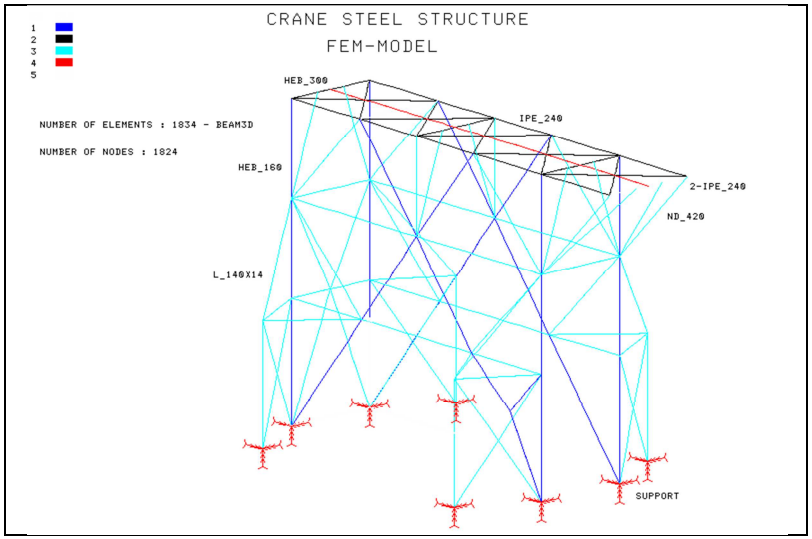

Fig. 2. Crane track on roof of tank.

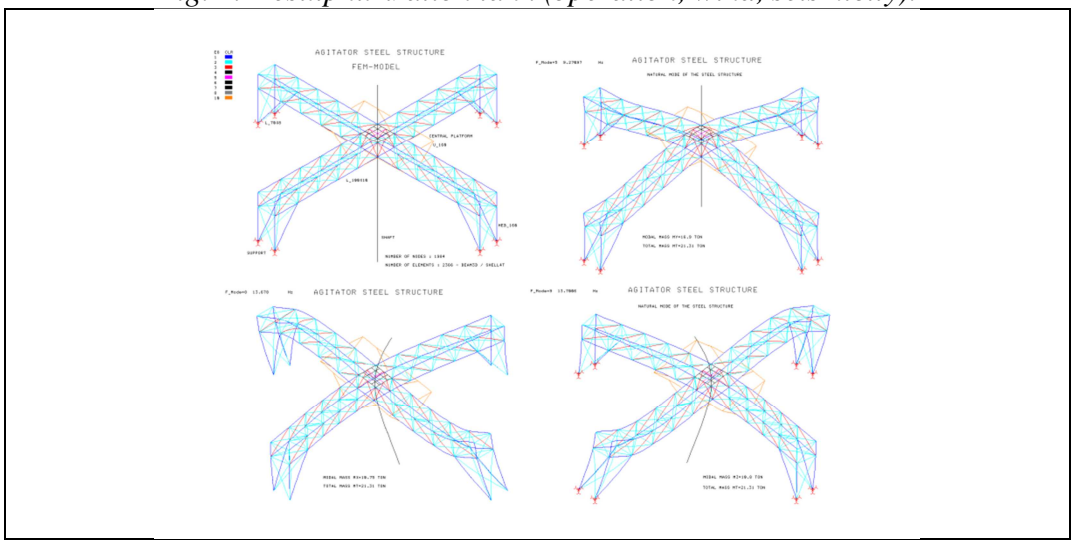

Fig. 3. Lowest natural shapes of structure with mixing device.

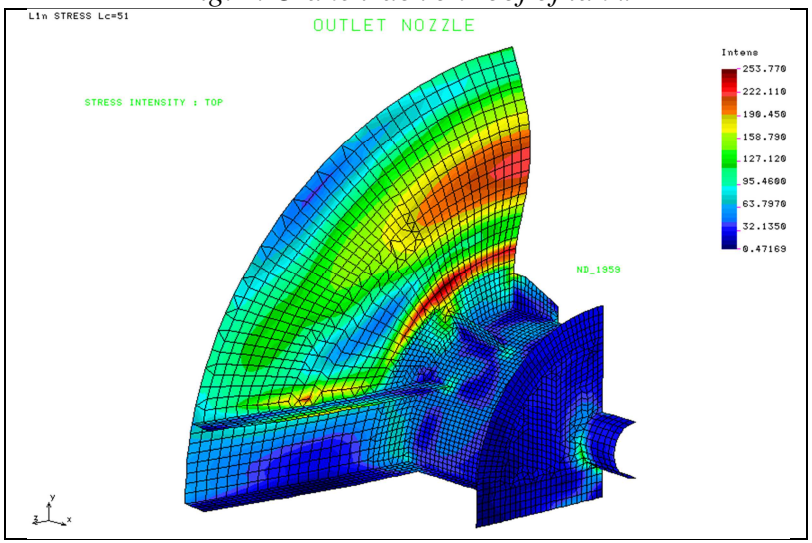

Fig. 4. Special output nozzle at bottom of tank.

Overview of selected computational finite element analyses

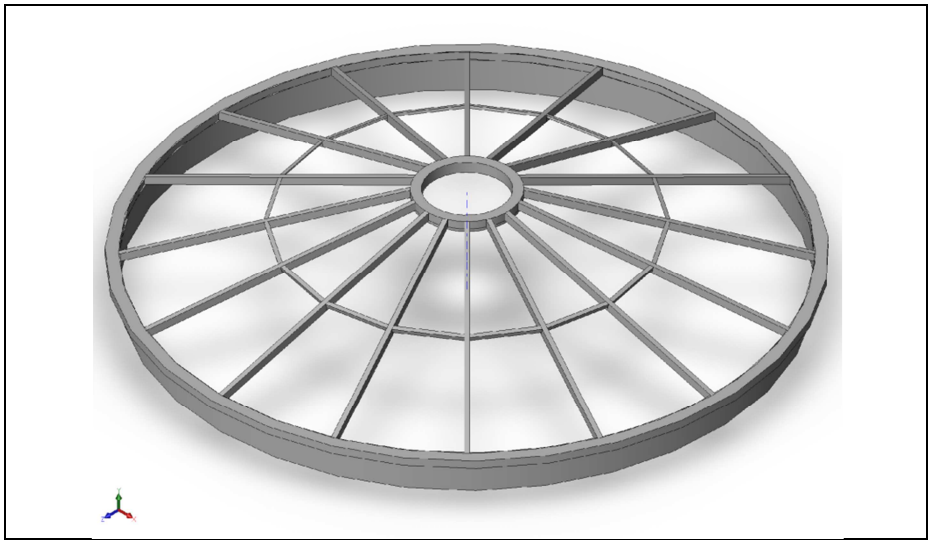

Fig. 1. Model of conical frame roof of vertical tank.

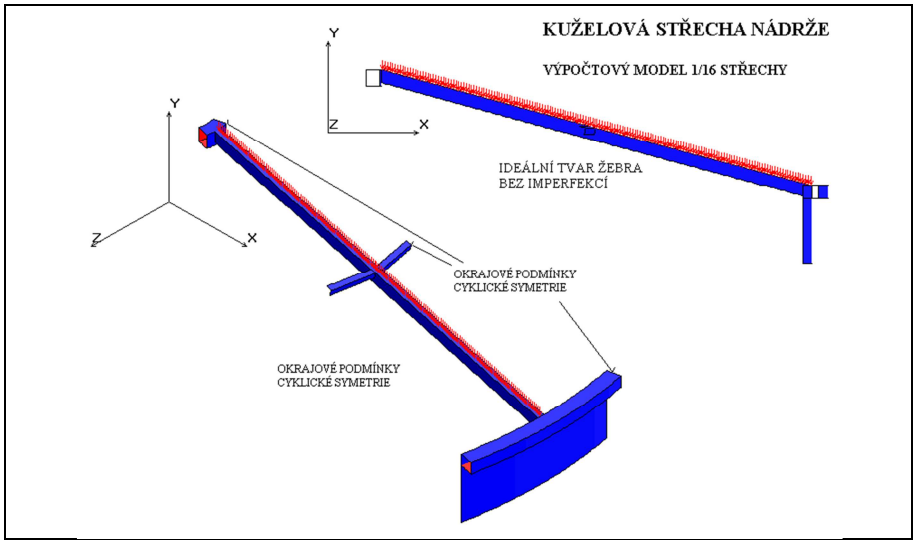

Fig. 2. Computational model with one meridian stringer.

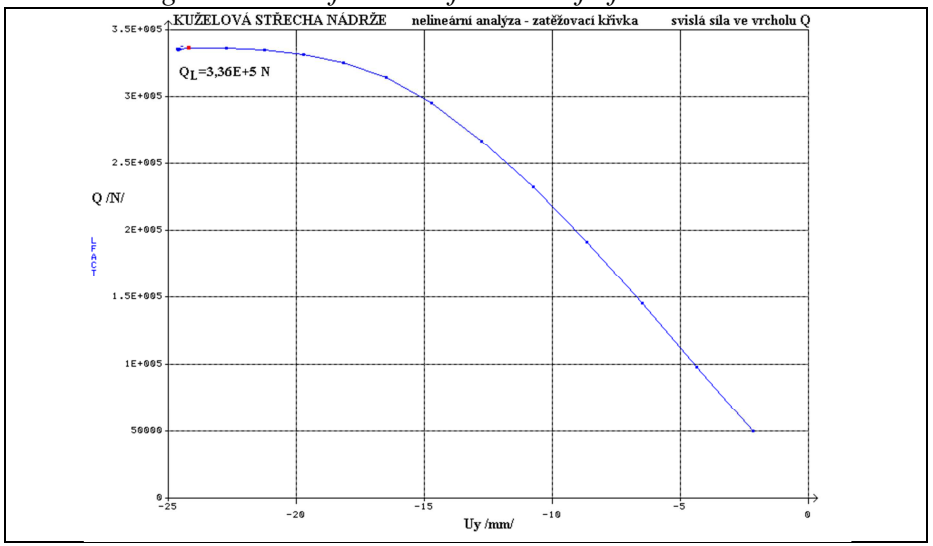

Fig. 3. Load curve of computational model – vertical force.

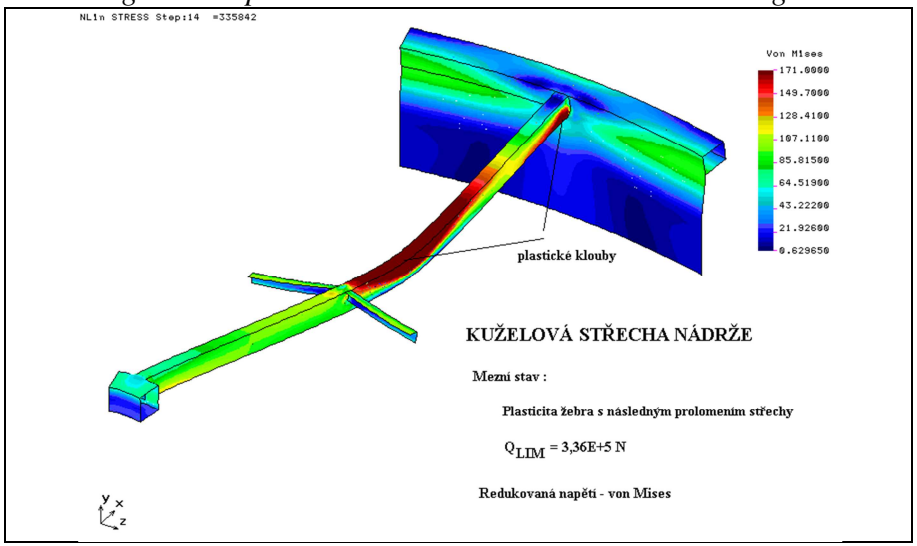

Fig. 4. Plastic snap-through into inverse position.

Overview of selected computational finite element analyses

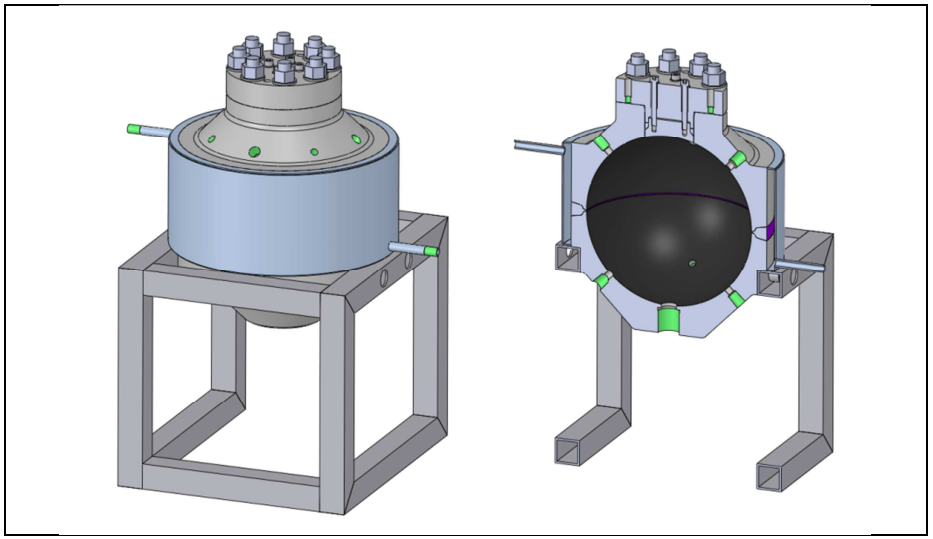

Fig. 1. Model of test equipment – explosion chamber.

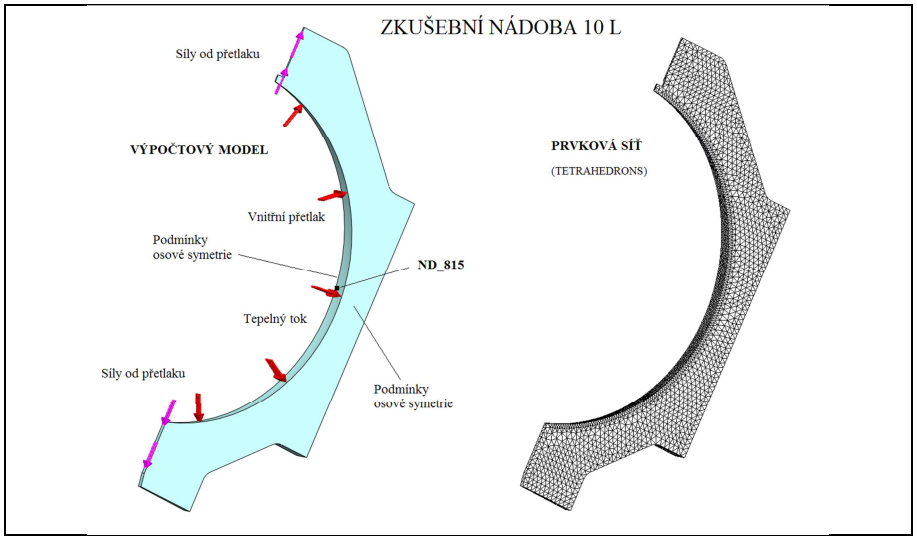

Fig. 2. Computational model of spherical pressure vessel.

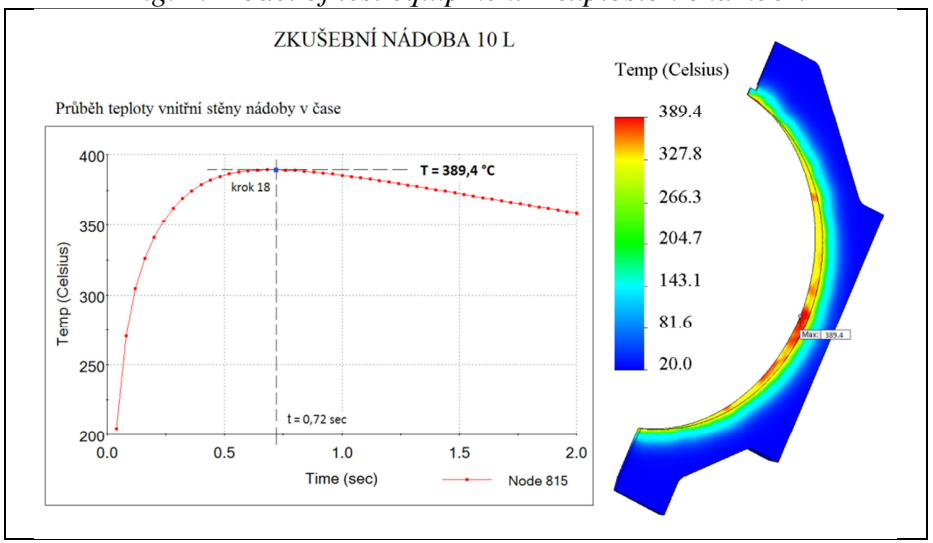

Fig. 3. Thermal analysis of wall – explosion inside vessel.

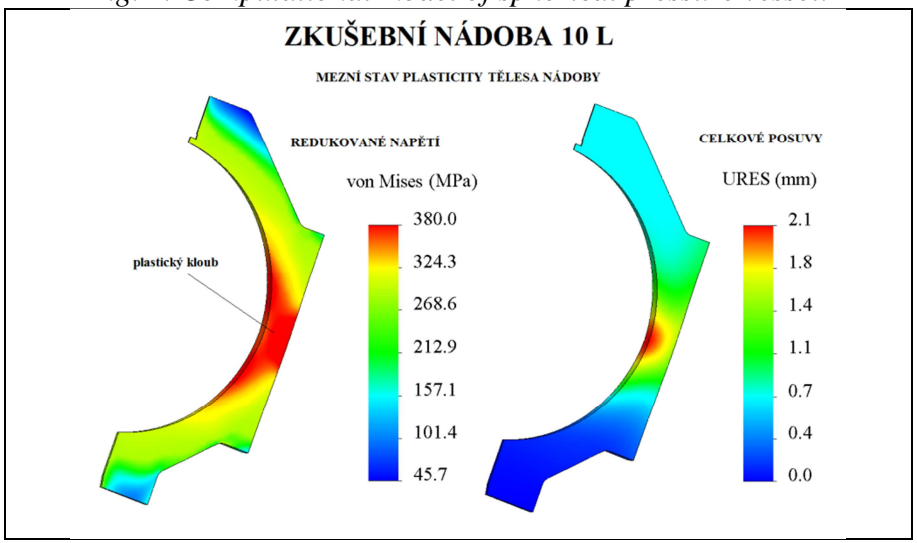

Fig. 4. Limit state of plasticity – strength analysis.

Overview of selected computational finite element analyses

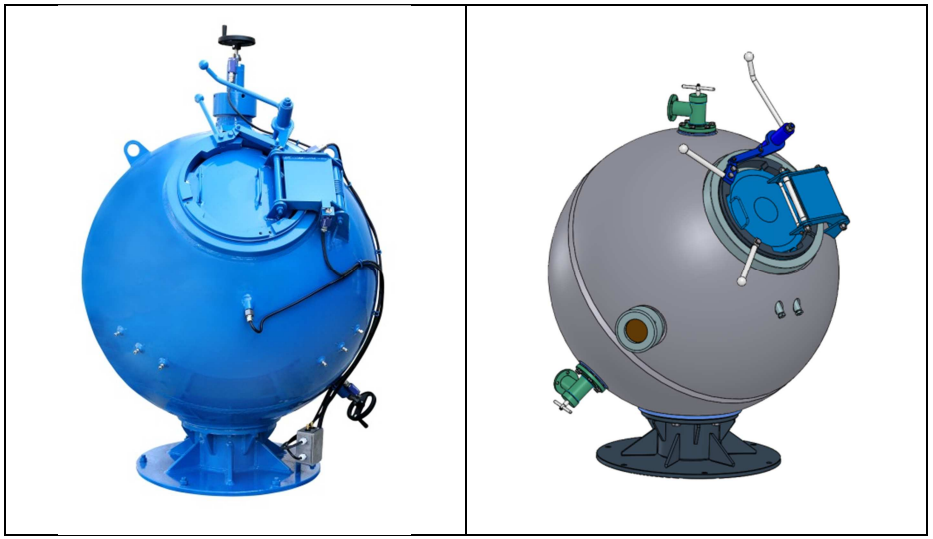

Fig. 1. Model of test equipment – detonation chamber.

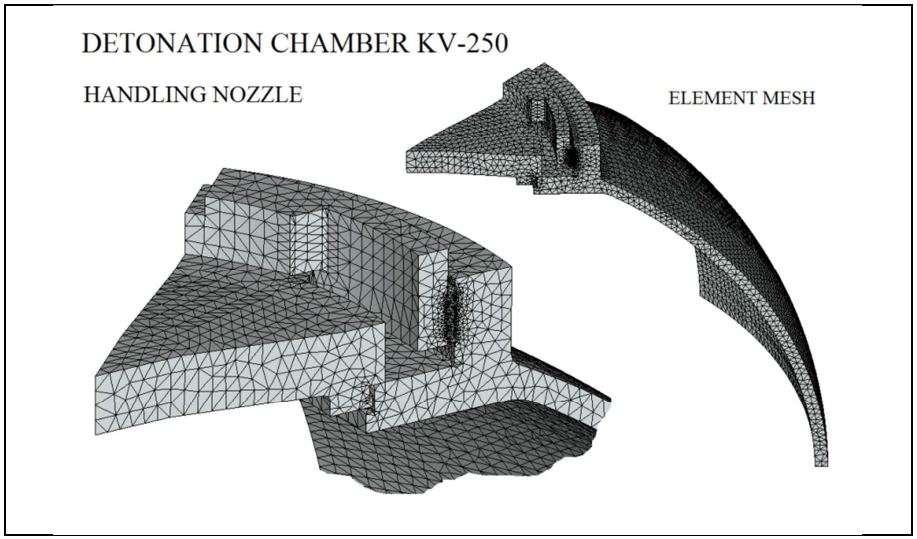

Fig. 2. Computational model of bayonet flange.

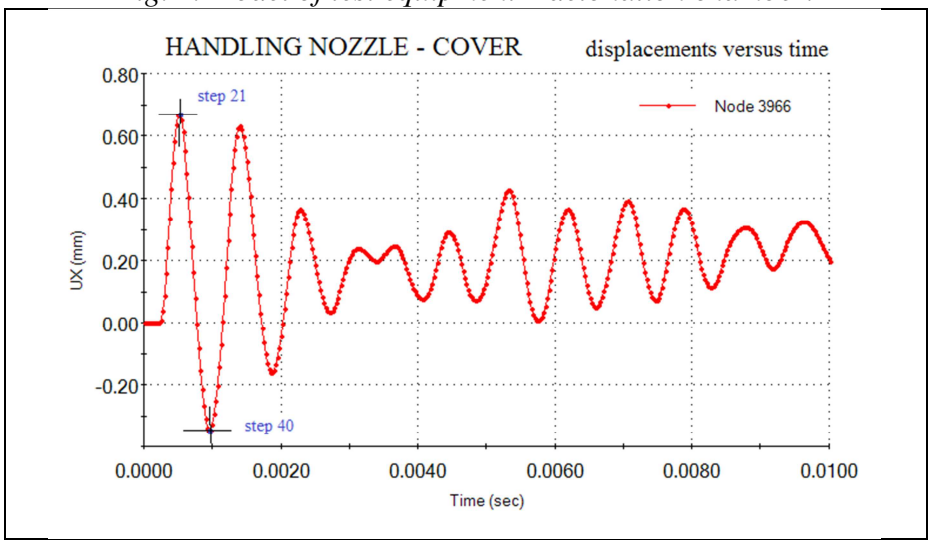

Fig. 3. Dynamic analysis – vibration of the central region of the nozzle cover.

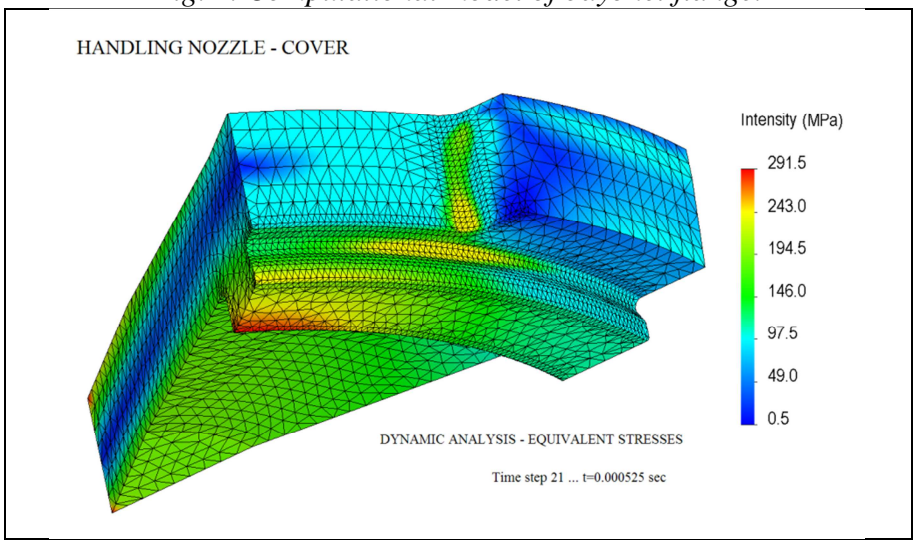

Fig. 4. Dynamic analysis – maximum stress intensity performed for fatigue evaluation.

Overview of selected computational finite element analyses

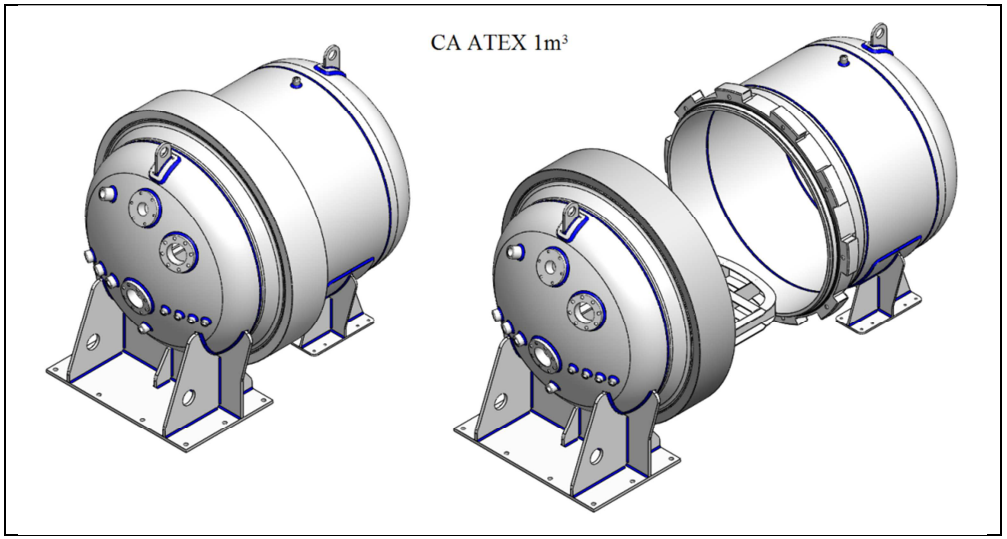

Fig. 1. 3D-model of the chamber (closed / open).

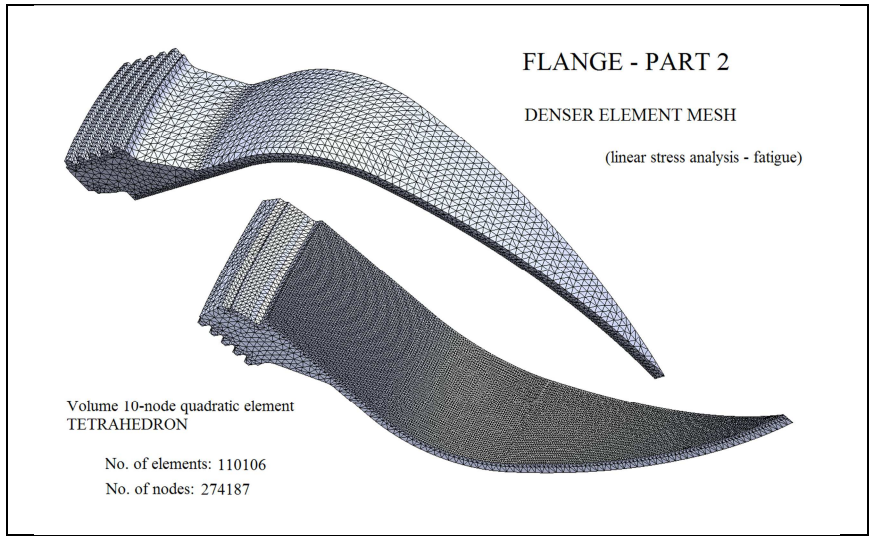

Fig. 2. Doomed bottom flange element mesh.

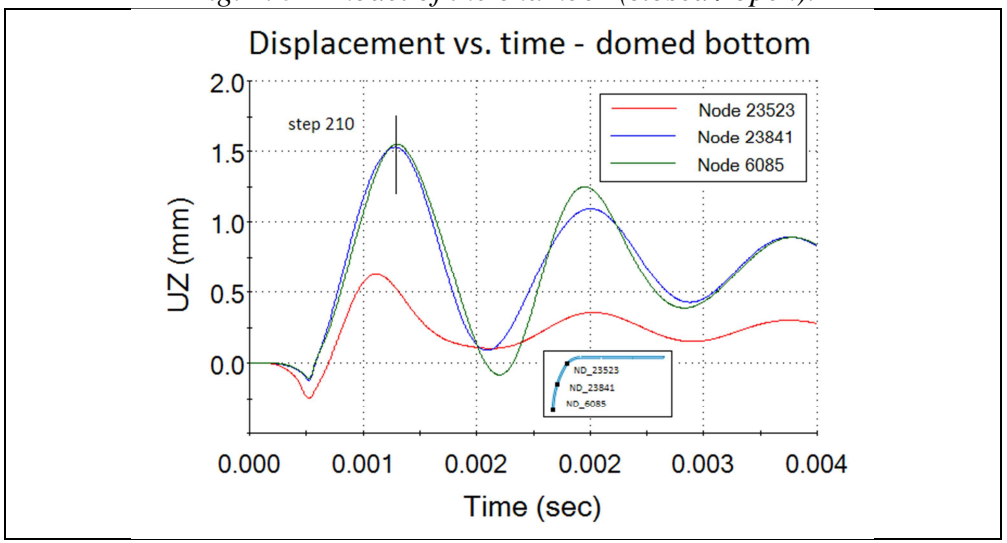

Fig. 3. Doomed bottom dymamic response in displacements.

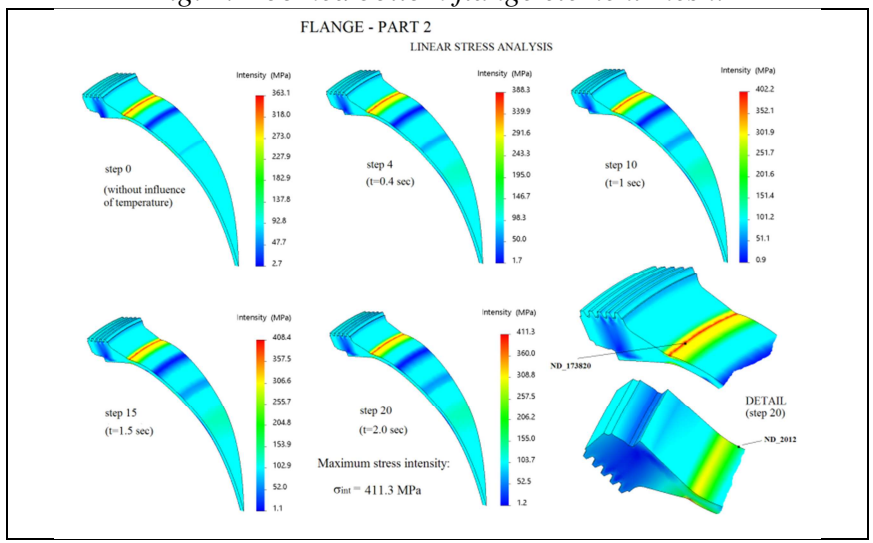

Fig. 4. Doomed bottom dymamic response in stresses.

Overview of selected computational finite element analyses

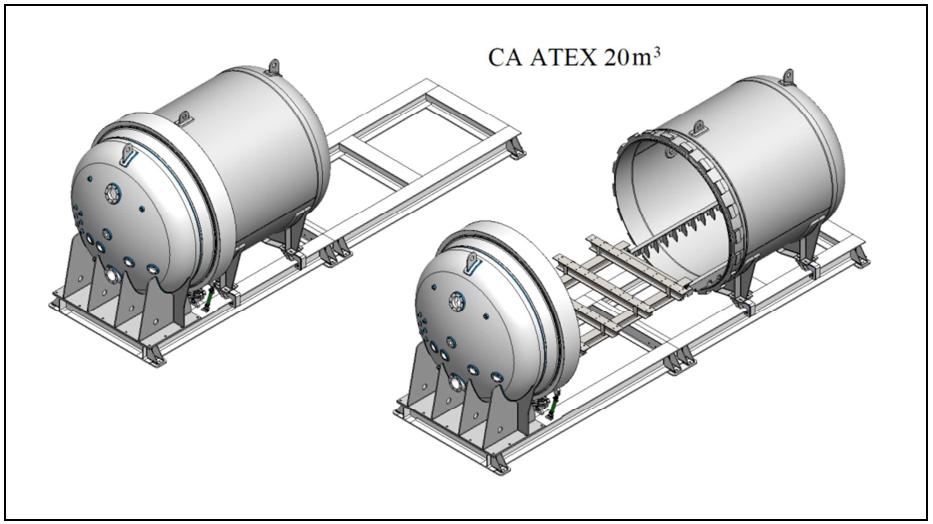

Fig. 1. 3D-model of the chamber (closed / open).

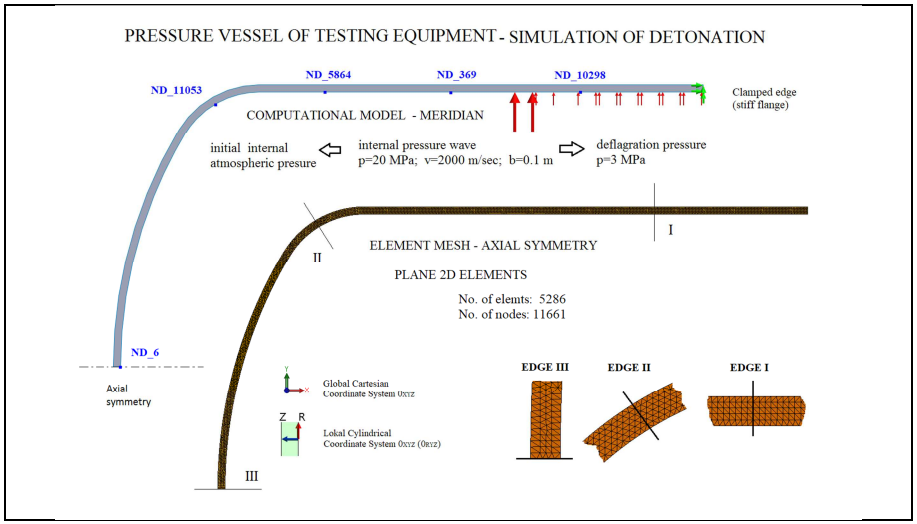

Fig. 2. Axially symmetric model of chamber (computational simulation of detonation).

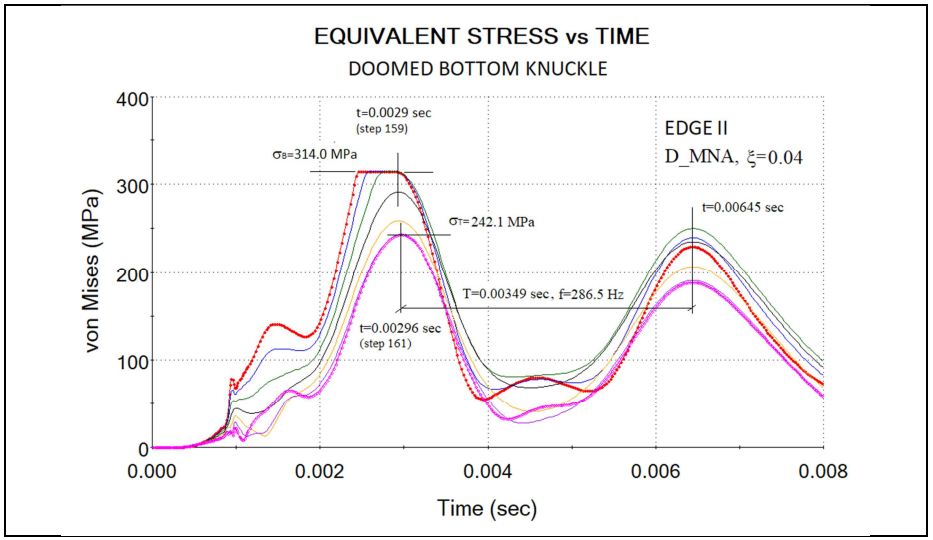

Fig. 3. Nonlinear dynamic response at knuckle.

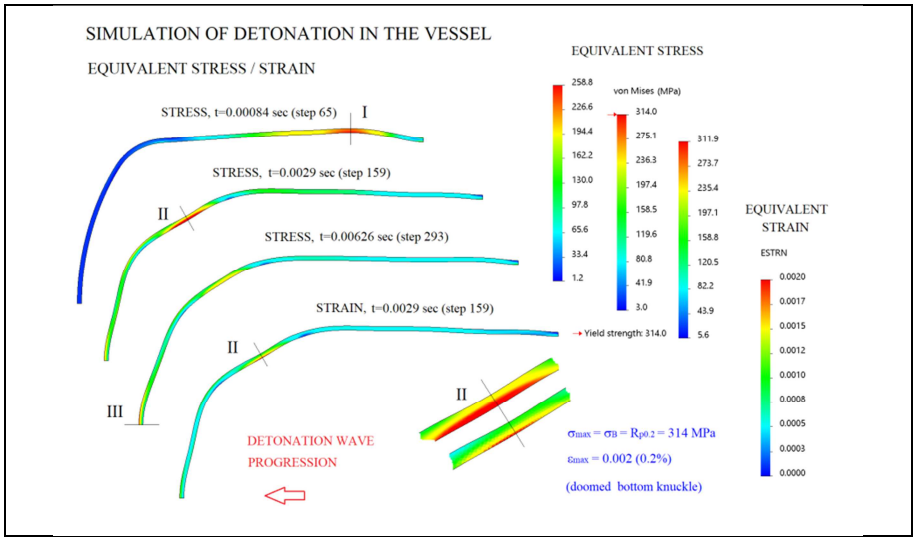

Fig. 4. Equivalent stress of the wall at various time steps.

Overview of selected computational finite element analyses

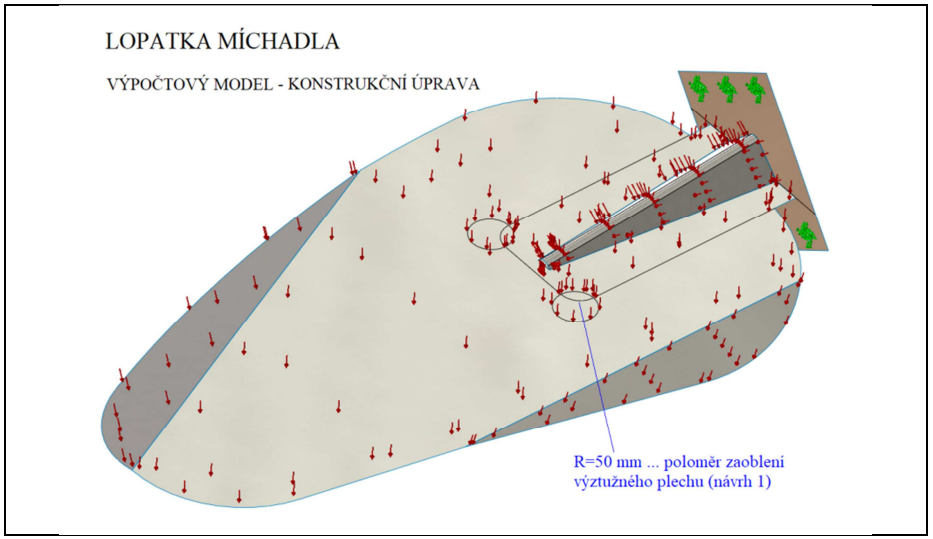

Fig. 1. Computational model of the stirrer blade.

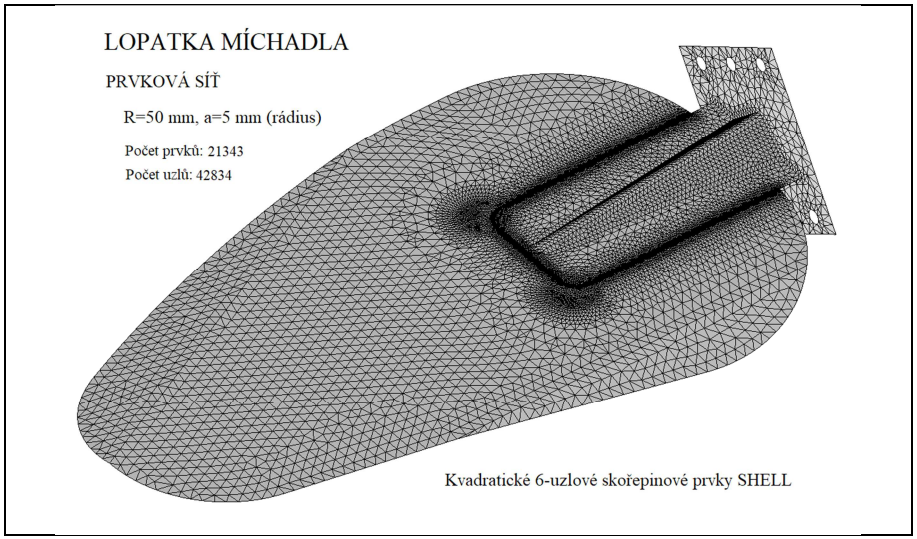

Fig. 2. Element mesh with increased density of elements.

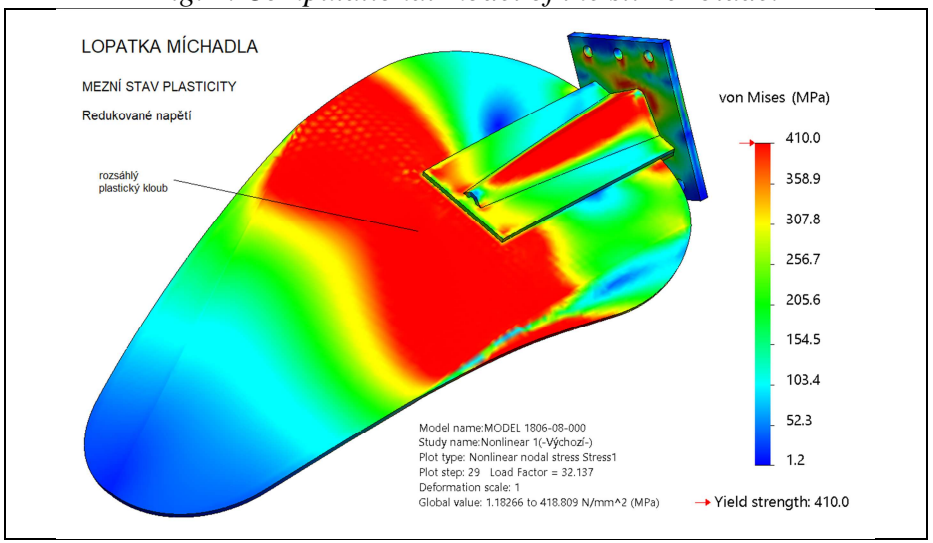

Fig. 3. Limist state of plastic carrying capacity - strength.

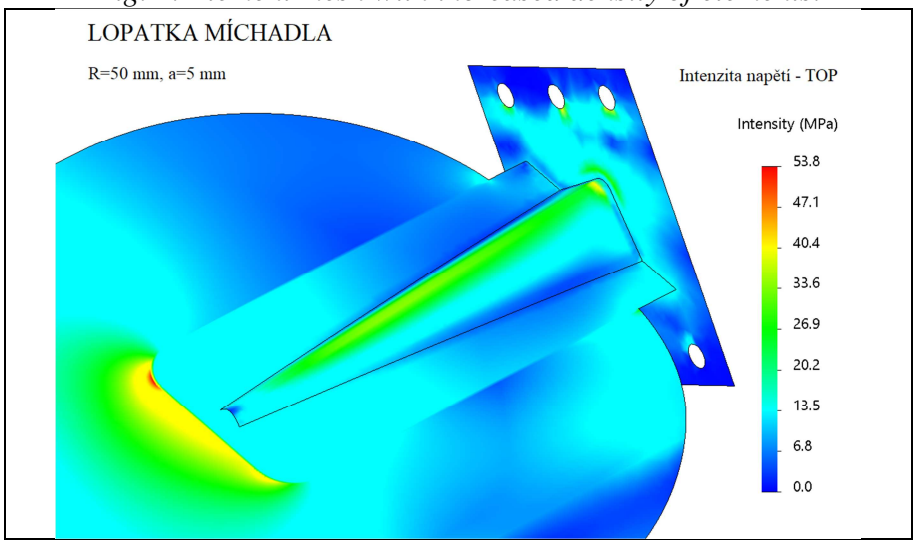

Fig. 4. Maximum elastic stresses - fatigue.

Overview of selected computational finite element analyses

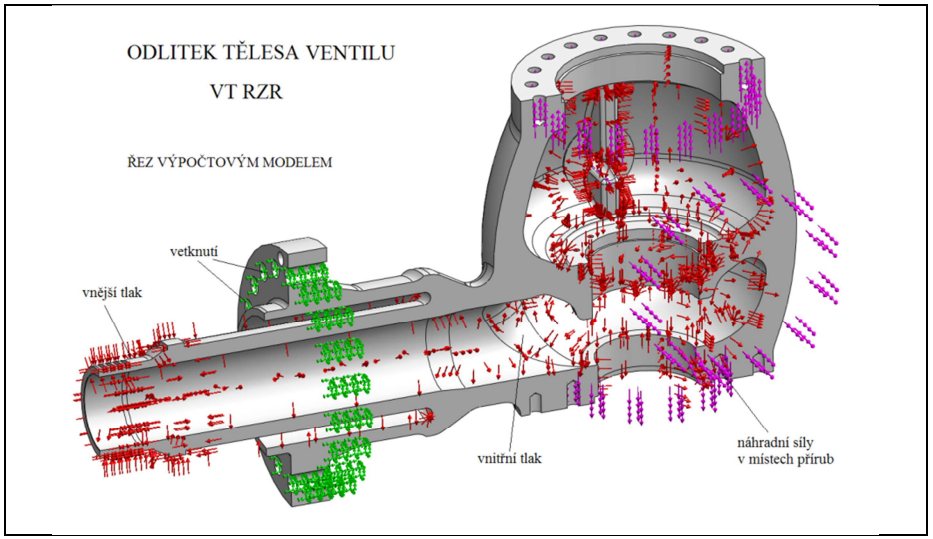

Fig. 1. Computational model of valve – body section.

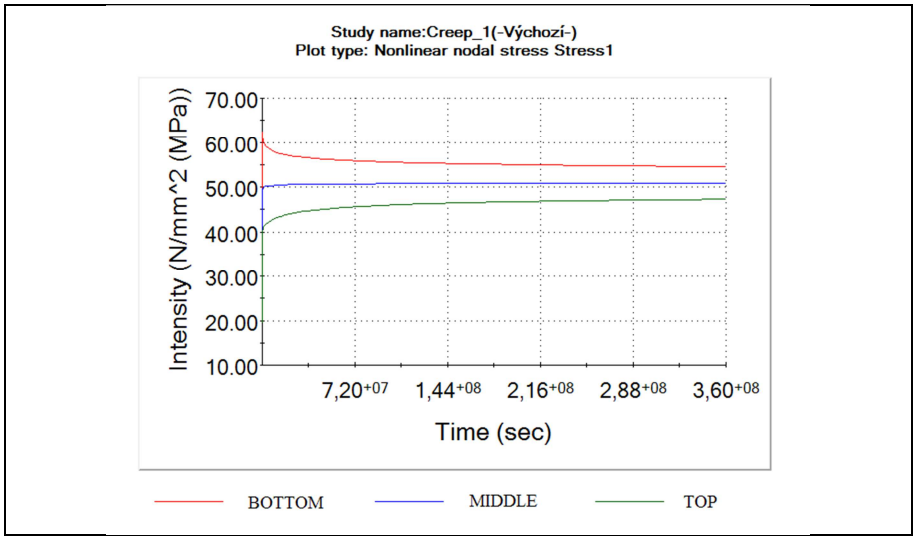

Fig. 2. Time course of stress intensity in section 1 - creep.

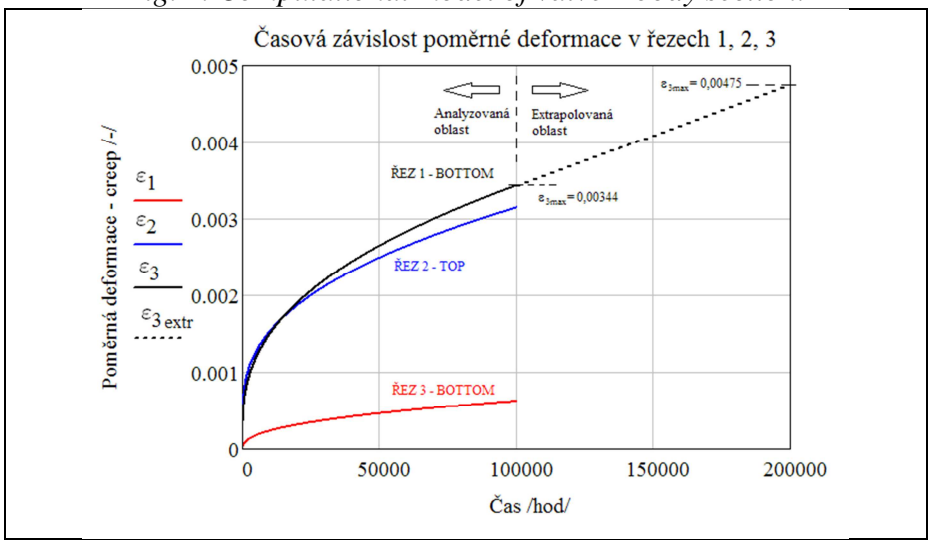

Fig. 3. Time course of strain in section 1 – creep.

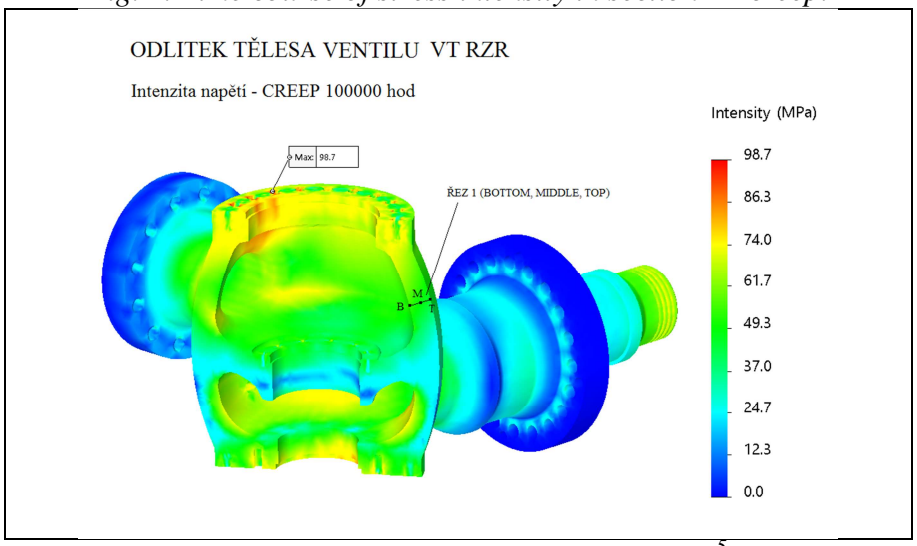

Fig. 4. Stress intensity with marked section 1 (10^5 hours).

PROCESS INDUSTRY

Overview of selected computational finite element analyses

Fig. 1. Disc drier of rendering material.

Fig. 2. Worn out rotor of disc drier.

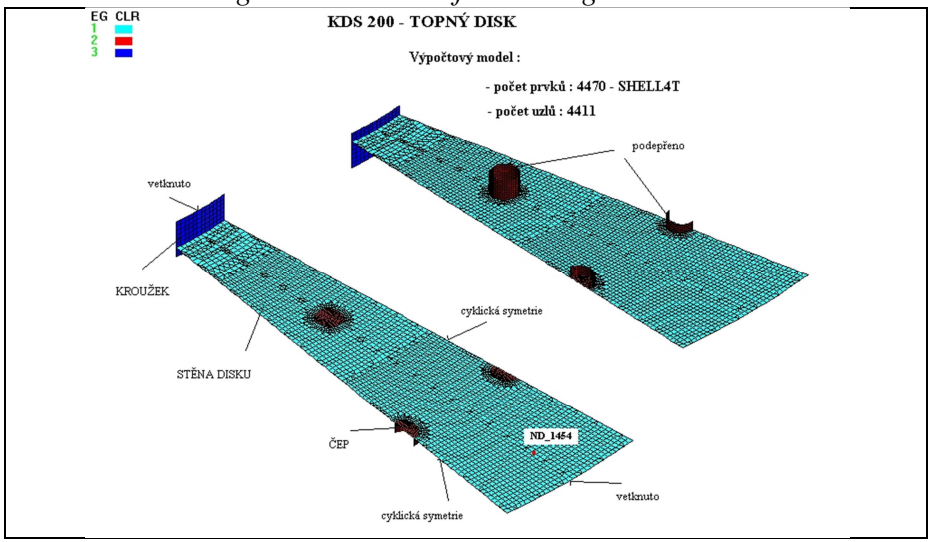

Fig. 3. FEM model of disc (strength and remaining service life).

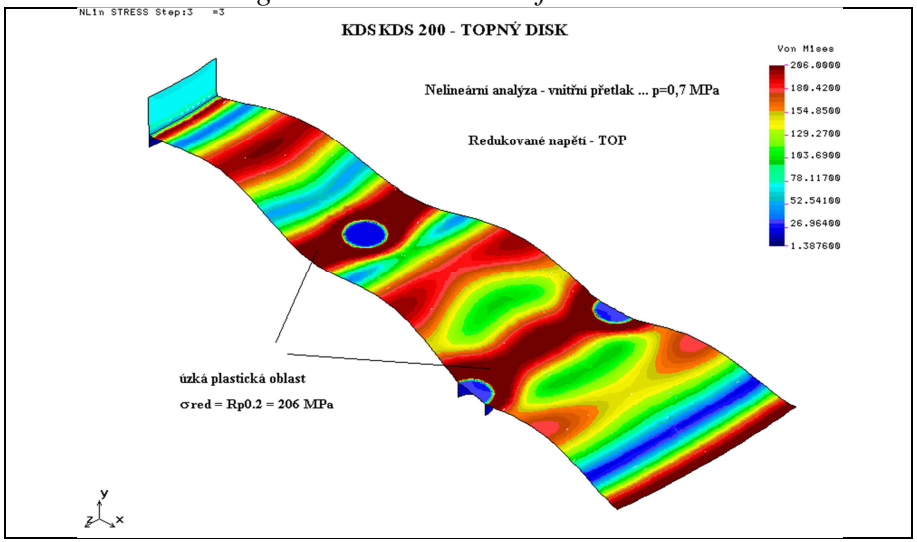

Fig. 4. Limit state of plasticity due to internal pressure of disc.

Overview of selected computational finite element analyses

Fig. 1. Pipe dryer for production of biodiesel.

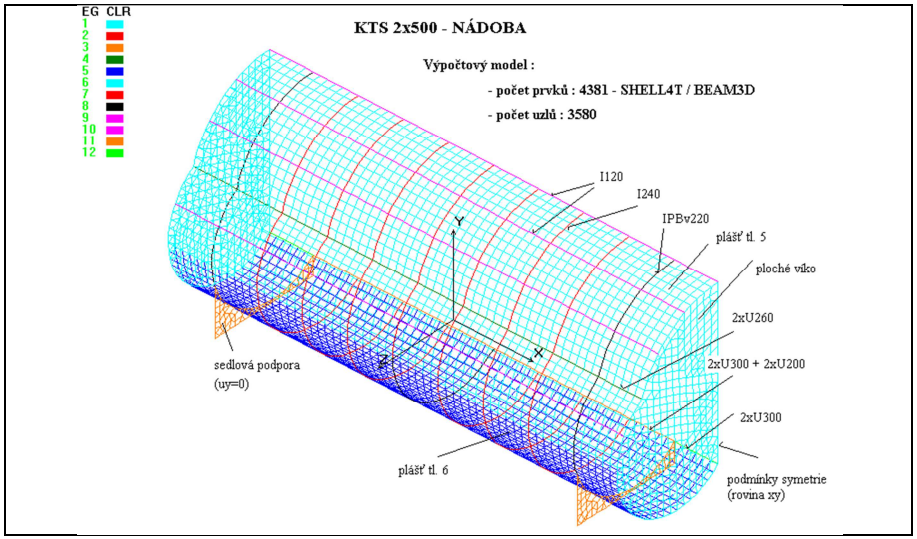

Fig. 2. Simplified model of dryer body.

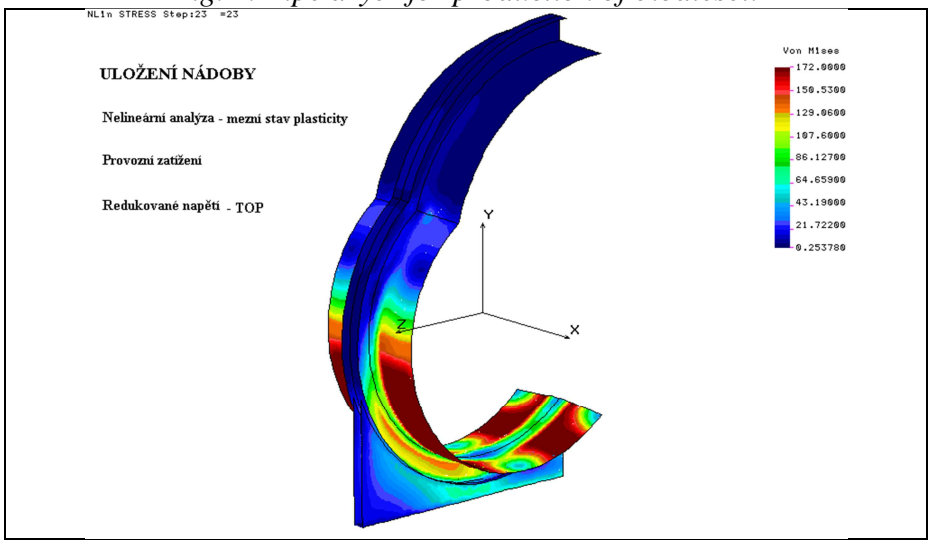

Fig. 3. Detailed model of section of dryer body - limit state.

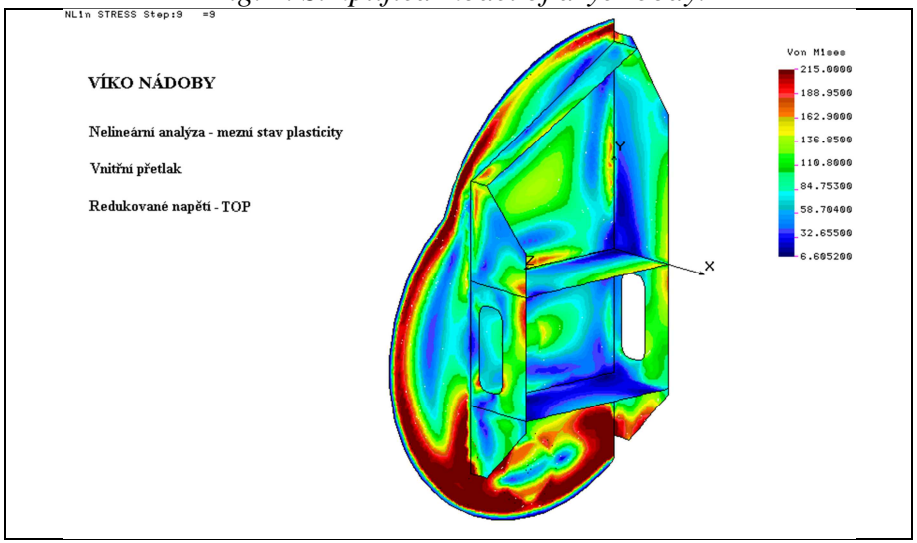

Fig. 4. Stiffened cover of drier – limit state.

Overview of selected computational finite element analyses

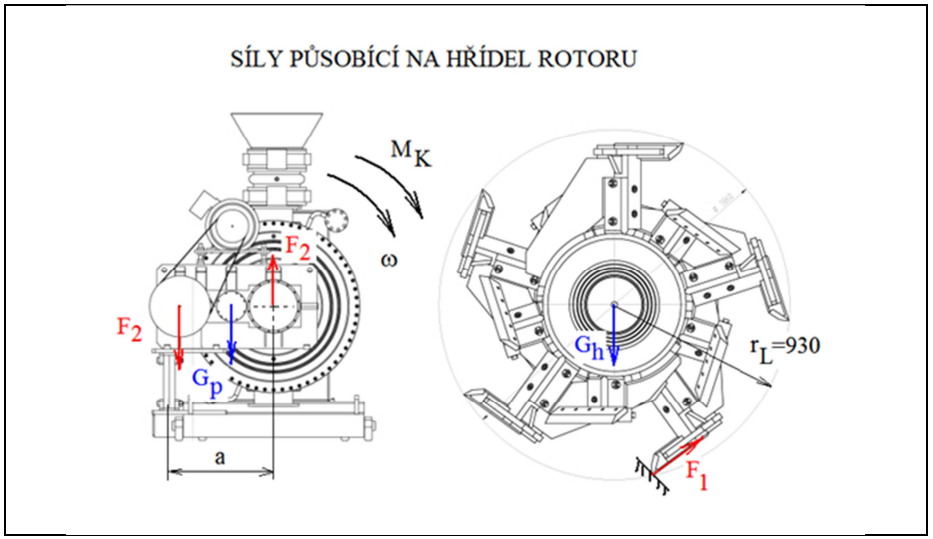

Fig. 1. Scheme of rotor loads of thermal desorption dryer.

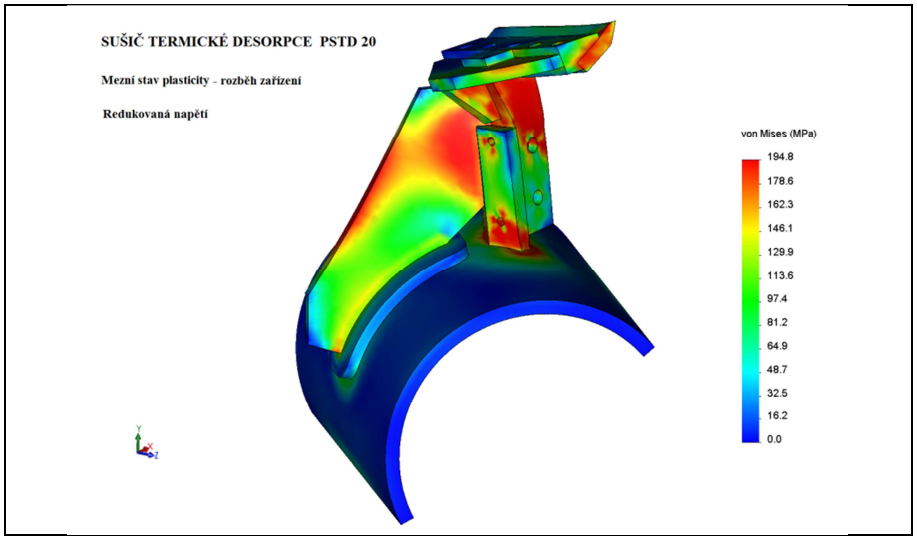

Fig. 2. Rotor blade in limit state of plasticity.

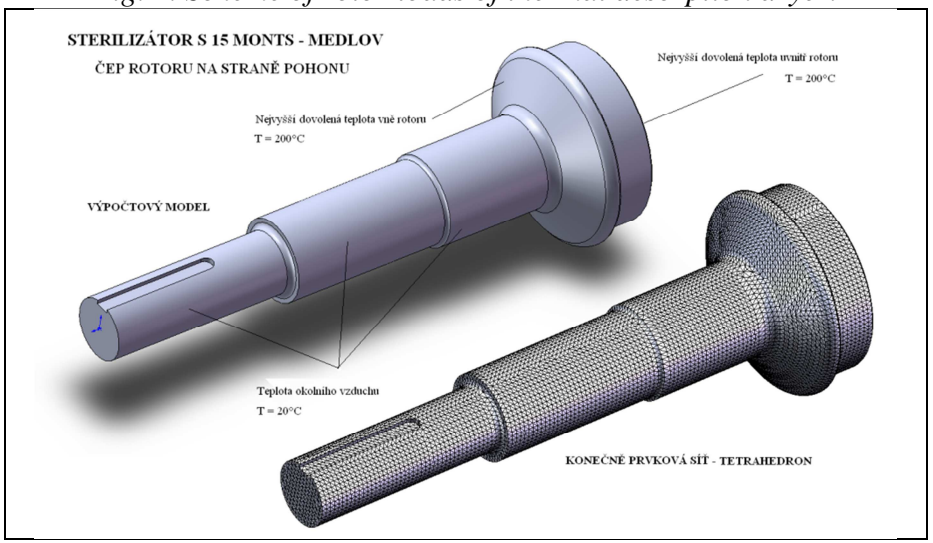

Fig. 3. Computational model of rotor drive shaft.

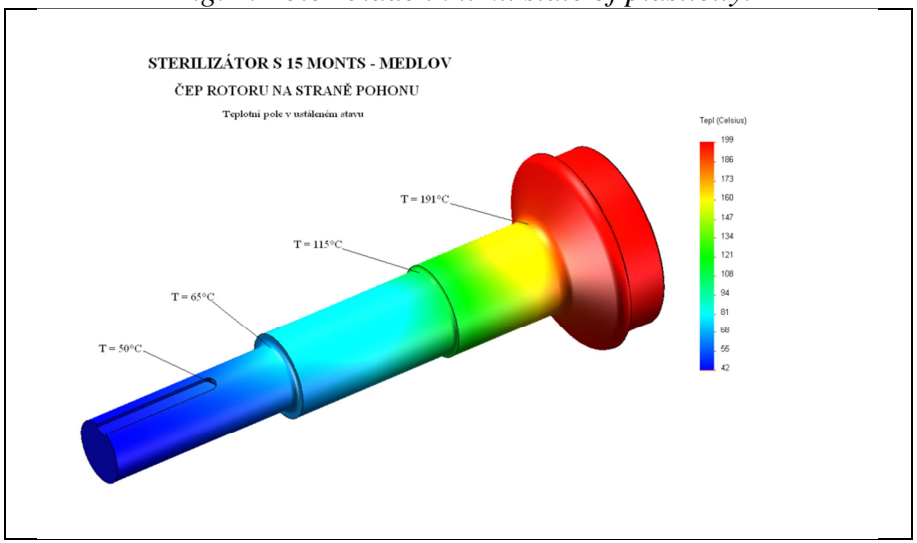

Fig. 4. Temperature field of shaft for design of bearings.

Overview of selected computational finite element analyses

Fig. 1. Photo of three / four beer tanks stacked atop one other.

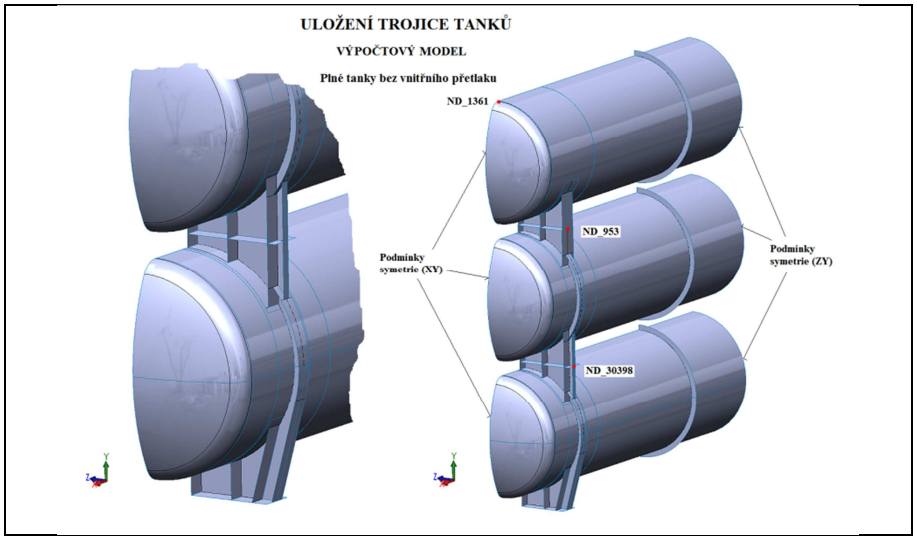

Fig. 2. Computational model of three tanks.

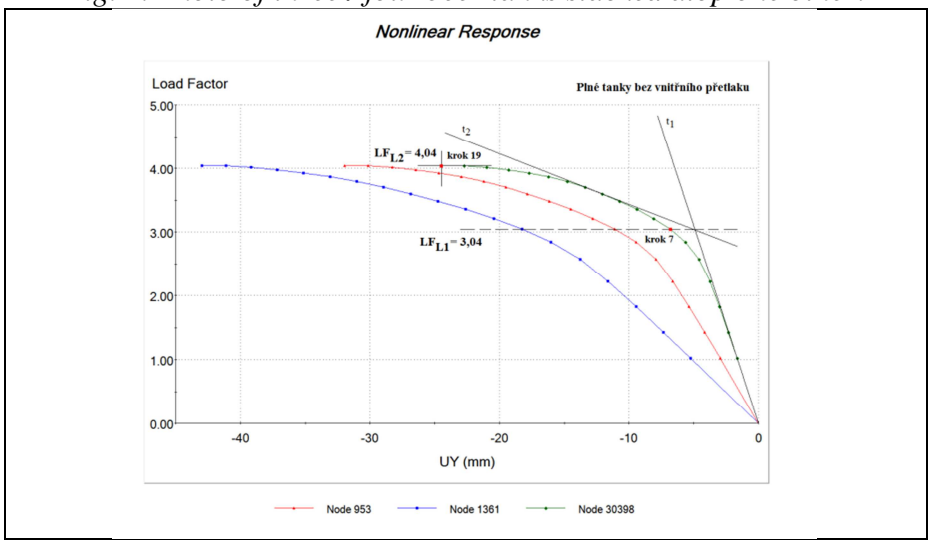

Fig. 3. Load curve of tanks loaded by weight of stored beer.

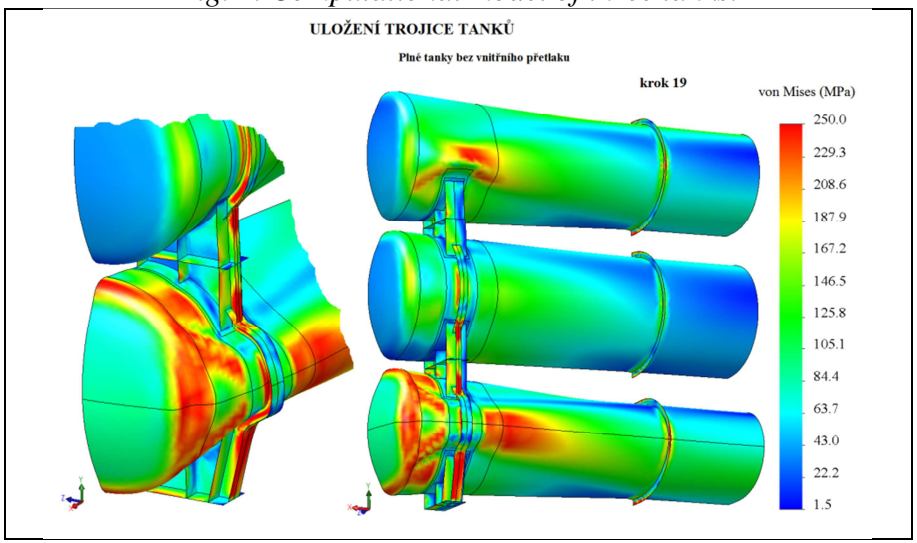

Fig. 4. Equivalent stress of computational model.

Overview of selected computational finite element analyses

Fig. 1. Flour sorter suspended in test station.

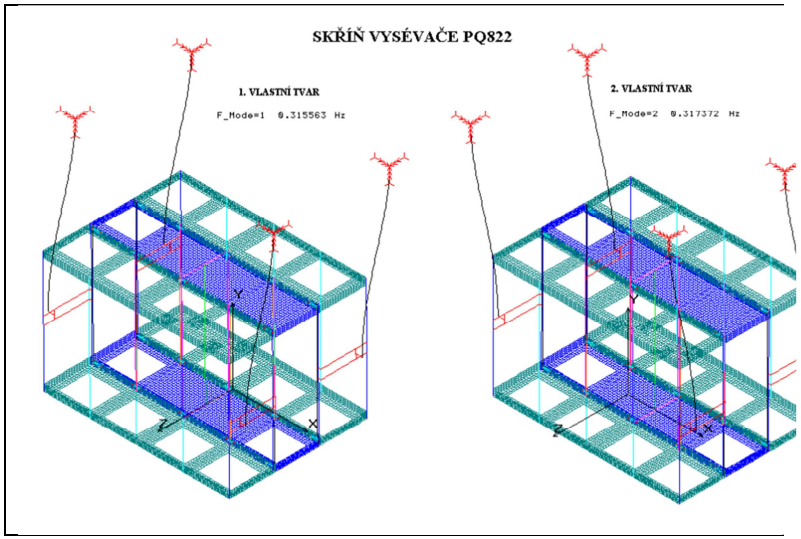

Fig. 2. Lowest natural modes of simplified FEM model.

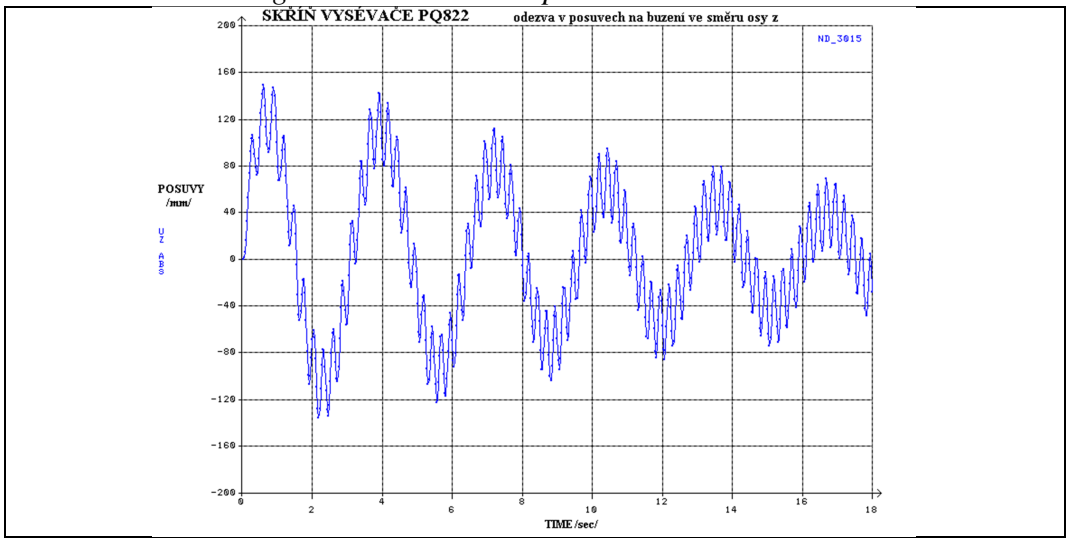

Fig. 3. Character of forced vibration of computational model.

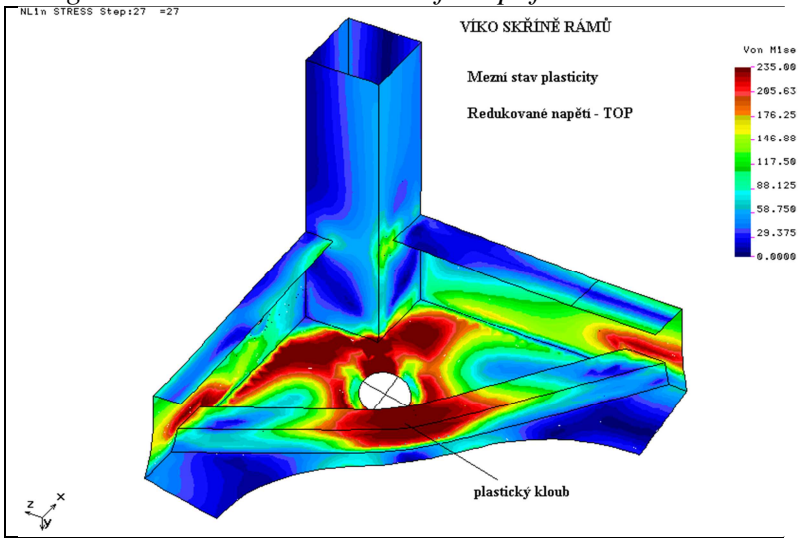

Fig. 4. Limit state of plasticity od detailed FEM model of one upper corner.

Overview of selected computational finite element analyses

Fig. 1. Cylindrical shell of vertical stainless steel tank with excessive shape imperfections.

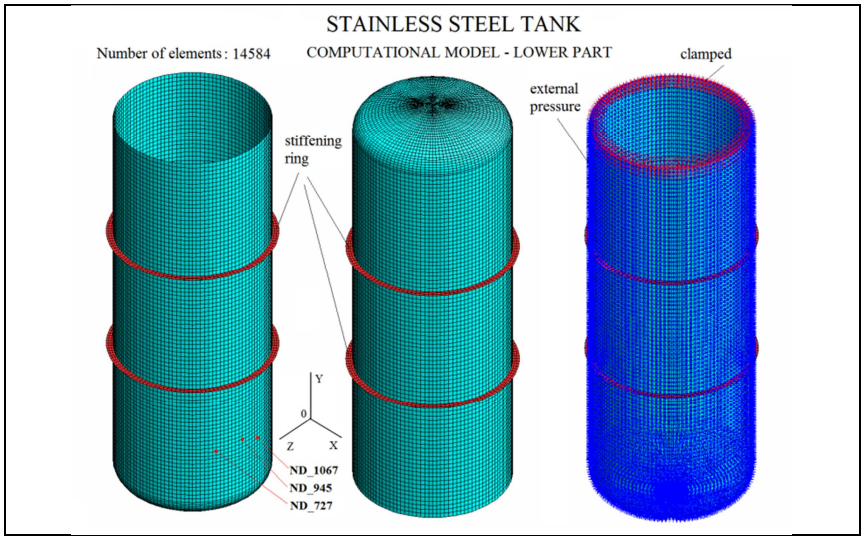

Fig. 2. Computational model of lower part of tank.

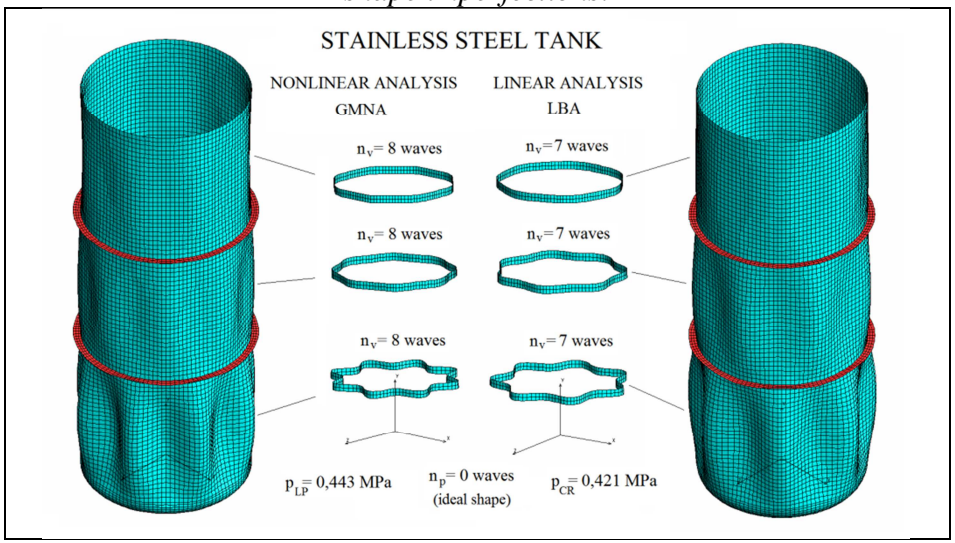

Fig. 3. FEM model deformed in 8 circumferential waves.

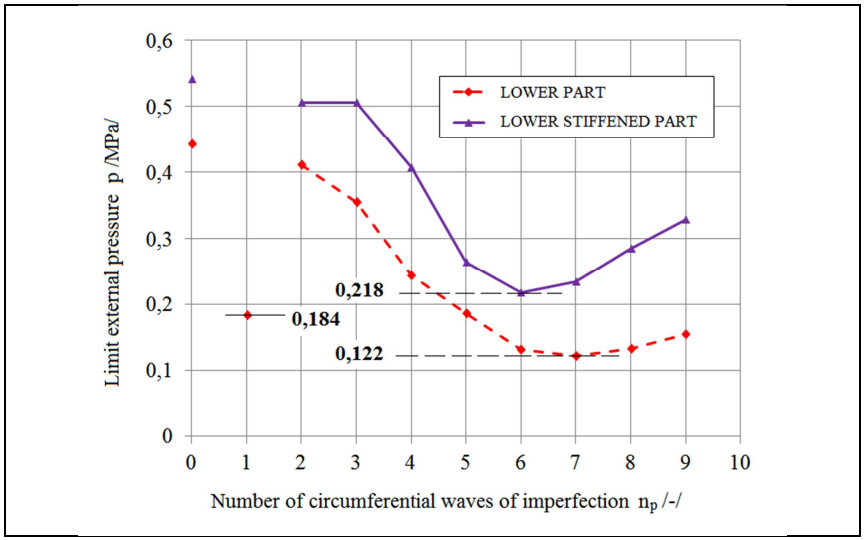

Fig. 4. Dependence of limit pressure on number of waves.

Overview of selected computational finite element analyses

Fig. 1. Loss of stability of vertical beer tank.

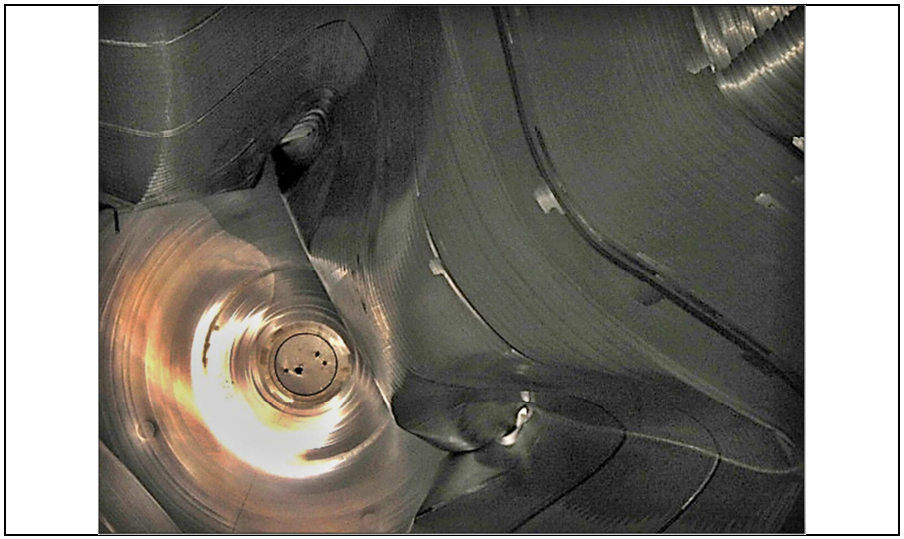

Fig. 2. View of the collapsed tank through nozzle in the bottom.

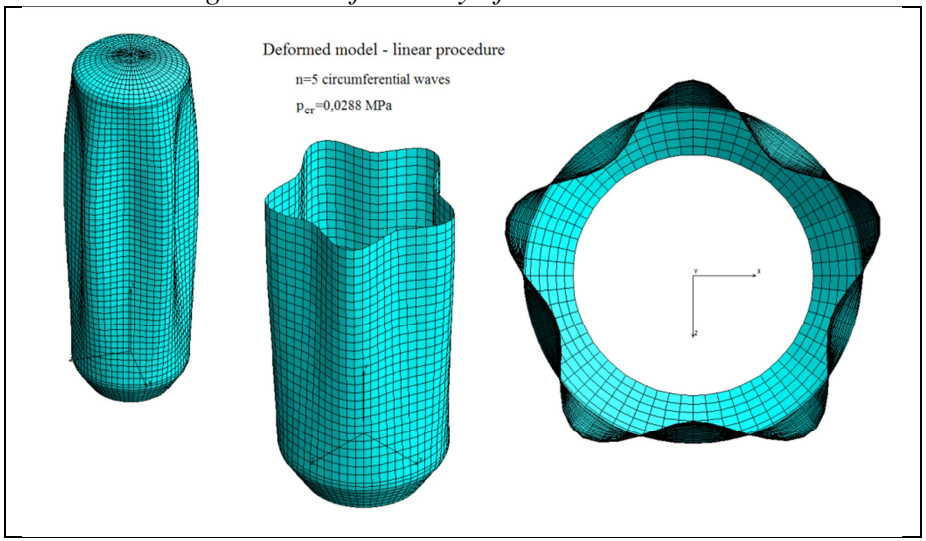

Fig. 3. FEM linear stability analysis with resulting 5 circumferential waves.

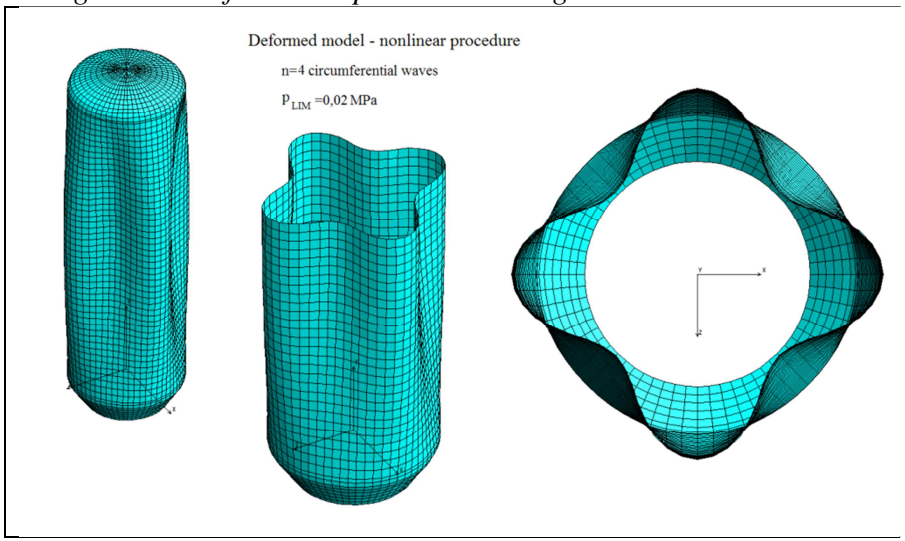

Fig. 4. FEM nonlinear stability analysis with resulting 4 circumferential waves (corresponds to reality).

Overview of selected computational finite element analyses

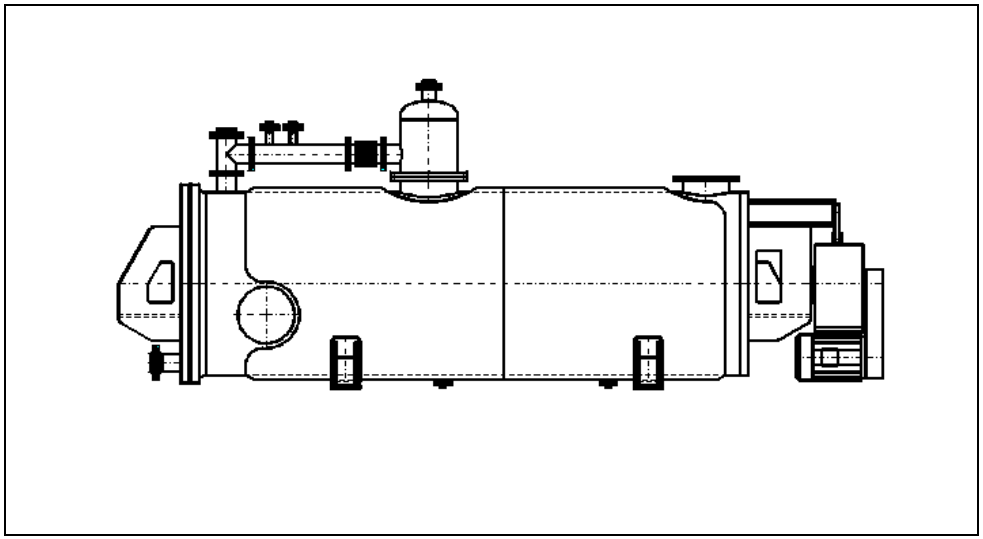

Fig. 1. Destructor for processing of rendering material.

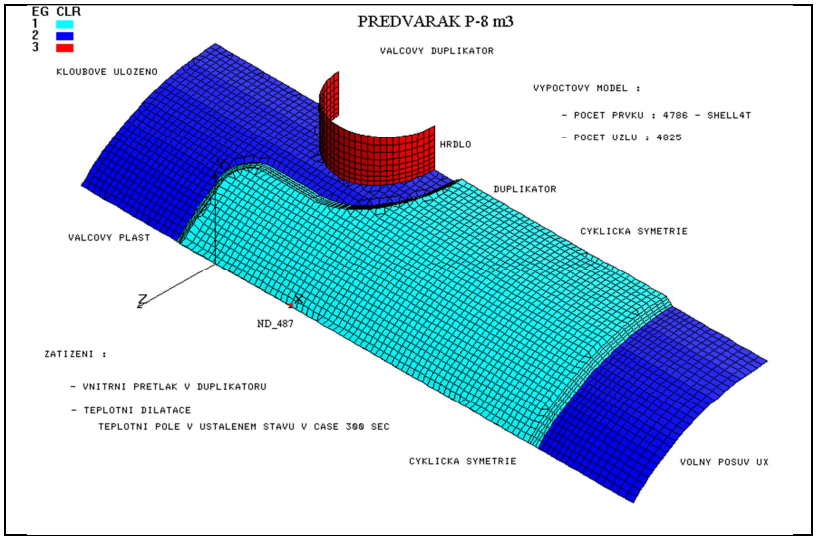

Fig. 2. Computational model of shell with jacket.

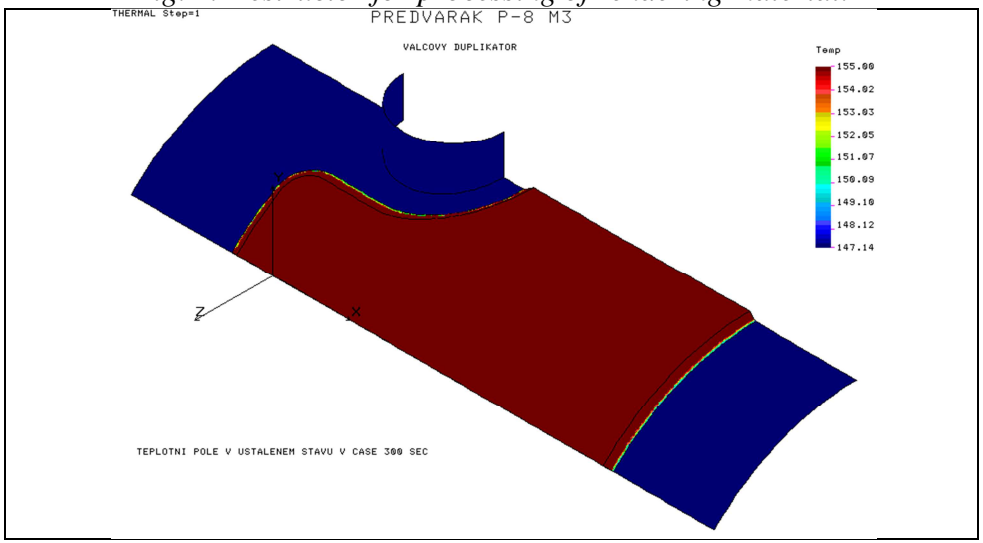

Fig. 3. Temperature field in steady state.

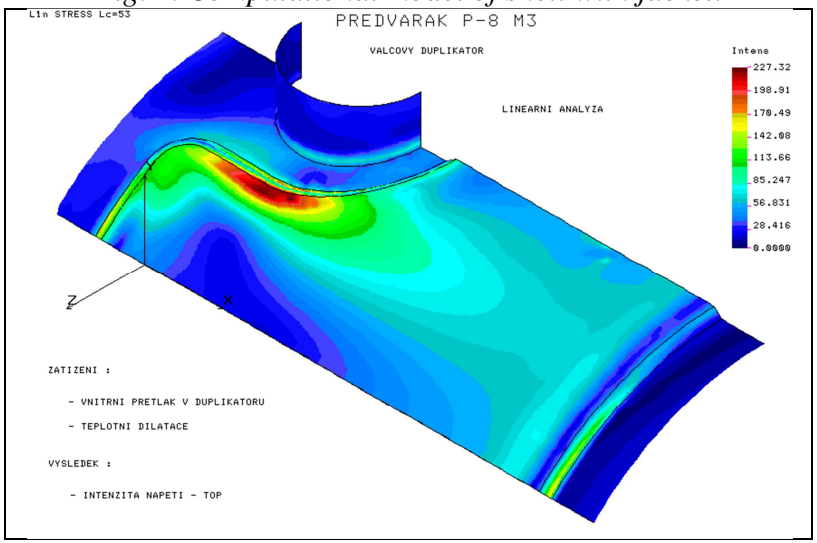

Fig. 4. Maximum stress intensity by pressure and temperature.

Overview of selected computational finite element analyses

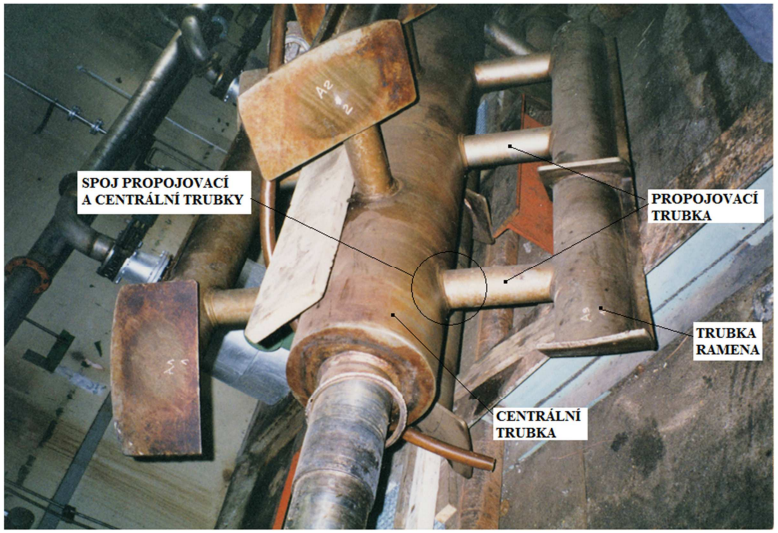

Fig. 1. Agitator of sterilizer heated by steam.

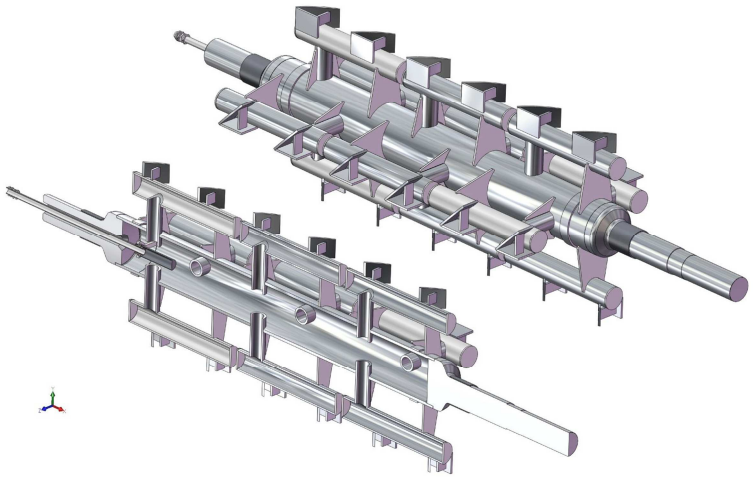

Fig. 2. Model of modified construction of agitator.

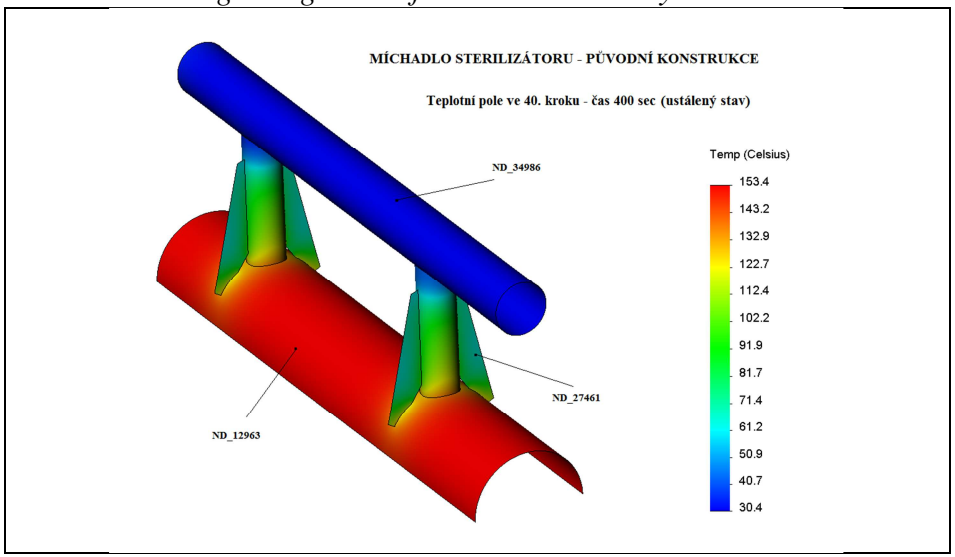

Fig. 3. Computational model with temperature field in steady state.

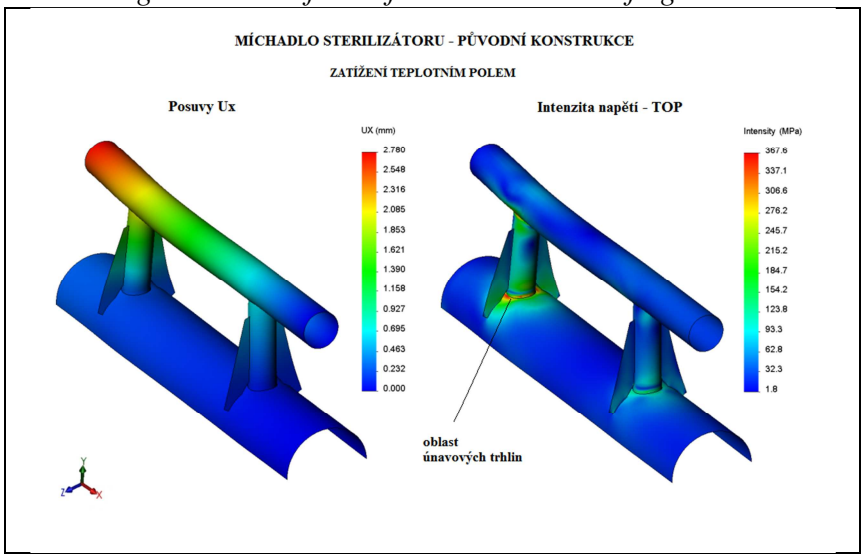

Fig. 4. Deformed model with displacements and stresses.

Overview of selected computational finite element analyses

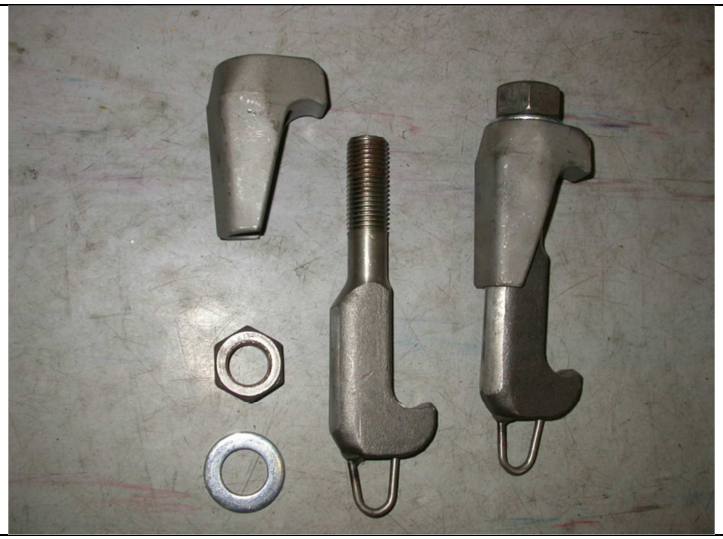

Fig. 1. Stainless steel C-clamp M27 short (for enameled vessels).

Fig. 2. C-clamp fastened to tensile test facility.

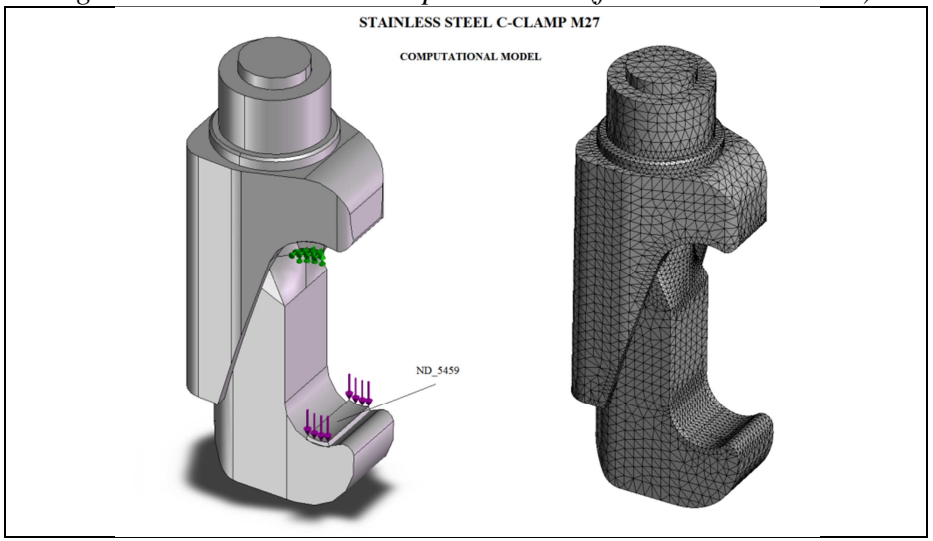

Fig. 3. Computational model of C-clamp.

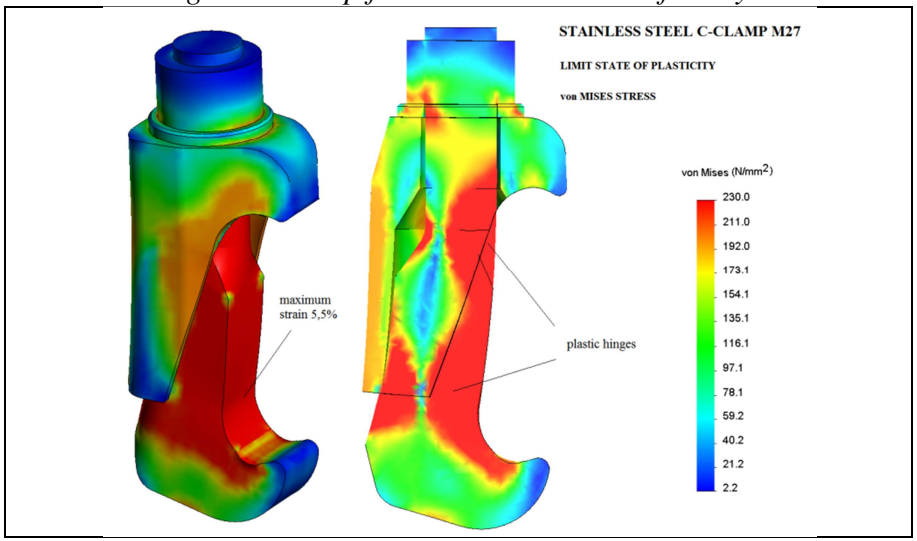

Fig. 4. Limit state of plasticity of computational model.

Overview of selected computational finite element analyses

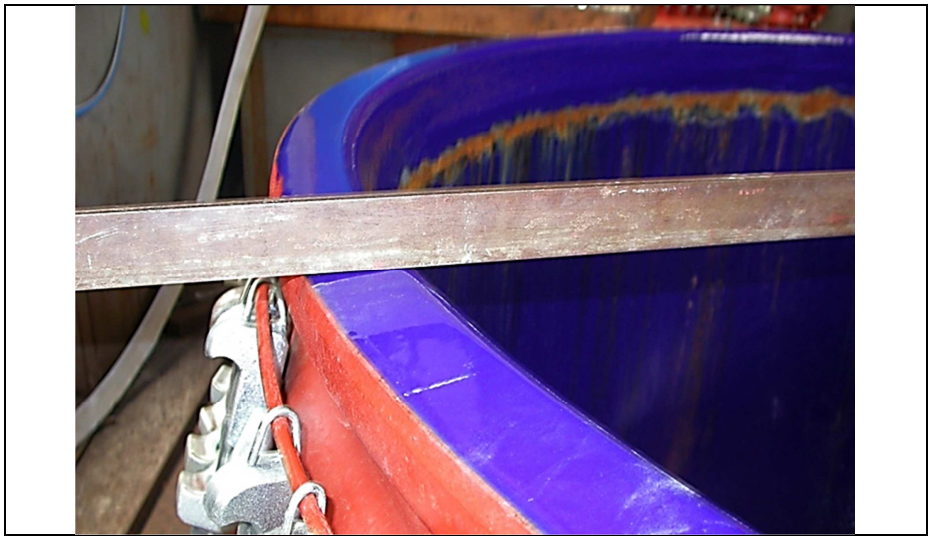

Fig. 1. Damaged enamel of vessel near imperfect flange.

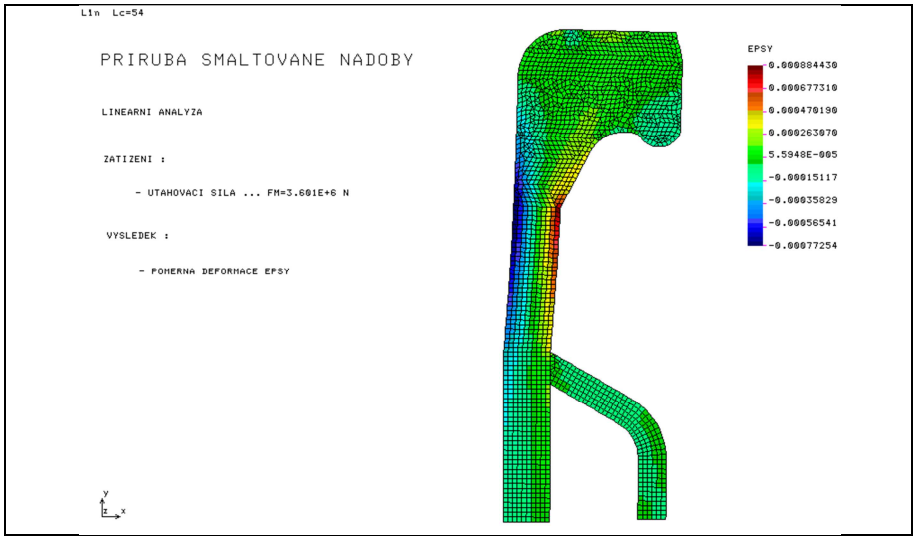

Fig. 2. Strain ε_y after tightening flange.

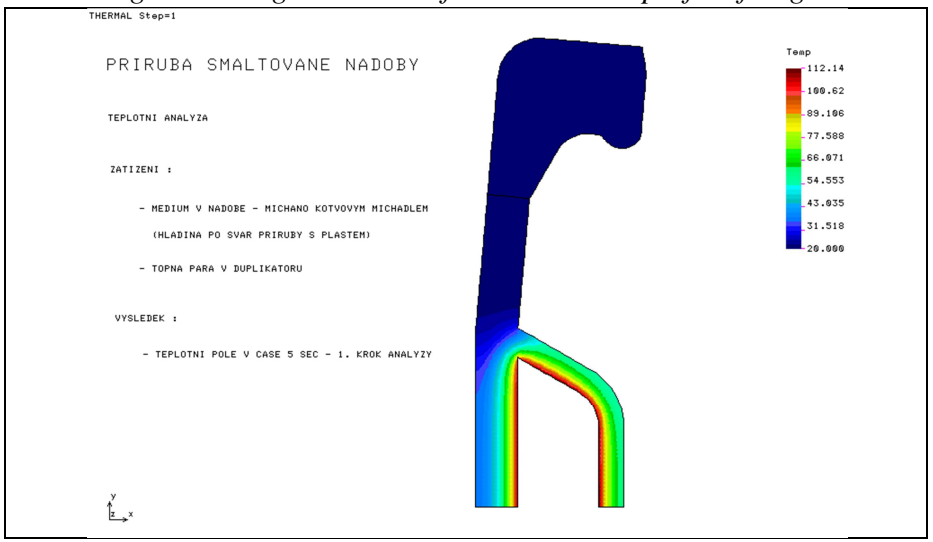

Fig. 3. Temperature field of vessel with jacket – heated by steam.

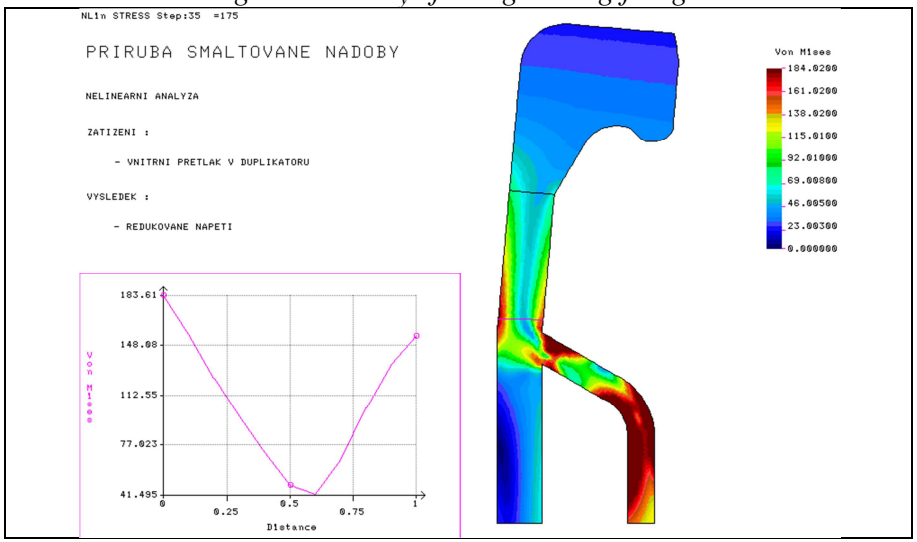

Fig. 4. Limit state of plasticity due to pressure in jacket.

Overview of selected computational finite element analyses

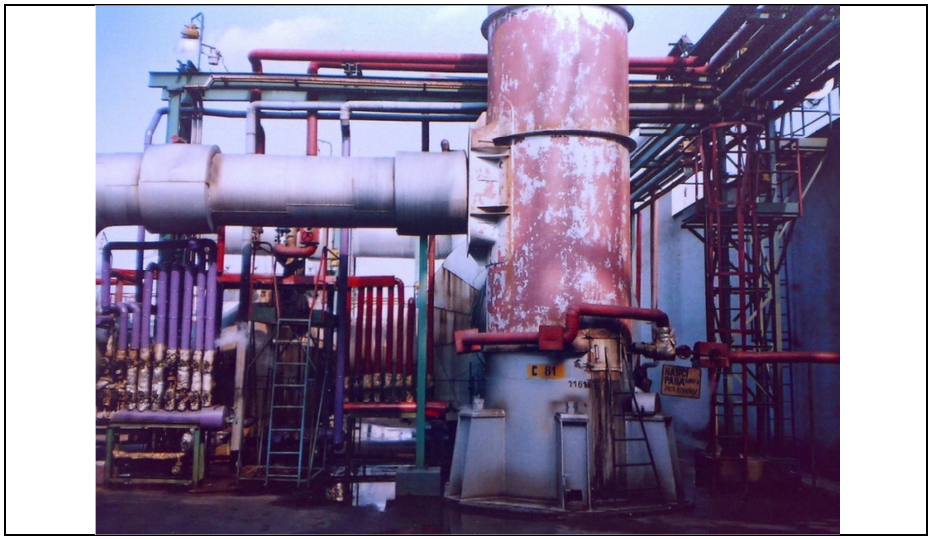

Fig. 1. Lower part of steel chimney with high 55 m.

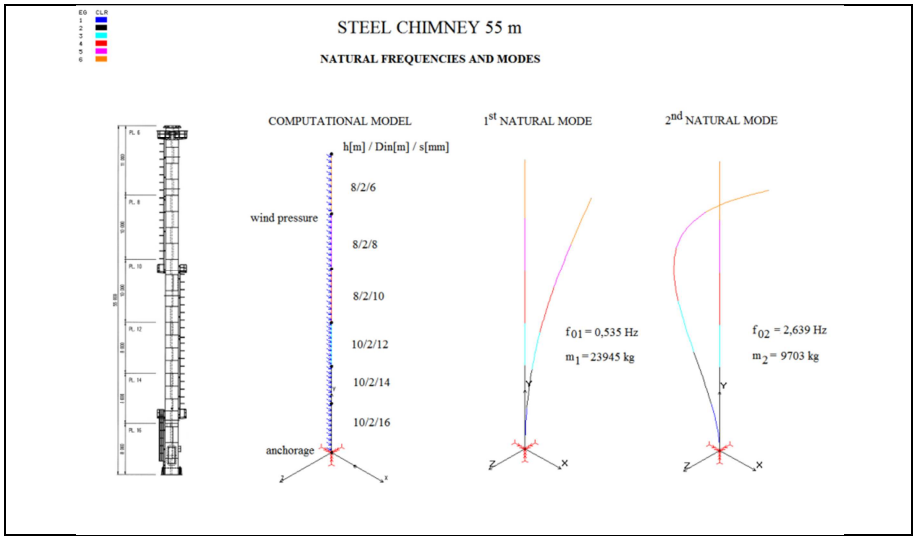

Fig. 2. Results of BEAM3D dynamic model loaded with wind.

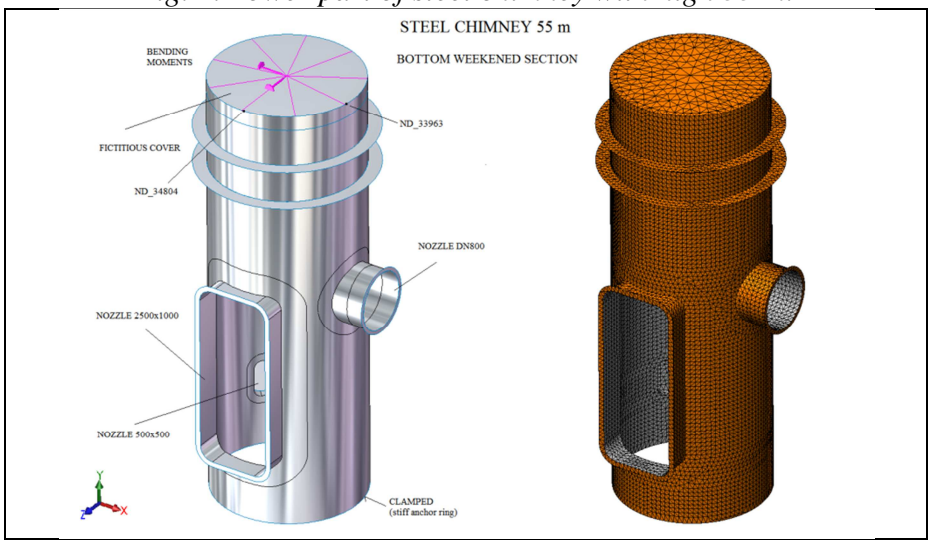

Fig. 3. Detailed shell computational model.

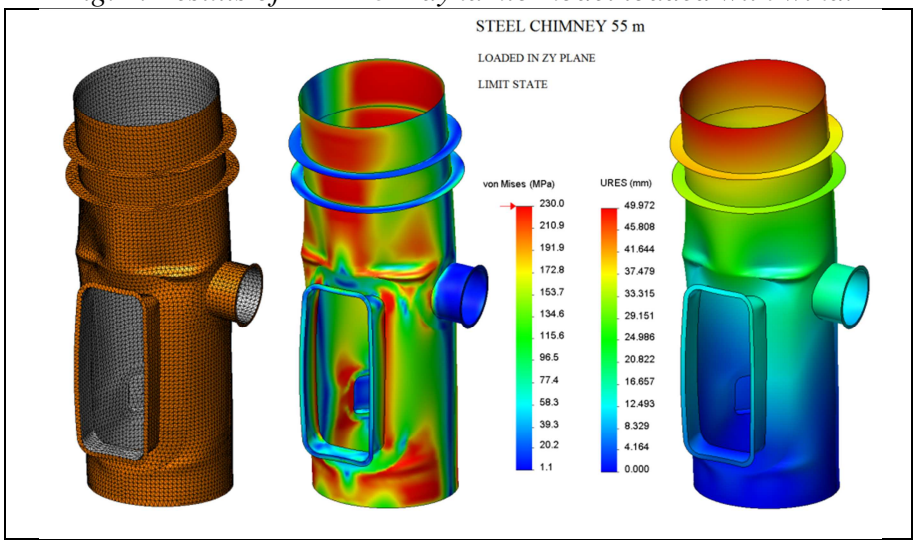

Fig. 4. Limit state - loss of stability in elastic-plastic area.

Overview of selected computational finite element analyses

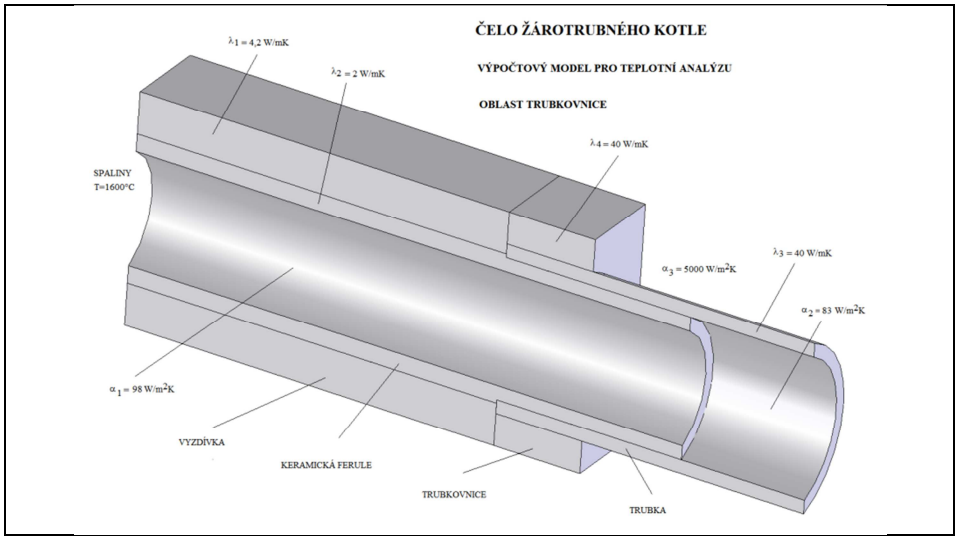

Fig. 1. Model of part of boiler tubesheet with thermal insulation (one tube).

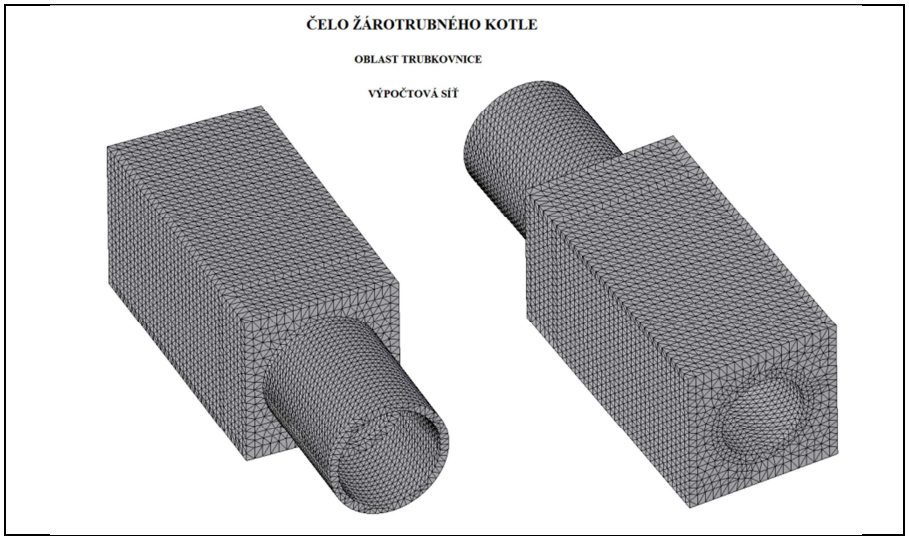

Fig. 2. Computational model.

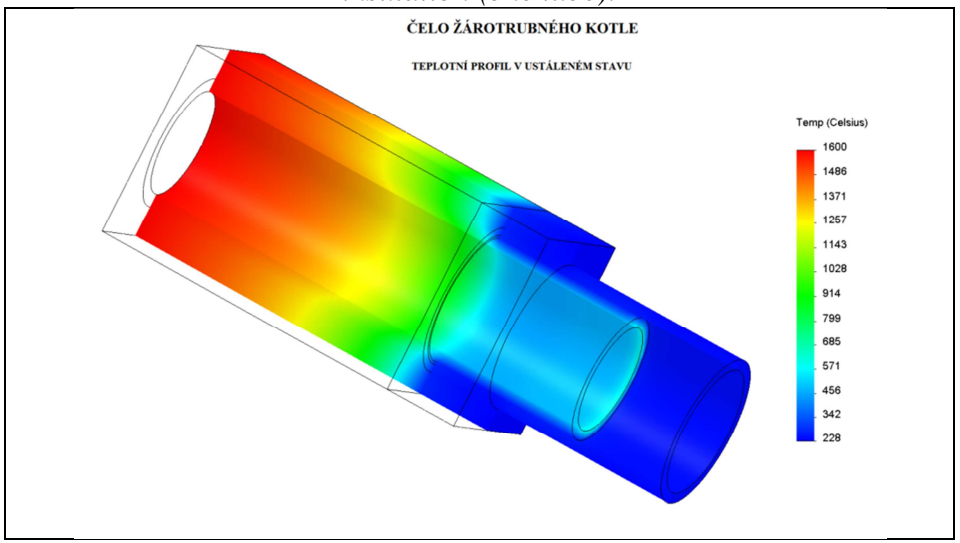

Fig. 3. Temperature distribution at steady state.

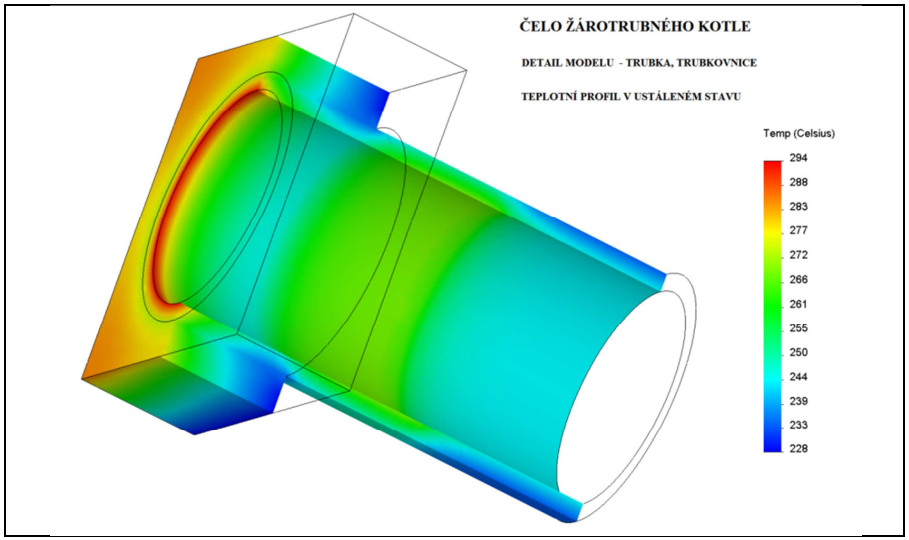

Fig. 4. Temperature distribution in weld tube and tubesheet.

Overview of selected computational finite element analyses

Fig. 1. Loss of stability of bulkhead of tank road due to external pressure (loss of stability of spherical cap).

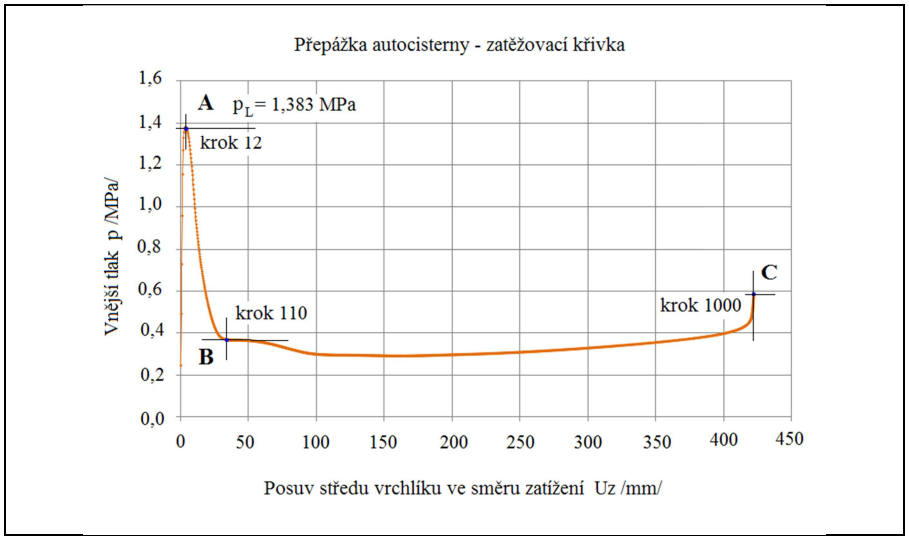

Fig. 2. Load curve representing relation between external pressure and center point displacements along axis of the cap.

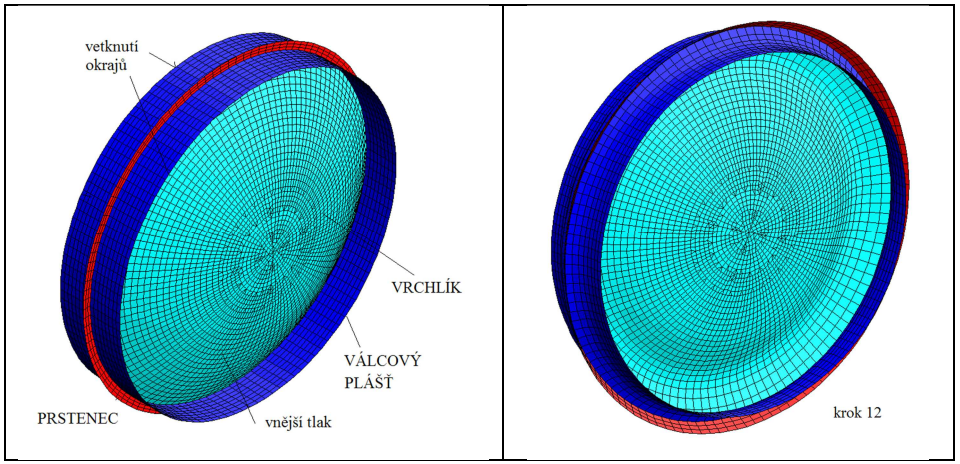

Fig. 3. Computational model and model deformed in step 12 (A).

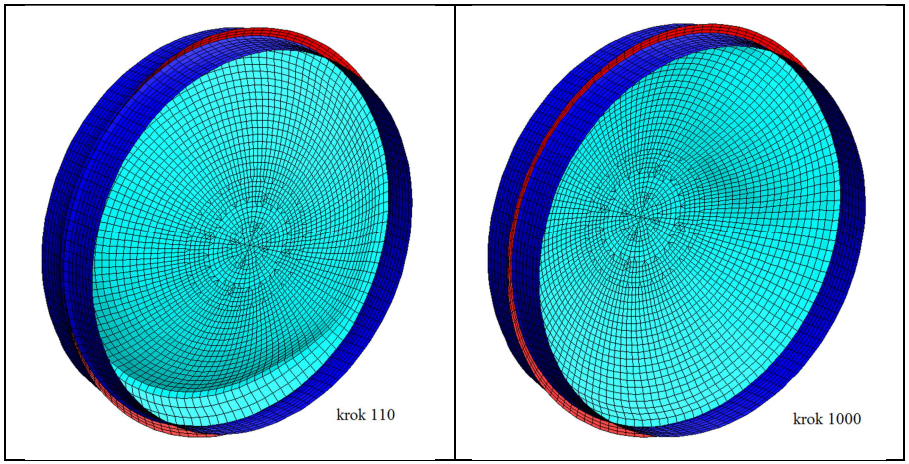

Fig. 4. Model deformed in step 110 (B) and 1000 (C).

Overview of selected computational finite element analyses

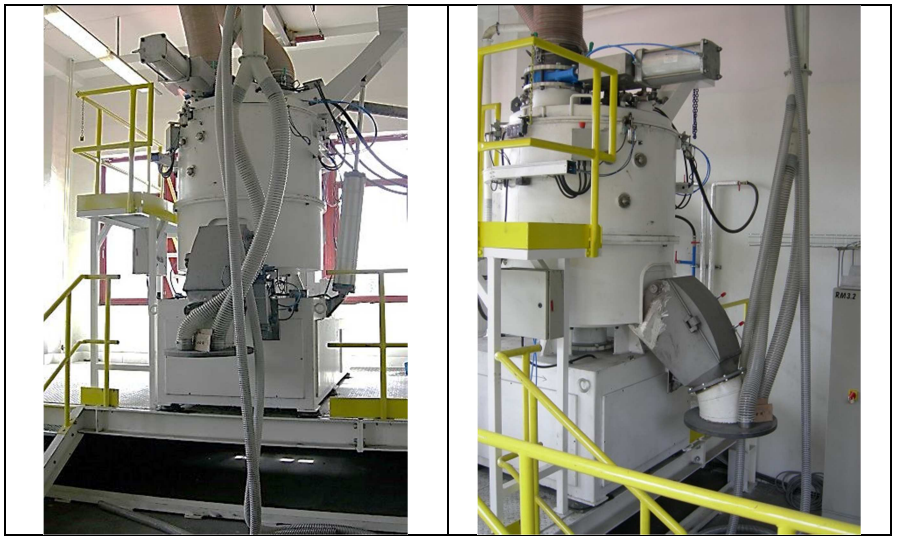

Fig. 1. Mixer of bulk materials – excessive vibrations.

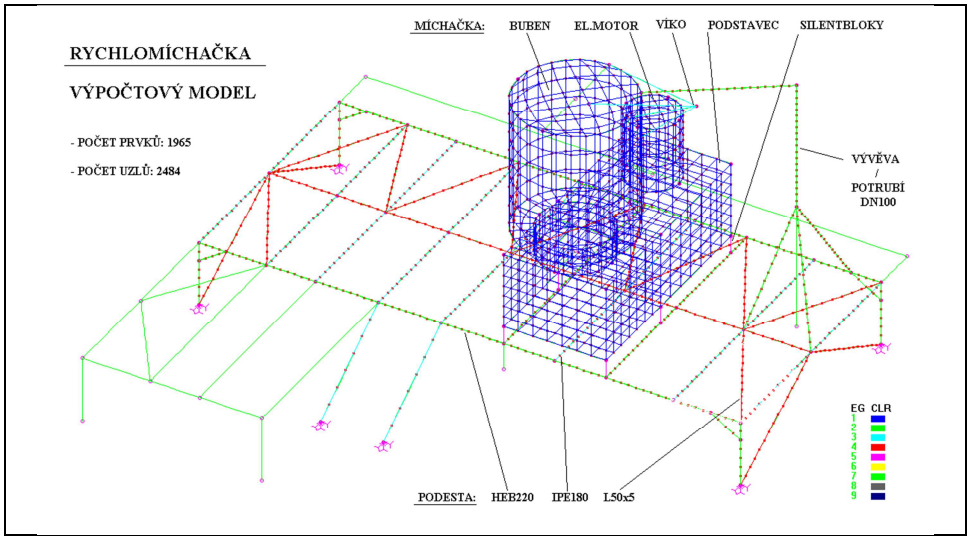

Fig. 2. Computational model of mixer.

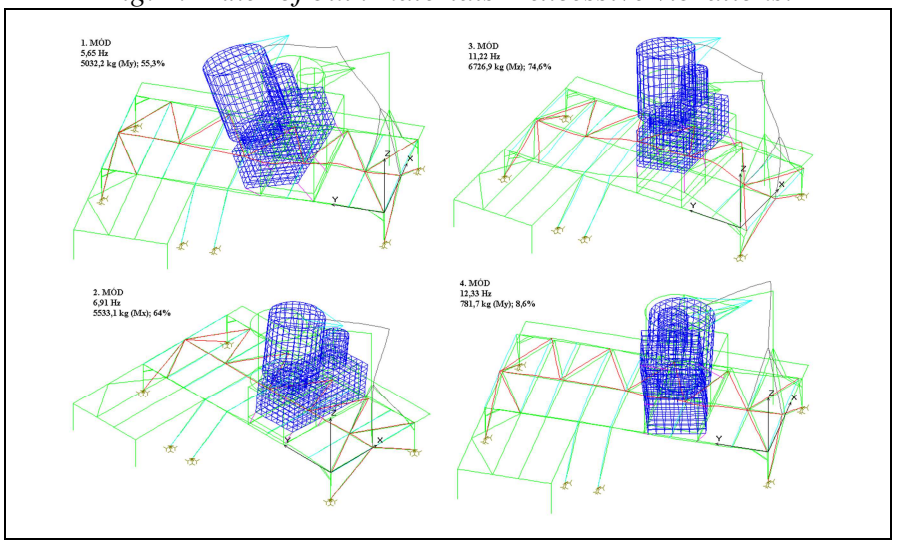

Fig. 3. Lowest natural modes of mixer.

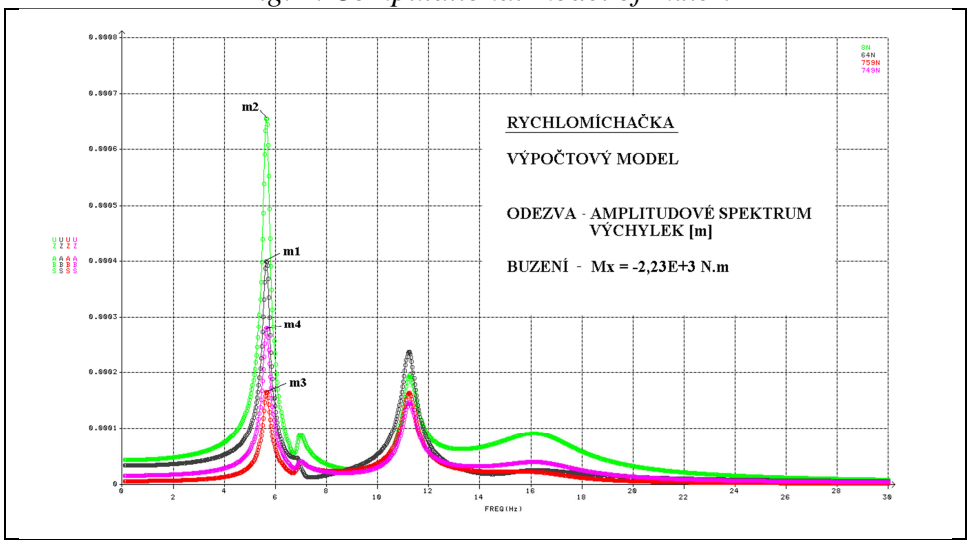

Fig. 4. Deflection amplitude spectrum.

Overview of selected computational finite element analyses

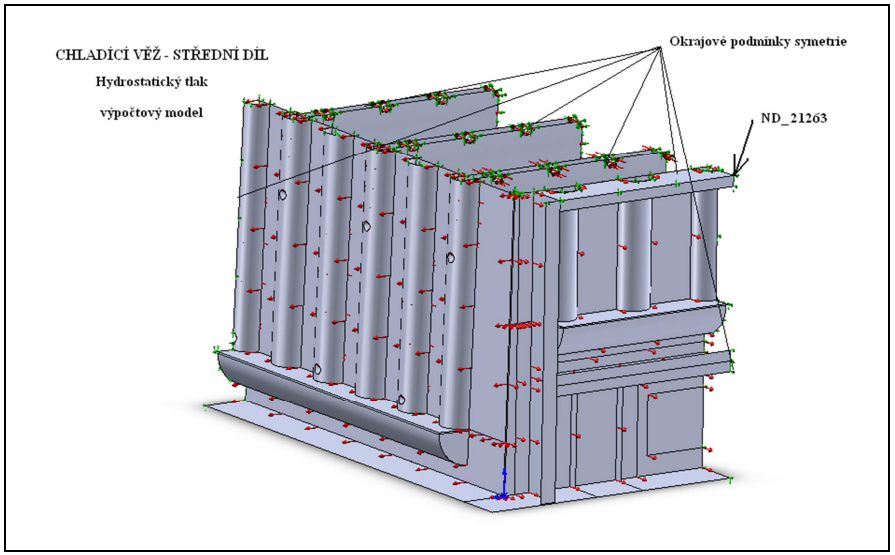

Fig. 1. Model of cooling tower.

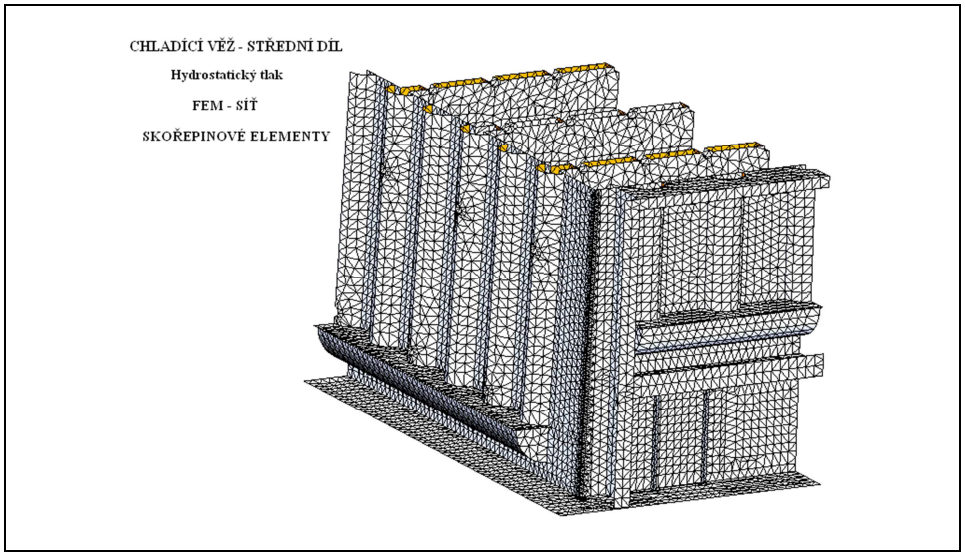

Fig. 2. Computational model.

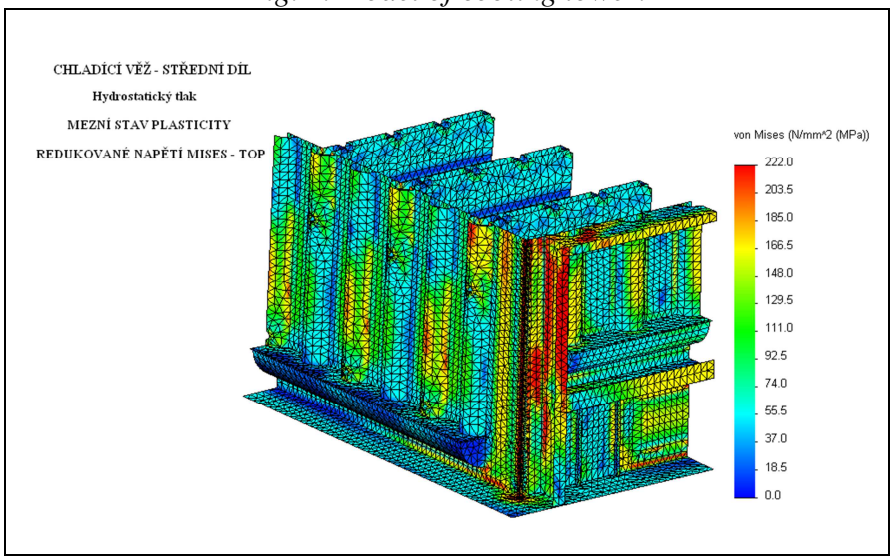

Fig. 3. Limit state of plasticity – strength evaluation.

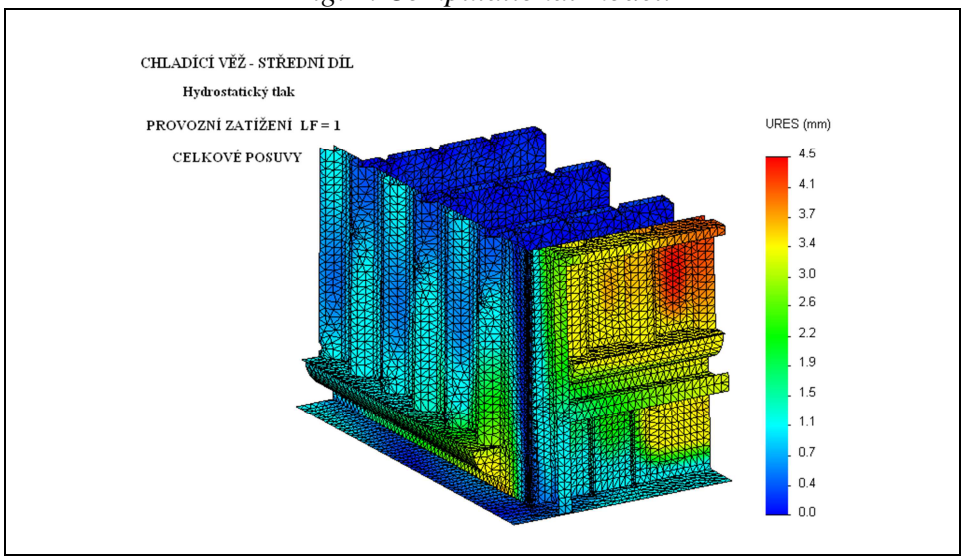

Fig. 4. Total displacements.

Overview of selected computational finite element analyses

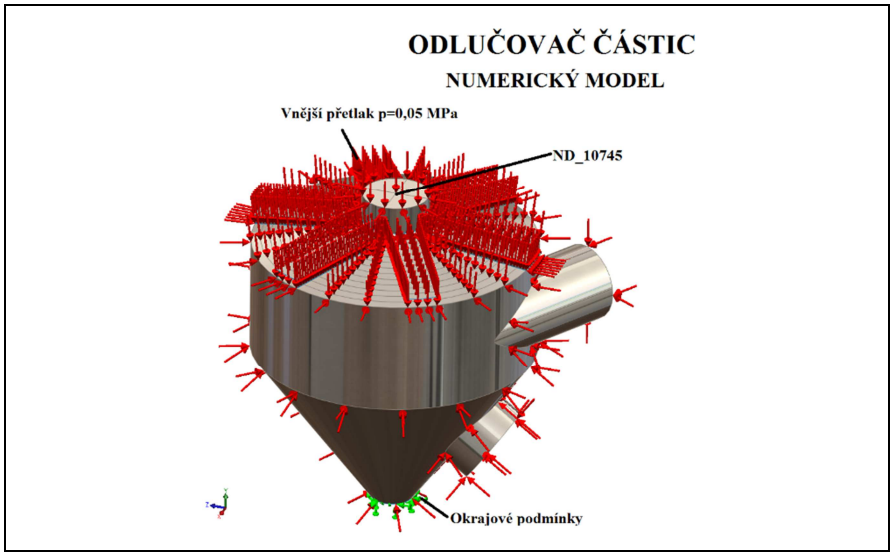

Fig. 1. Model of particle separator.

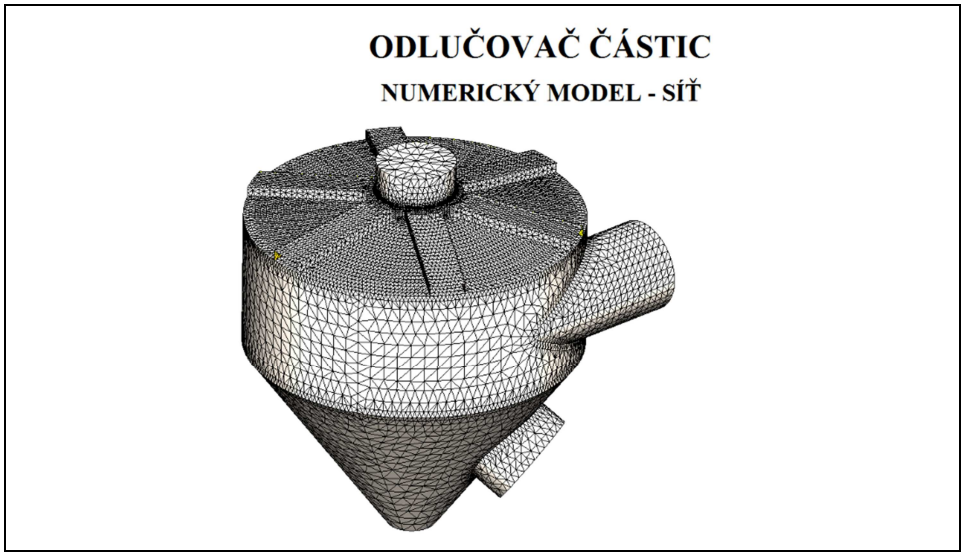

Fig. 2. Computational model.

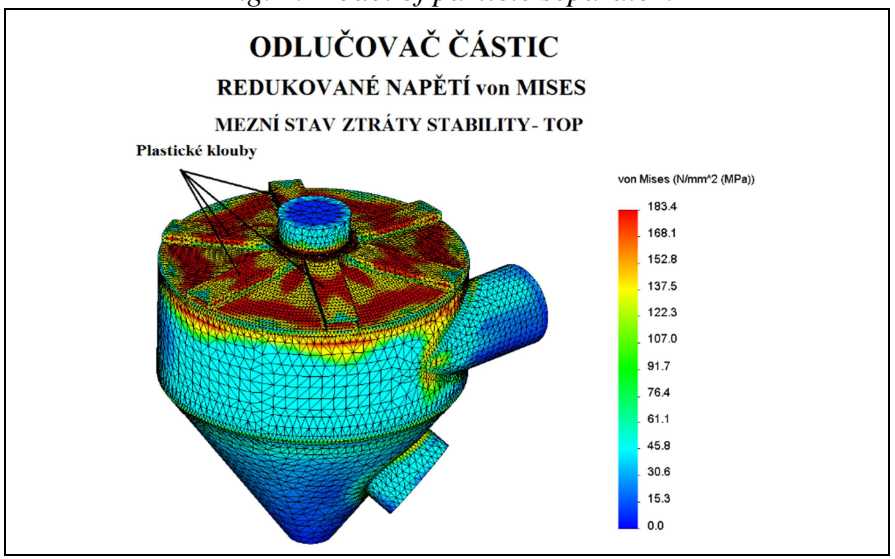

Fig. 3. Limit state of plasticity – strength evaluation.

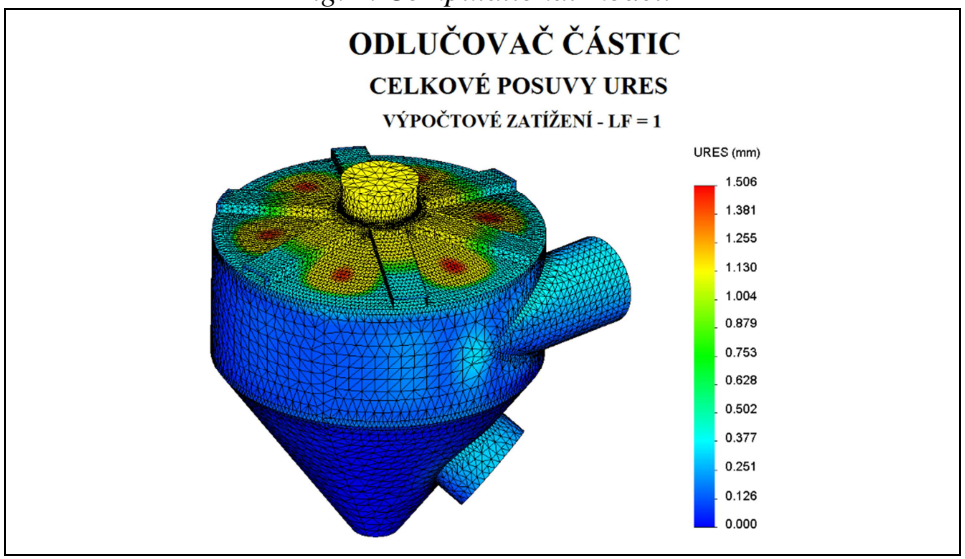

Fig. 4. Total displacements.

Overview of selected computational finite element analyses

Fig. 1. Steel construction with reactor R301A, R301B, R301C (measurement of excessive vibrations).

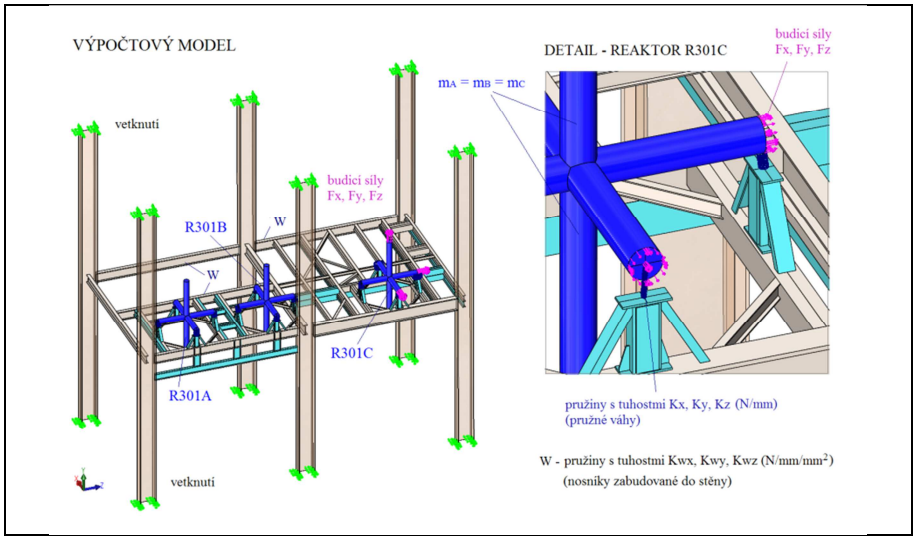

Fig. 2. Computational model of the reinforced steel structure.

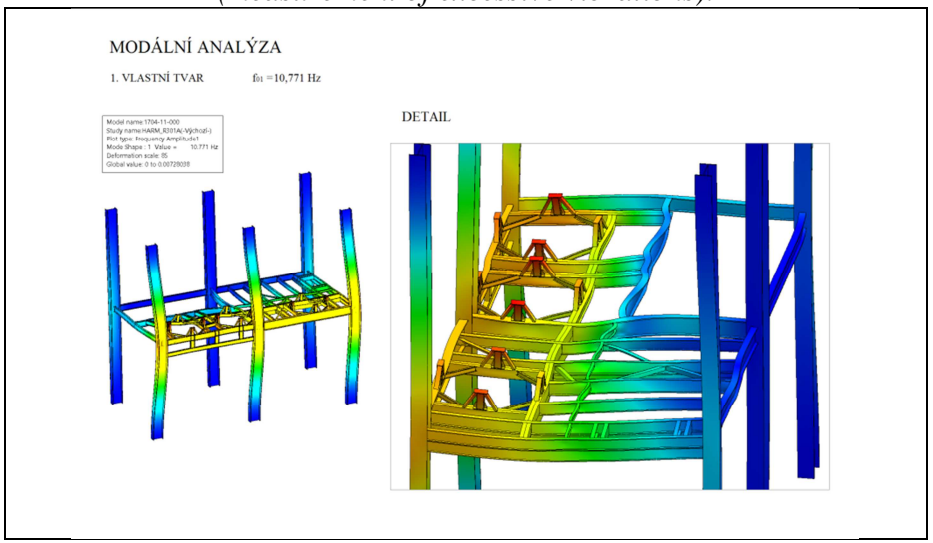

Fig. 3. Modal analysis – the firs significant eigenmode.

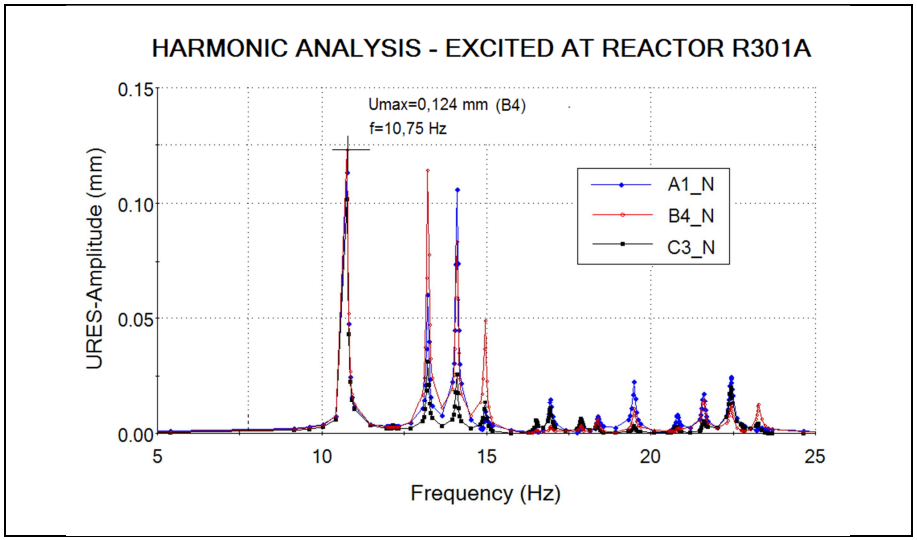

Fig. 4. Harmonic analysis – response spectrum in displacements.

Overview of selected computational finite element analyses

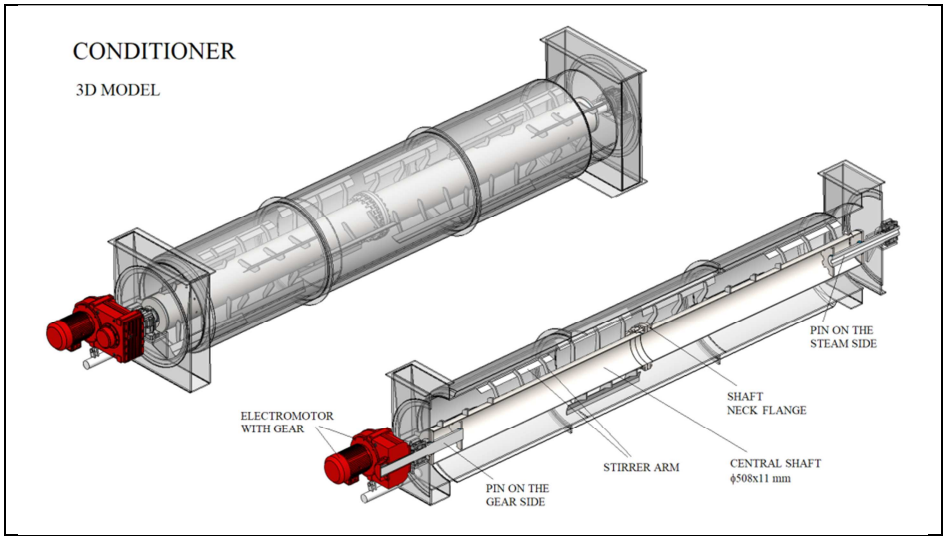

Fig. 1. Conditioner – 3D-model.

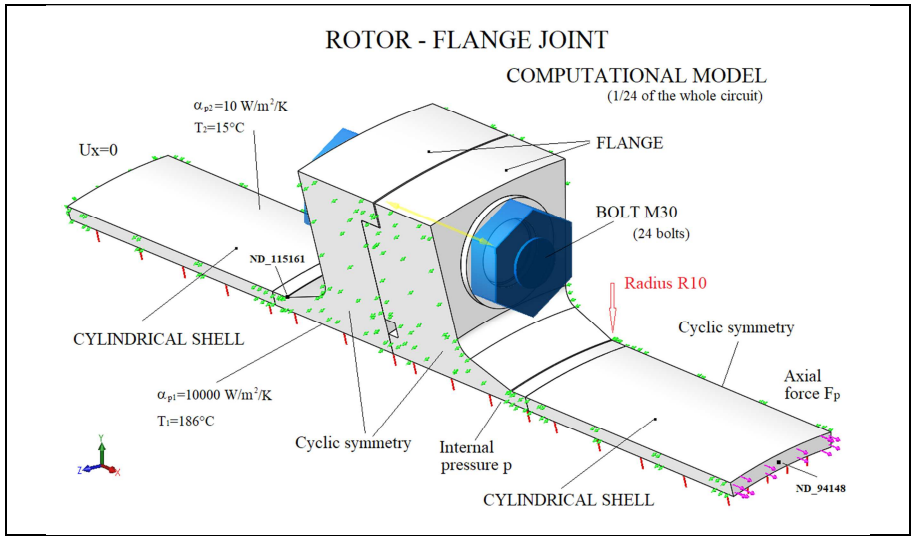

Fig. 2. Computational model of the shaft neck flange.

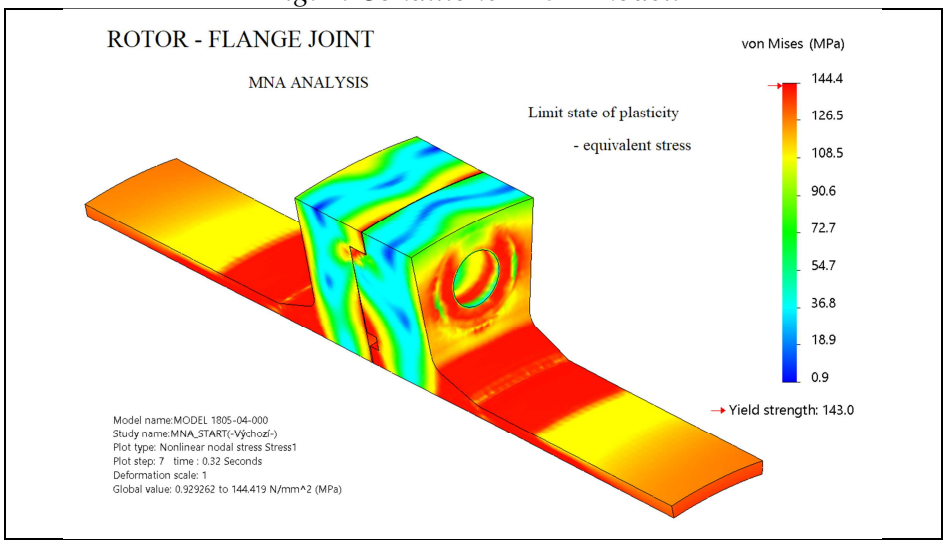

Fig. 3. Limit state of carrying capacity - strength.

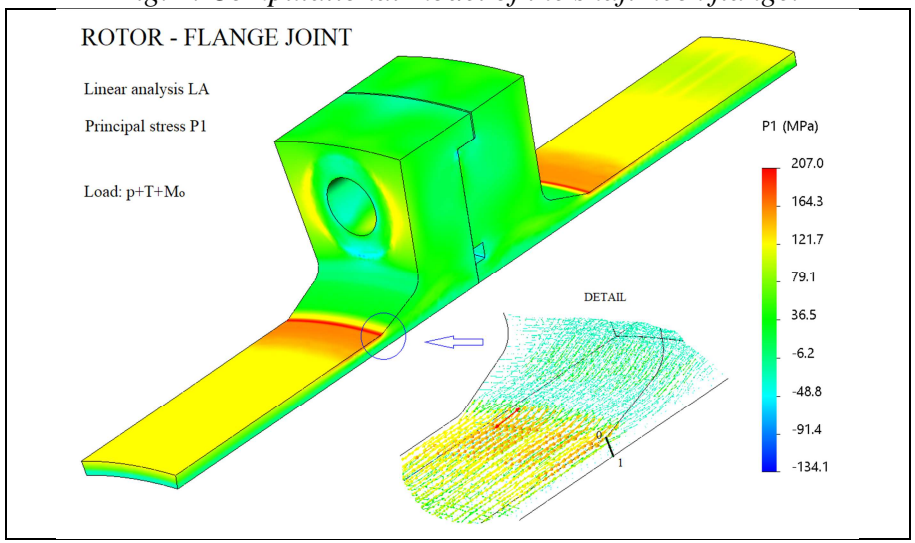

Fig. 4. Principle stress P1 (load combination p+T+M_0) - fatigue.

Overview of selected computational finite element analyses

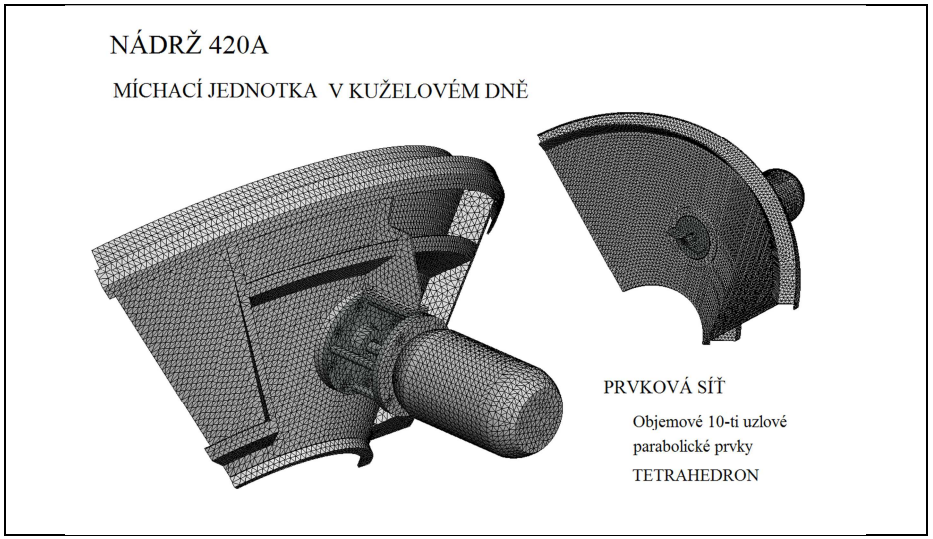

Fig. 1. Vessel conical bottom with mixing device.

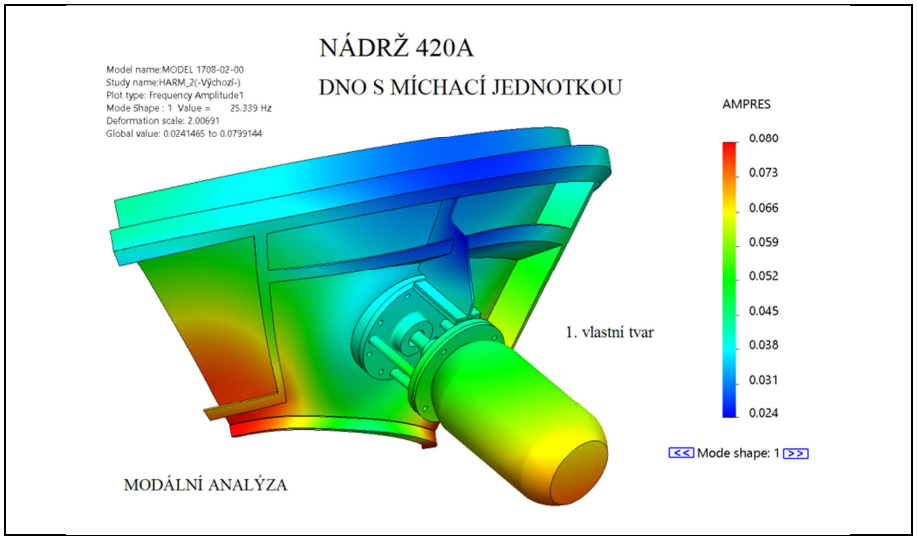

Fig. 2. Modal analysis – the first significant eigenvalue.

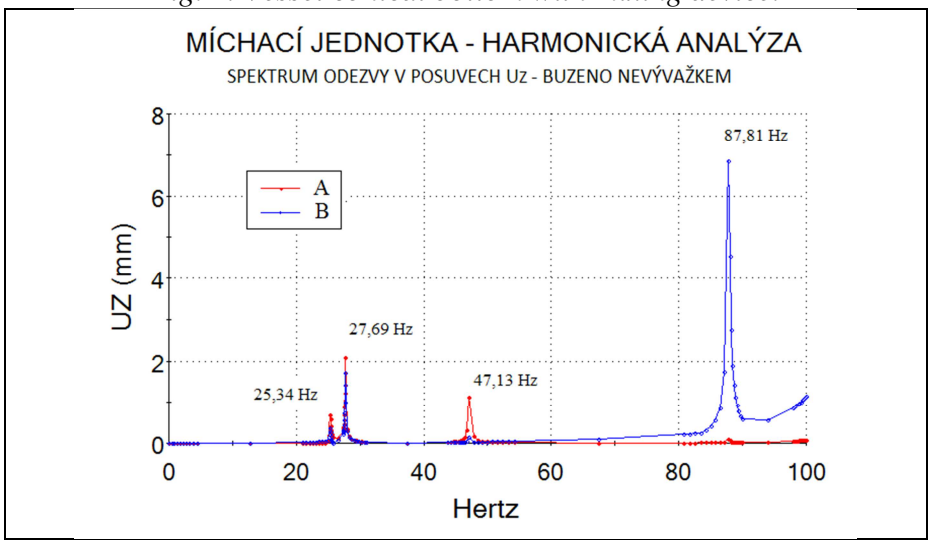

Fig. 3. Harmonic analysis – response spectrum in displacements.

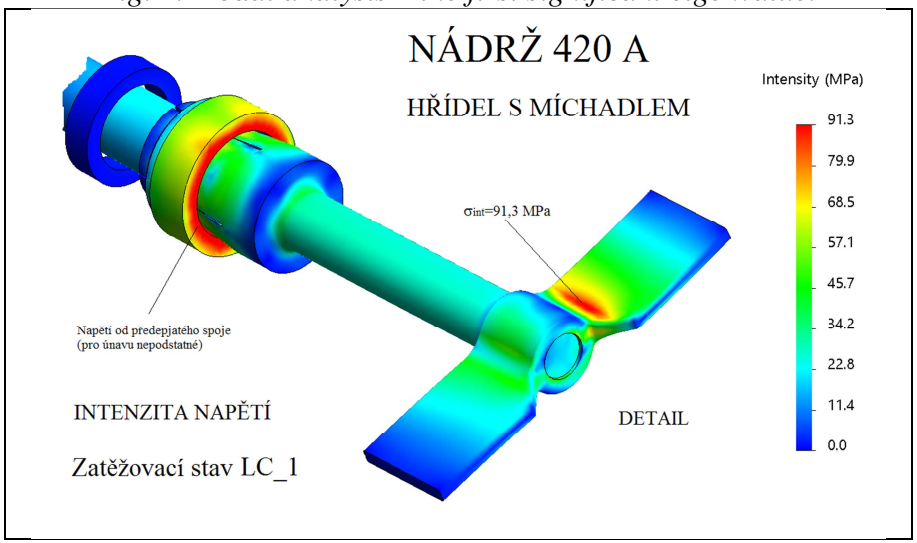

Fig. 4. Harmonic analysis – response in maximum stresses.

Overview of selected computational finite element analyses

Fig. 1. Photo of the rotor.

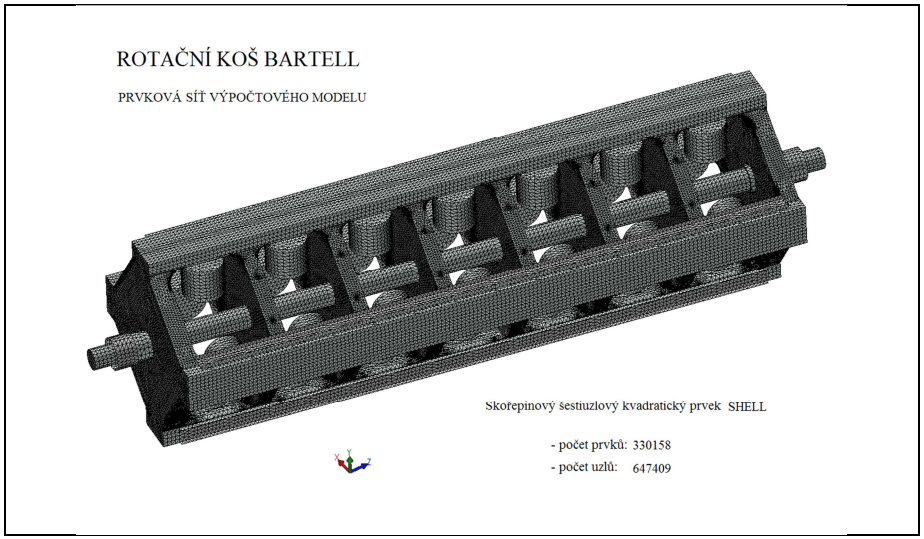

Fig. 2. Computational model - mesh.

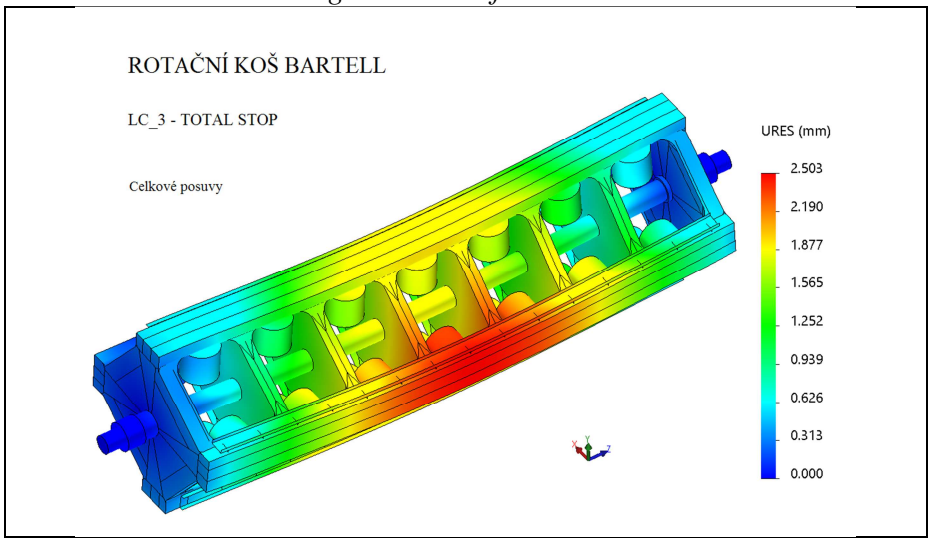

Fig. 3. TOTAL STOP – total displacements.

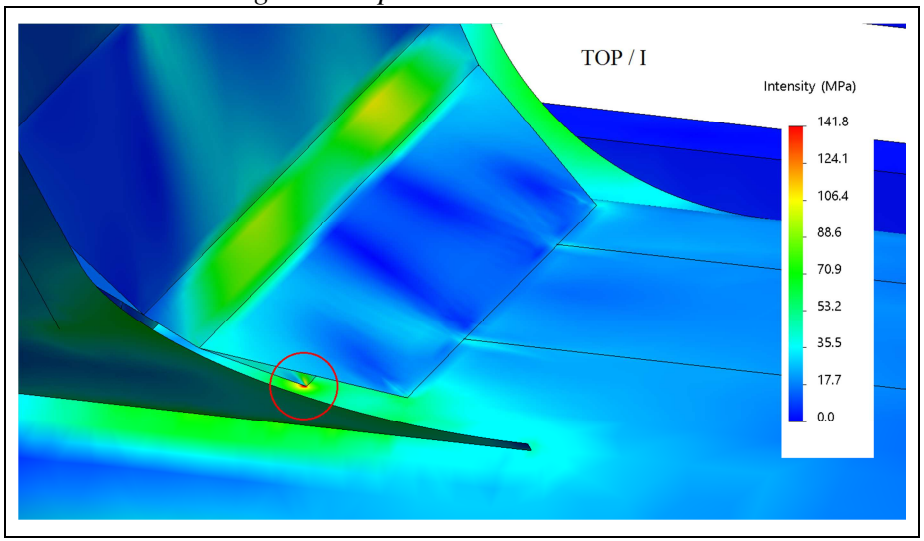

Fig. 4. Total stop – stress intensity peak (TOP).

Overview of selected computational finite element analyses

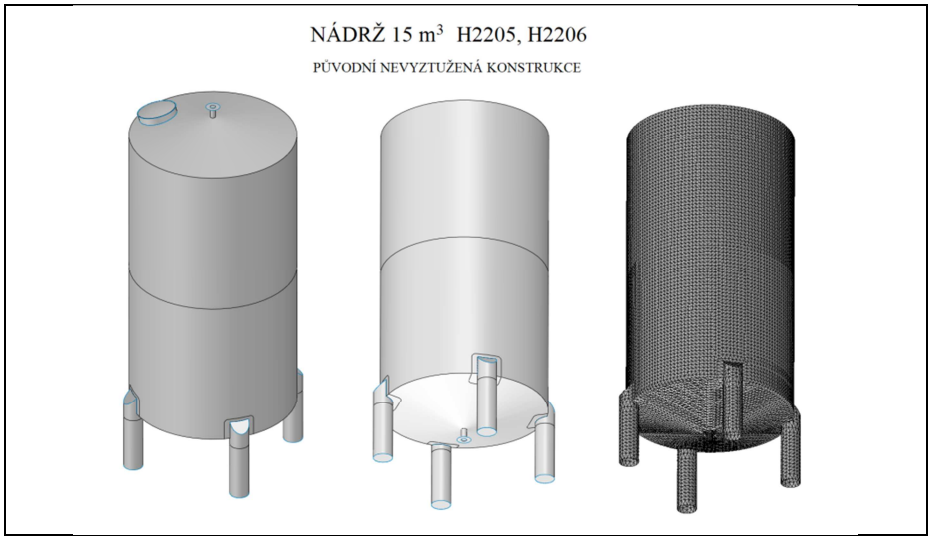

Fig. 1. Unreinforced original tank design – computational model.

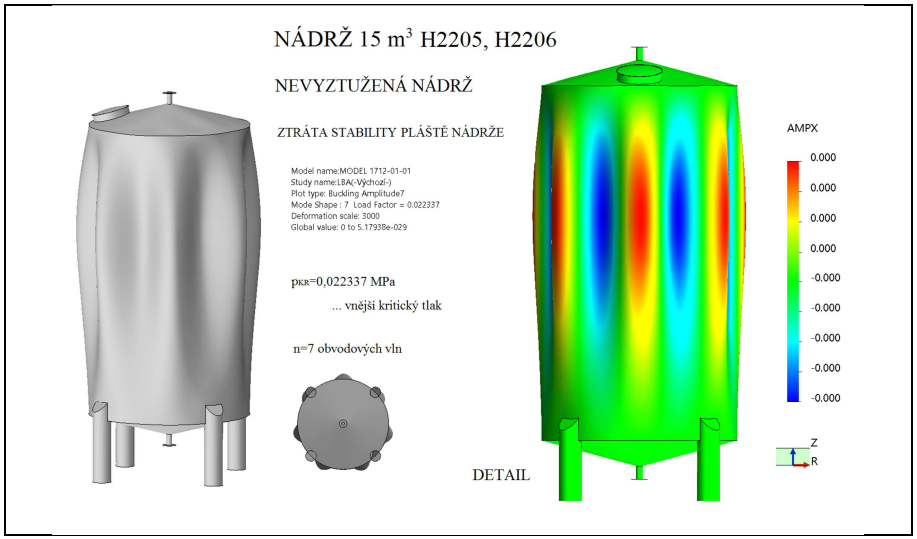

Fig. 2. Loss of stability of unreinforced original tank.

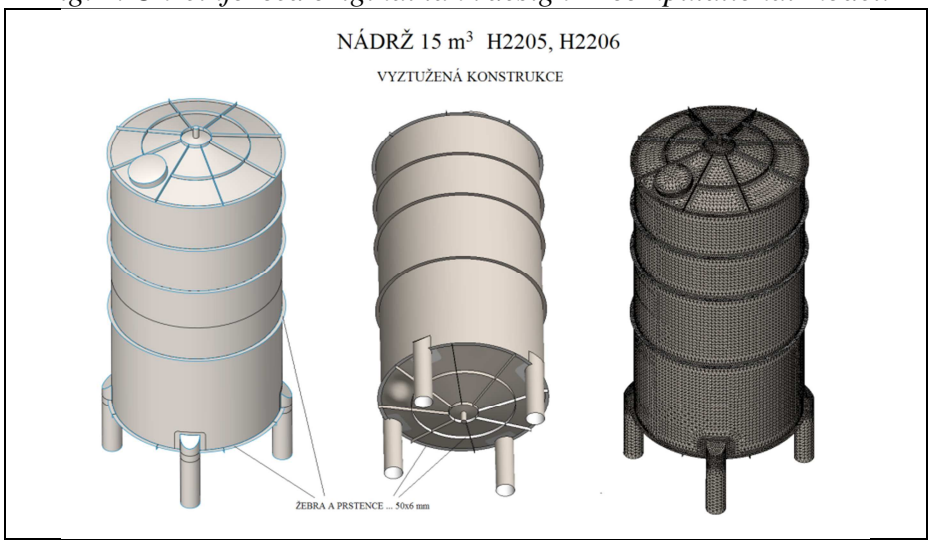

Fig. 3. Reinforced tank – computational model.

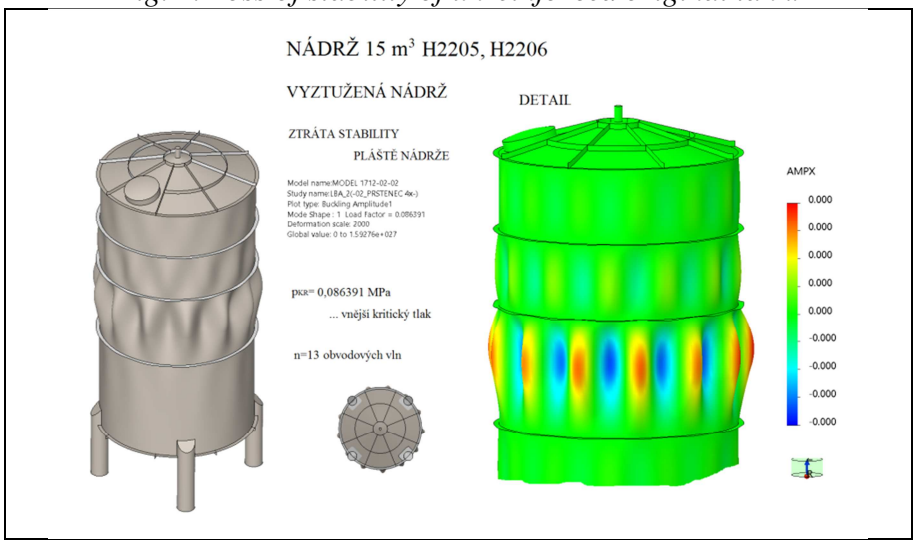

Fig. 4. Loss of stability of reinforced tank.

ELECTRICAL INDUSTRY

Overview of selected computational finite element analyses

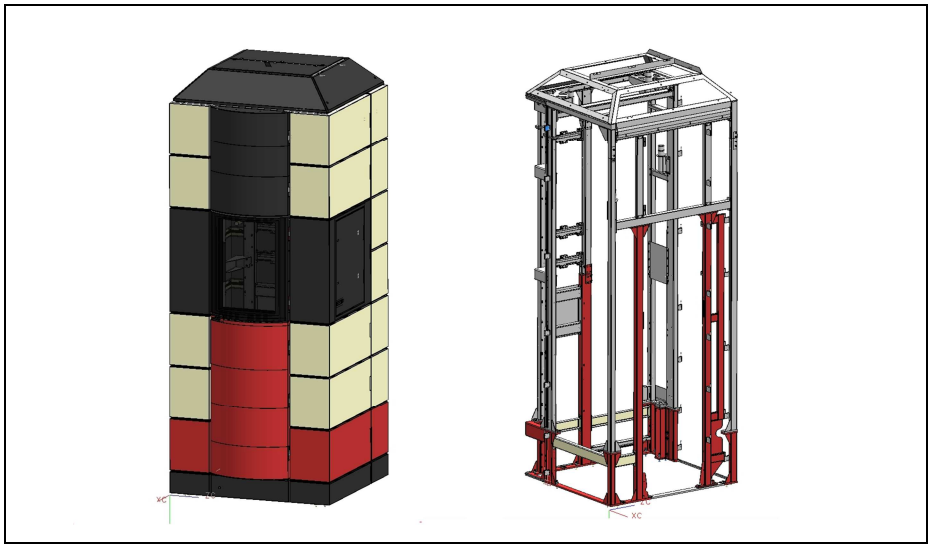

Fig. 1. Acoustic box of electron microscope.

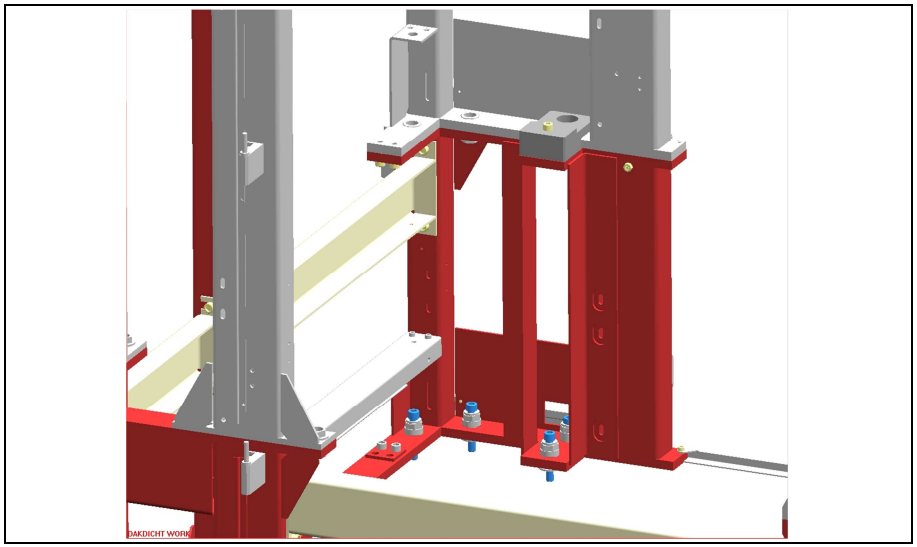

Fig. 2. Model of box corner anchored to the ground.

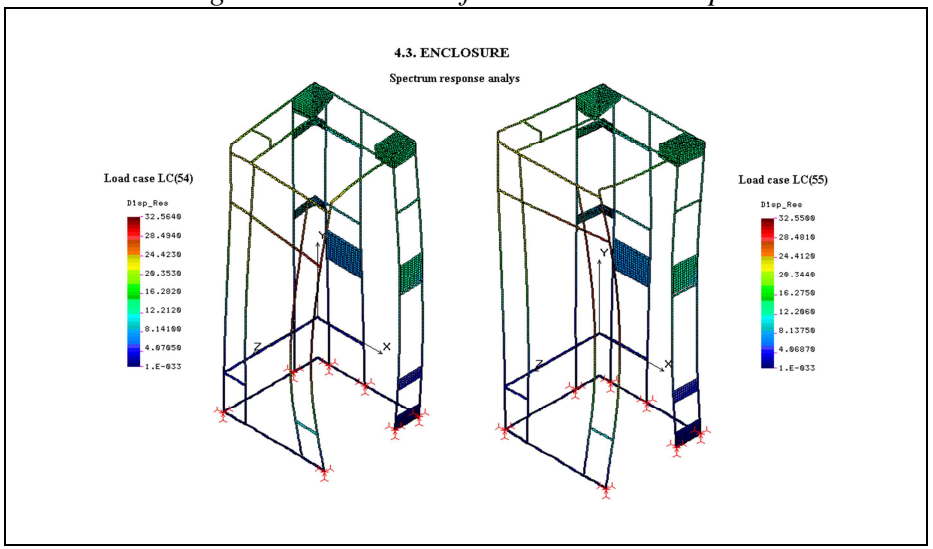

Fig. 3. Seismic analysis results of BEAM3D model.

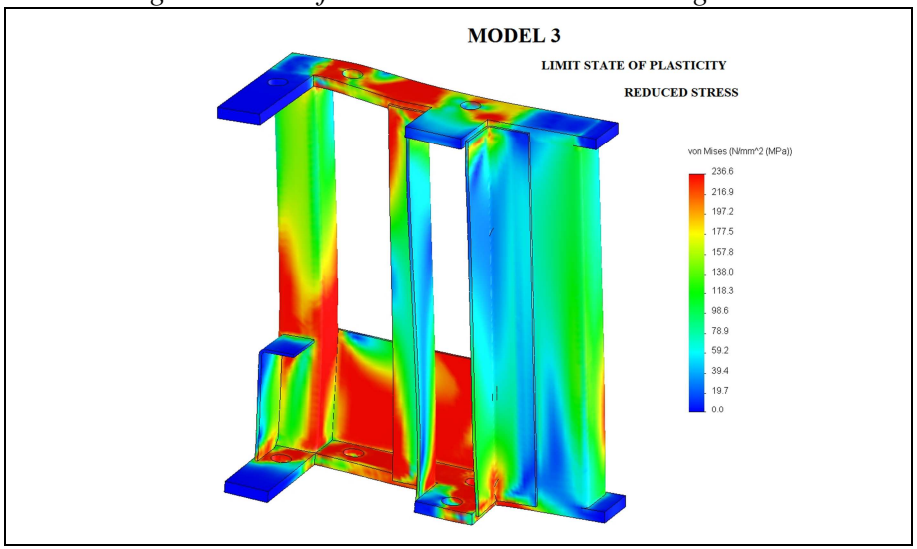

Fig. 4. Limit state of plasticity – strength evaluation.

Overview of selected computational finite element analyses

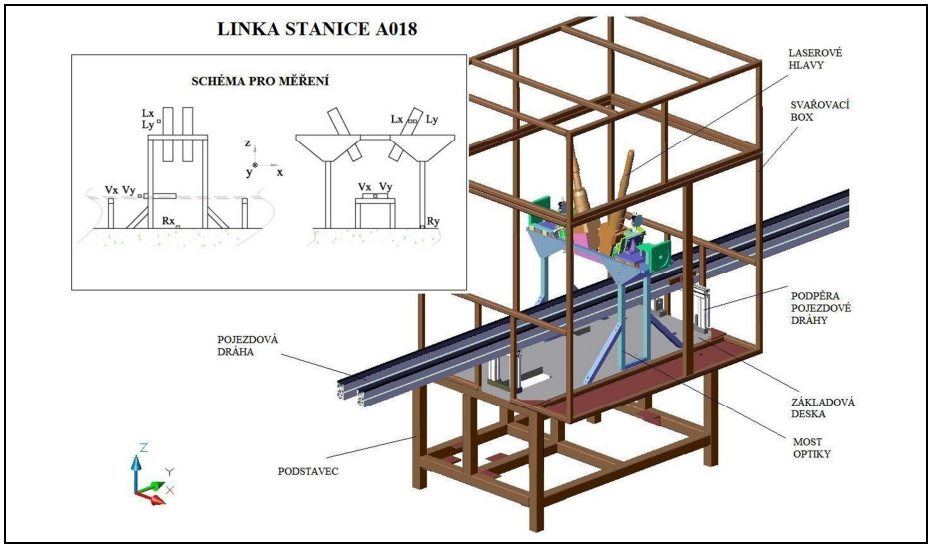

Fig. 1. Model of laser welding station with path for carriers.

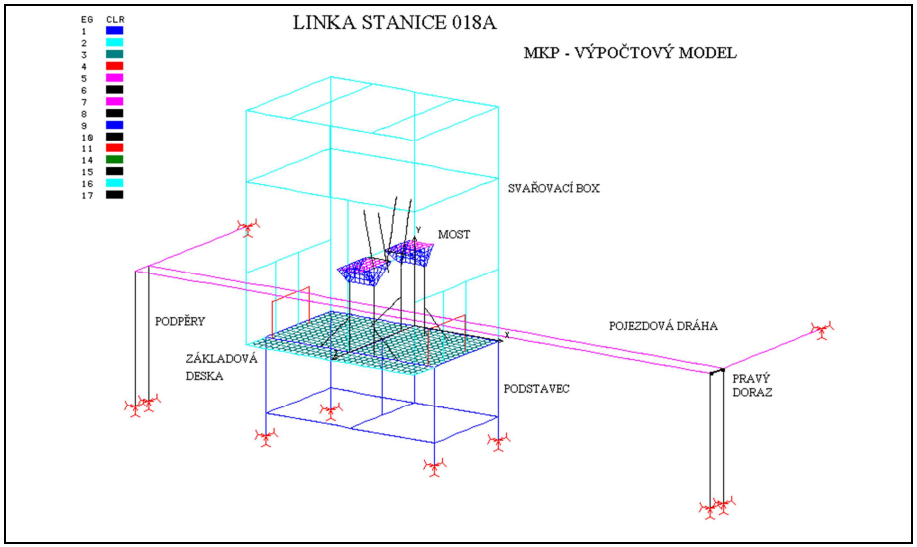

Fig. 2. Computational model of welding station.

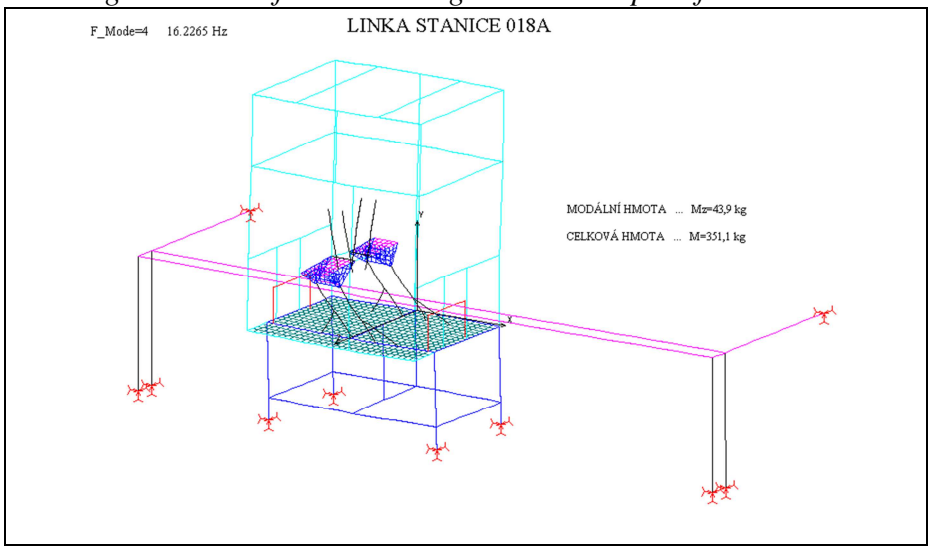

Fig. 3. Excessive vibrations due to resonance with stepping motor.

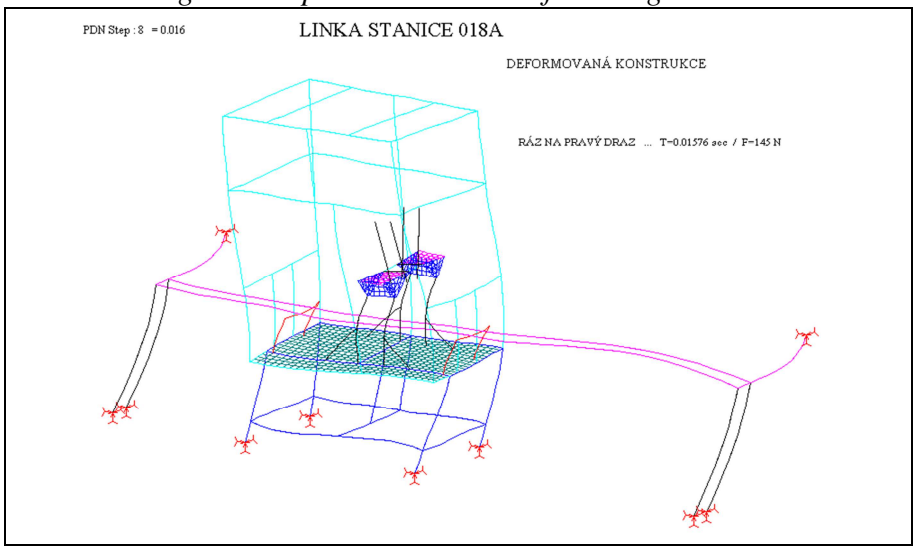

Fig. 4. Excessive vibrations due to impacts in path for carriers.

Overview of selected computational finite element analyses

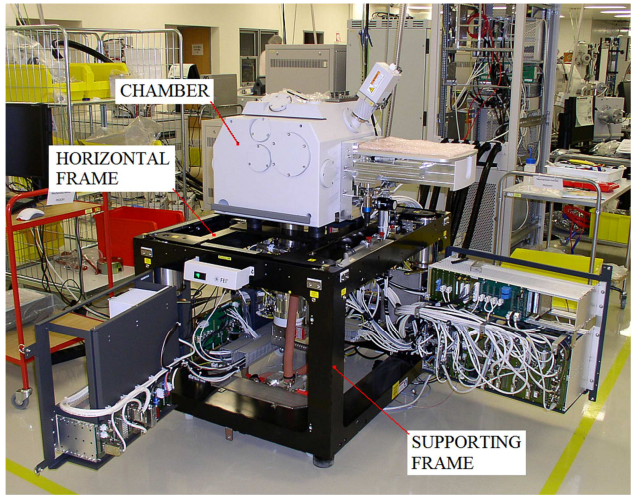

Fig. 1. Electron microscope perched on support frame.

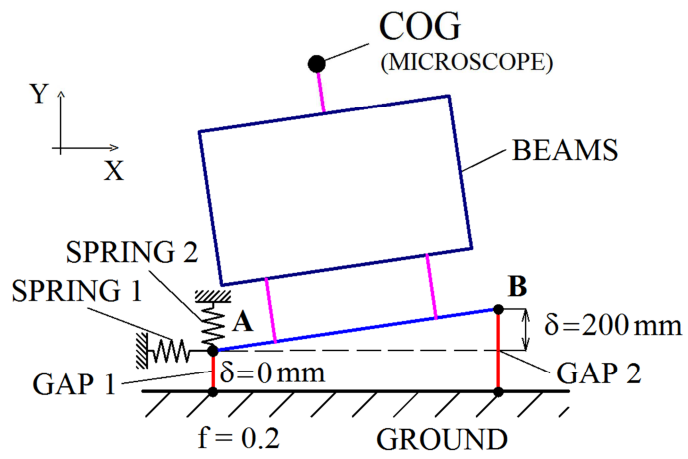

Fig. 2. Computational simulation of drop test – inertial forces.

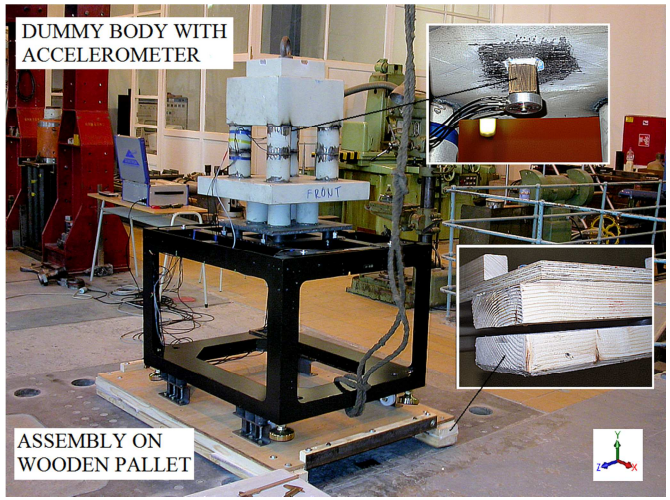

Fig. 3. Test assembly with dummy microscope.

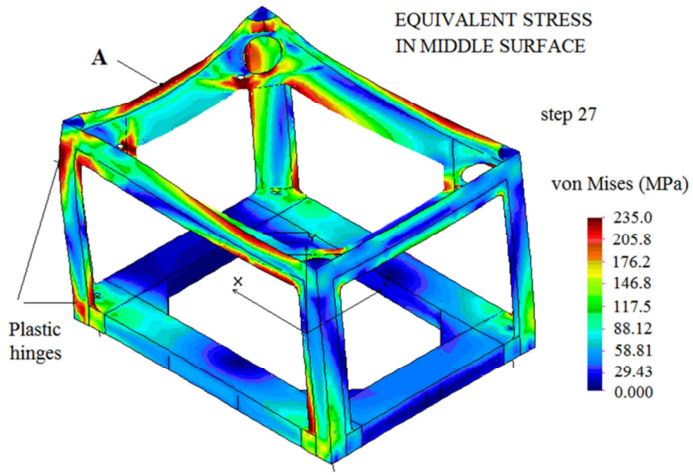

Fig. 4. Limit state of plasticity – strength evaluation.

Overview of selected computational finite element analyses

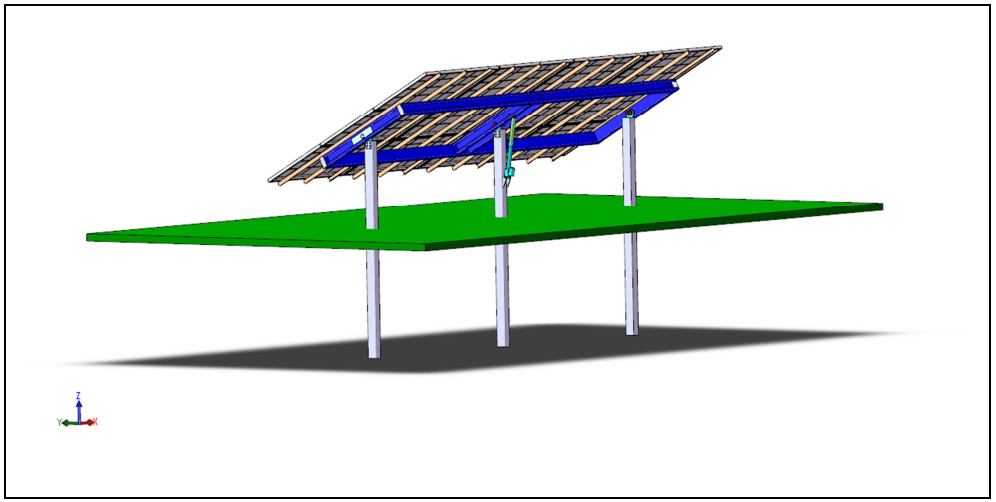

Fig. 1. Model of photovoltaic panel.

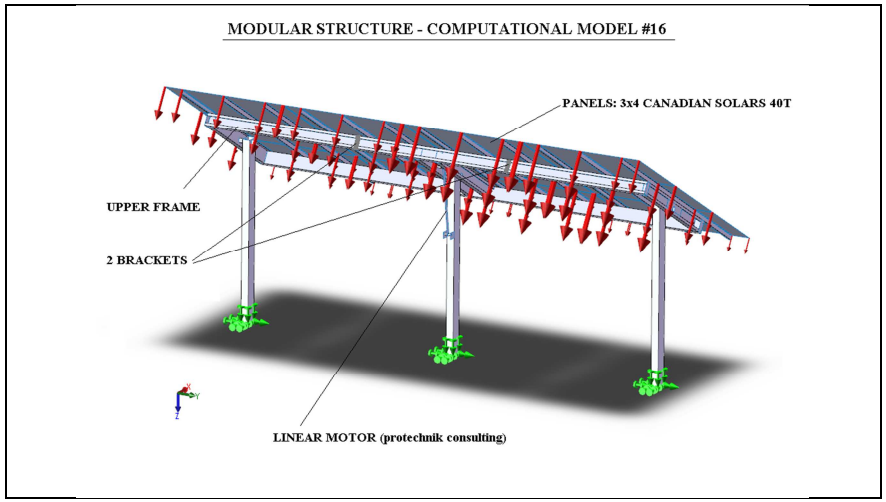

Fig. 2. Computational model of modular construction (snow, wind).

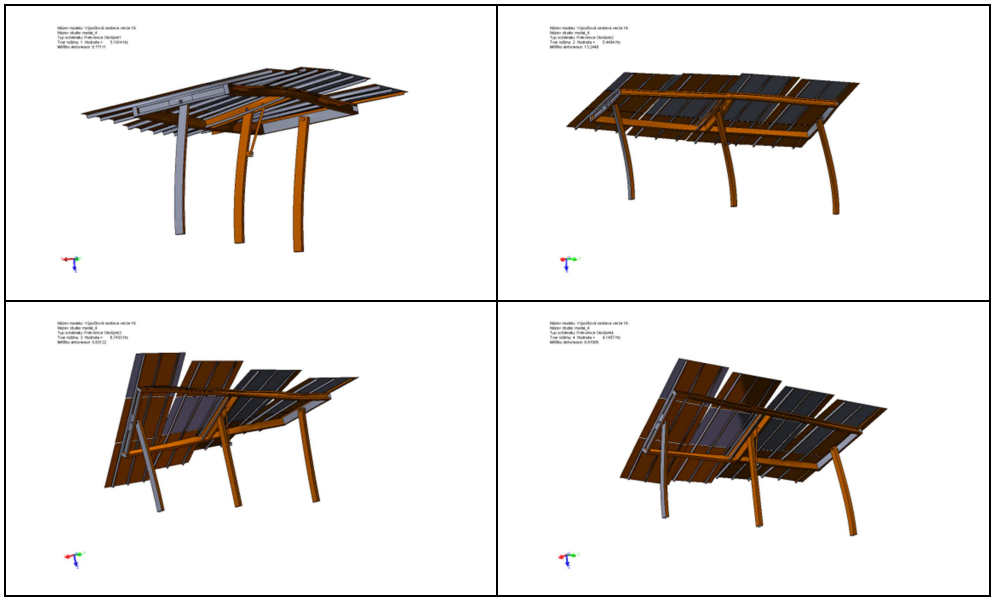

Fig. 3. Modal analysis – first four natural modes.

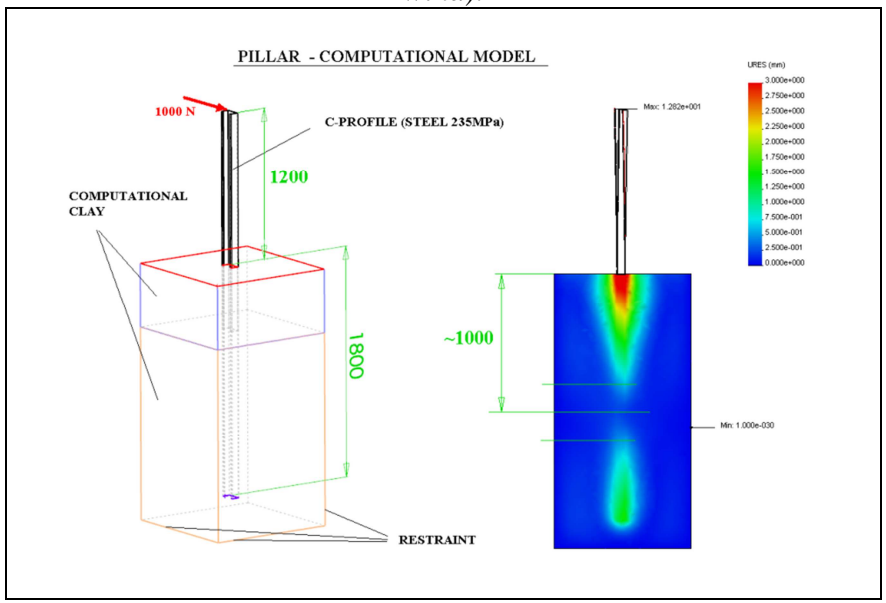

Fig. 4. Computational analysis of anchored column.

OTHER AREAS

Overview of selected computational finite element analyses

Fig. 1. Whirlpool (SPA).

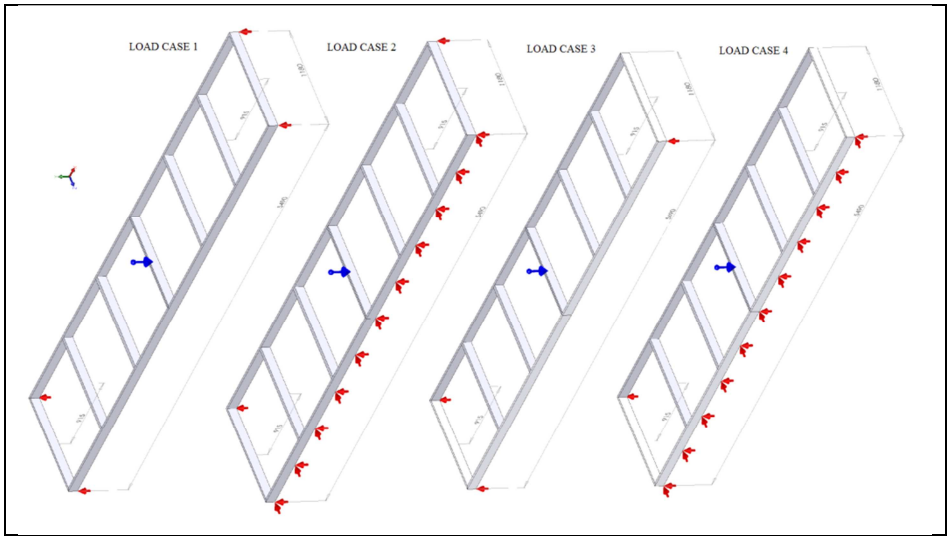

Fig. 2. Model of whirlpool cover frame.

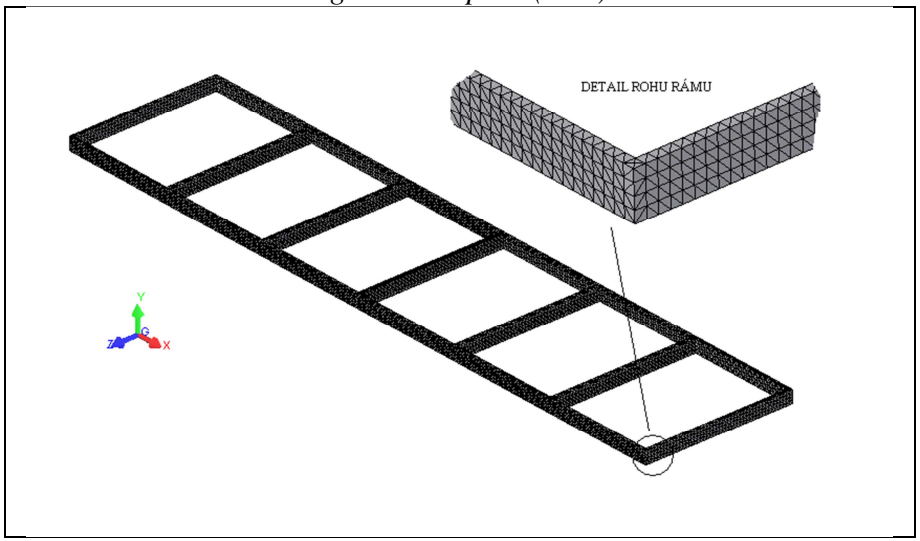

Fig. 3. Computational model.

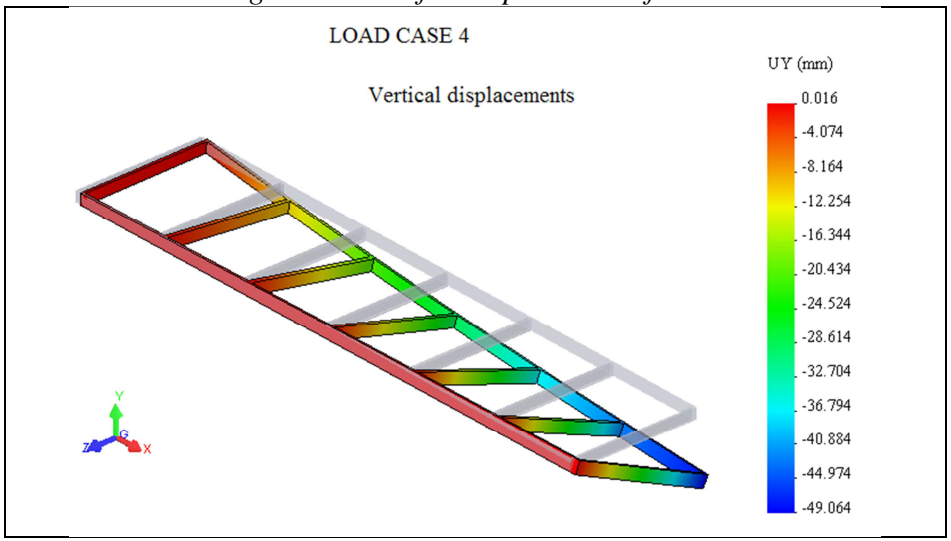

Fig. 4. Vertical displacements of frame.

Overview of selected computational finite element analyses

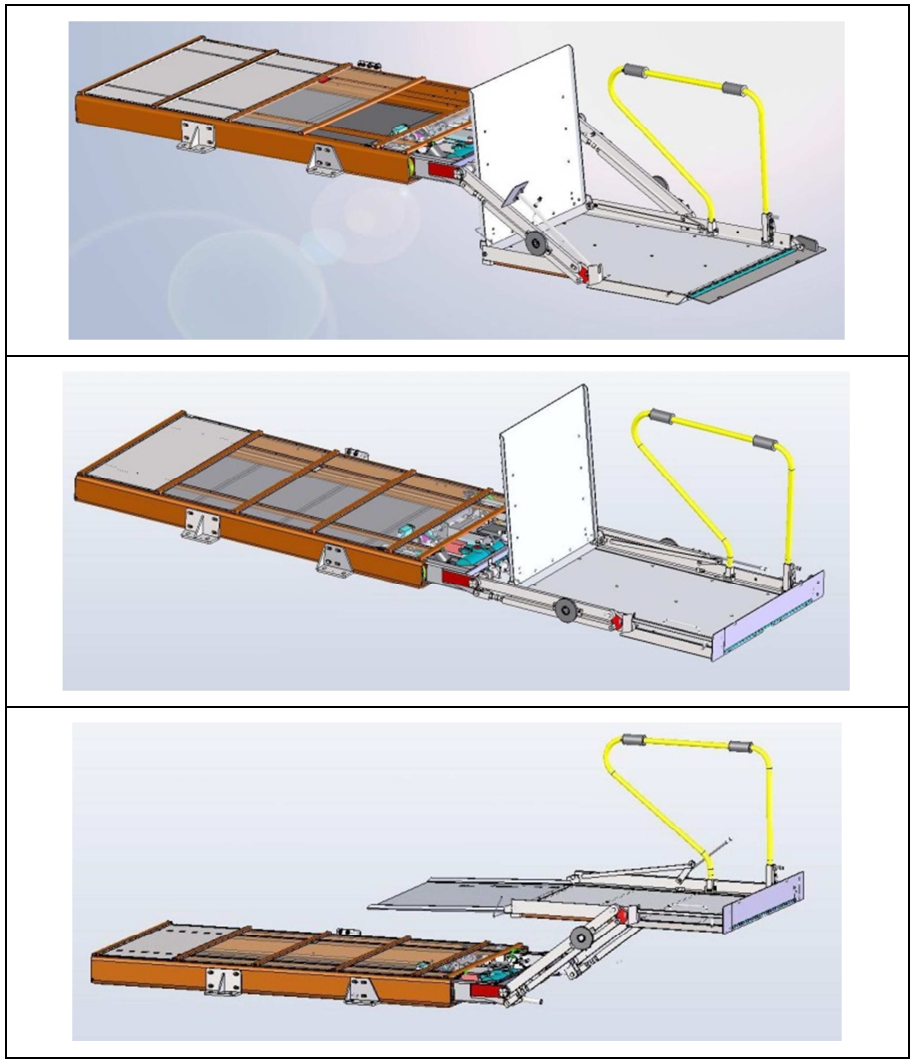

Fig. 1. Model of elevator for the handicapped - different positions.

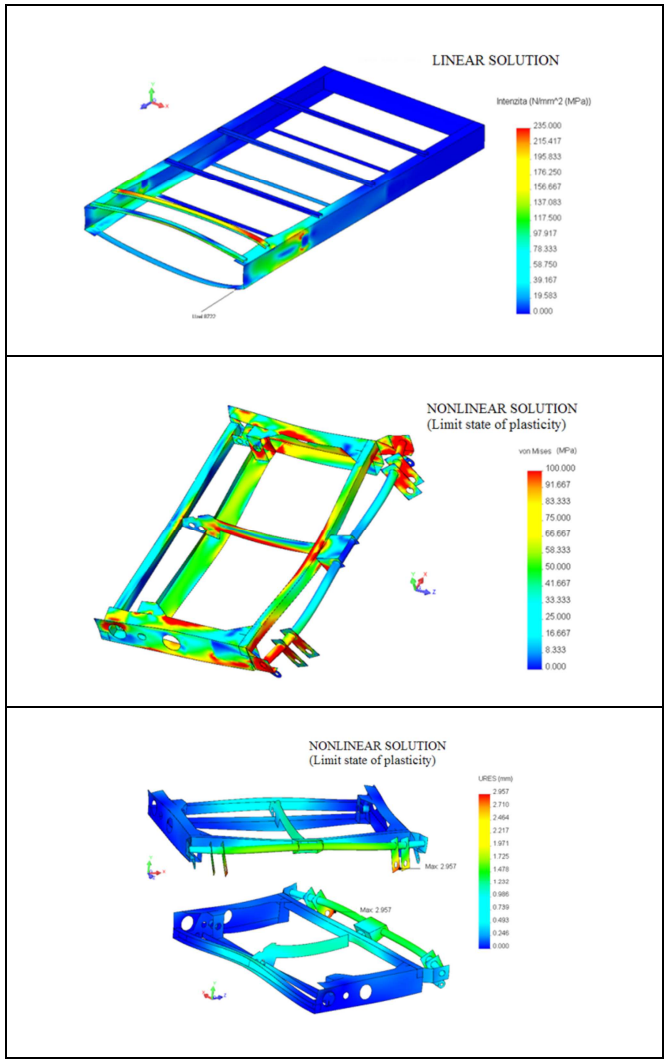

Fig. 2. Computational analysis of strength and stiffness.